AN INVESTIGATION INTO THE WAVE DIFFRACTION BY SMALL OBSTACLES FOR DIRECTIVE PROPAGATION AND MEASUREMENT OF DIELECTRIC CONSTANT OF BANGLADESH SOIL

BY

MAHBUBUL HOQUE

A THESIS

SUBMITTED TO THE DEPARTMENT OF ELECTRICAL ENGINEERING, BANGLADESH UNIVERSITY OF ENGINEERING AND TECHNOLOGY DACCA, IN PARTIAL FULFILMENT OF THE REQUIREMENTS FOR THE DEGREE OF MASTER OF SCIENCE IN ENGINEERING (ELECTRICAL).

DEPARTMENT OF ELECTRICAL ENGINEERING, BANGLADESH UNIVERSITY OF ENGINEERING AND TECHNOLOGY, DACCA

DECEMBER- 1977.

THIS IS TO CERTIFY THAT THIS WORK HAS DONE BY ME AND IT HAS NOT BEEN SUBMITTED ELSEWHERE FOR THE AWARD OF ANY DEGREE OR DIPLOMA.

SIGNATURE OF THE SUPERVISOR

SIGNATURE OF THE CANDIDATE

AN INVESTIGATION INTO THE WAVE DIFFRACTIONAL BY SMALL OBSTACLES FOR DIRECTIVE PROPAGATION AND MEASUREMENT OF DIELECTRIC CONSTANT OF BANGLADESH SOIL

ACCEPTED AS SATISFACTORY FOR PARTIAL FULFILMENT OF THE REQUIREMENTS FOR THE DEGREE OF MASTER OF SCIENCE IN ENGINEERING (ELECTRICAL).

EXAMINERS

S Ahmed 5/12/77
PROF. S. U. AHMED
DEPTT. OF ELECT. ENGG.
BUET., DACCA. — CHAIRMAN

5/12/77
KAZI ABDUR ROOF
MEMBER, T & T BOARD
BANGLADESH. — EXTERNAL MEMBER

PROF. A.M. ZAHOORUL HOQ
HEAD, ELECT. ENGG. DEPTT.
BUET, DACCA. — MEMBER

5/12/77
PROF. A.M. PATWARI
DEPTT. OF ELECT. ENGG.
BUET, DACCA. — MEMBER

A C K N O W L E D G E M E N T

It is a matter of great pleasure on the part of the author to express his profound gratitutes to his superviser Professor Shamsuddin Ahmed for his invaluable guidance throught the whole work and without whose aid and encouragement this work would not been completed. Thanks are also conveyed to Professor A.M. Zahoorul Haq Head of the Department of Electrical Engineering, for providing departmental facilities.

Thanks are also conveyed to the staff of the Department of Electrical Engineering, Bangladesh University of Engineering and Technology, Dacca particularly to Mr. Saroj Kanti Biswas and Mr. B.M. Azizur Rahman for their kind co-operation and help extended to the author in preparing computer programme.

The author.

ABSTRACT:

The thesis is composed of two parts based on two different topics. In the first part electromagnetic diffraction by knife-edge obstacle has been studied. An investigation has also been made by introducing the effect of antenna directivity in the Fresnel-Kircheoff theory and then the theoretical results were compared with that of experimental values. A theoretical and experimental investigation has also been made. [redacted] on electromagnetic diffraction by a "flat-top double edge obstacle. Numerical solutions have been obtained with the help of digital computer (IBM-360) . The results have been compared with experimental values. Finally an alternative approach to the solution of the above problem has been proposed.

The second part of the thesis deals with the measurement of the dielectric constant of Bangladeshi soil. Two different procedures, namely the "freee-space propagation measurement" and " wave- quide measurement Techniques" have been applied for the dielectric measurement. The variations of the dielectric constant with the change of the applied signal-frequncies hav been shown in graphs, for a few seletive samples. Finally the dc conductivity of the soil samples has also been measured.

C O N T E N T S

Page-

*****

CHAPTER 1

INTRODUCTION

1.1 GENERAL :

During the past few decades Microwave systems have grown and developed into one of the most important means of communication system. Growing out of the max-well's concept of Electromagnetic waves microwave engineering has been drawing much interest and attention of electrical engineers and physicist. Modern civilization's growing demand for better and reliable communication system has led to extensive research in this field. Research work on the various problems and new possibilities in microwave systems is going on all over the world. Among the wide range of topics the reflection and diffraction of electromagnetic waves by various natural obstacles propagation of electromagnetic waves in the open atmosphere under various atmospheric conditions should be of interest.

In this thesis two different problems on microwave communication system have been discussed separately. The first part of this thesis is concerned with problems on electromagnitic waves scattering and diffraction from obstacles. The second part deals with a study on the dielectric properties of Bangladesh soil at microwave frequencies. For this purpose dielectric constant of a number of soil samples collected from Dacca, Comilla, Noakhali and Chittagong districts have been measured at microwave frequencies.

Basically, analysis of scattering and diffraction of electromagnetic waves falls in the domain of boundary-value problems. The exact analysis of such a problem is a very difficult one and in most of the cases, solutions in compact form do not exist. In practice the exact solution to the problem is not always necessary, while the asymptotic solutions i.e. the solutions at large distances are mostly necessary. This approach to the solution greatly simplifies the problem. When a electromagnetic wave impinges on an object either conducting or dielectric, it induces currents on the object. This induced currents reradiates electromagnetic field in the space. For exact solution, information regarding the nature of induced current distribution on the scattering object must be known. To solve such a problem, numerous methods theoretical, semi-theoretical and numerical have been developed by various scientists and engineers. On the other hand when asymptotic solutions or the solution at large distances are required, a more simpler approach commonly known as " optical approach" can be used.

This approach is completely based on the wave properties of the electromagnetic radiation. At microwave frequencies, the wave properties of the electromagnetic waves closely resembles that of light waves. So, the scattering and diffraction phenomena of electromagnetic waves can be solved by considering them as obeying the basic laws of light waves. Since, in practice, only the far-distance field is of interest, hence this approach yields quite satisfactory result. In this thesis a simple modification of the original diffraction theory(Fresnel-Kirchoff diffraction theory) has been developed. Also theoretical solutions and practical measurements have been obtained for electromagnetic wave diffraction from a prototype conducting obstacles representing the model of a building.

The second part of this thesis deals with the measurements of dielectric constant of Bangladesh soil. Main object of this study was to prepare a Radio-data and to perform a study on reflection and diffraction of electromagnetic waves over various natural obstacles (mountain, flat land etc.) in Bangladesh. It has been an established fact, that reflection and diffraction of electro-magnetic waves from an obstacle depends on the shape and electrical characteristics of the obstacle. For this reason, a detail study on microwave- communication in our country requires an elaborate knowledge on electrical characteristics of Bangladesh soil at mocrowave-frequencies.

1.2 HISTORICAL REVIEW PART-I:

The problem of diffraction of electromagnetic waves by various natural obstacles have been extensively studied both theoretically and experimentally by various research workers. The basic approach to the study of diffraction phenomena was to consider the obstacle as a knife-edged semi-infinite perfectly conducting half plane. Rigorous mathematical solutions have also been obtained by a number of authors [1] for diffraction of electromagnetic waves by one or more infinitely thin half-planes. Again some author,[2] have also solved the problem by using the principles of optics. The basic theory established from this view point(principles of optics) is known to be the Fresnel-Kirchoff[3] diffraction theory which yields a satisfactory theoretical results for diffraction of electromagnetic waves by a knife-edged obstacles, under certain approximation. There is a general validity of this classical approach[4,5,6] which expresses the diffraction loss over a sharp ridge as a function of frequency 'f', the distance d_1, d_2 and height h.[4,5,6], with reference to Fig. 1.

In practice most of the obstacles cannot be approximated as a knife-edged obstacle. As for example, situation some times encountered when electromagnetic waves are diffracted by one or more mountains situated in between the transmitter and the receiver. In the usual theoretical treatment the mountains have been replaced by a vertical half-plane and the predictions of propagation condition by knife-edge theory have been found to agree reasonably well with experimental results obtained in different mountanous areas[1,2].

Though frequently encountered in this field, the case of two or more knife-edge obstacle has not been formally studied until Levine[5,6] Y has studied the nature of the diffracted fied in the presence of two semi-infinite screen. A close agreement between theory and experiment was also observed[7].

Bullington in his paper[8] published an approximation method for solving diffraction due to multiple knife-edge. Late, the method was modified by Epsten and Peferson[9], These two approaches are simple and easily extendable to three or more knife-edge obstacles. In 1962 Millington in his paper[10] obtained a complete mathematical analysis of the problem of diffraction of micro-waves by multiple knife-edge obstacles. Because of the unwieldly nature of the computation involved this mathematical solution is unsuitable for a quick estimate and is impracticable whenever there exists three or more intervening hills.[11] JacKuis presented another approximation which seems better than other solutions discussed earlier. This solution has been suggested at the French-School[12] and by French Army[3] as a replacement of the above methods.

So far, the presence of one or more knife-edge obstacles have been studied. It shoud be mentioned here that, though the presence of mountainous and dominant-ridges have been replaced by a vertical half-plane, and the predictions of this knife-edge theory have been found to agree reasonably well with experimental results[1,2], but the agreement have not been good enough in several other experiments. Reference is made to a paper by Crysdale [14]. One reason for such discrepencies may be due to the fact that the knife-edge approximation is not adequate to take into account of the effect of mountain tops. A better approximation should be to replace the mountains with a smooth cylindrical crest. Rice [15] has derived a theory for parabolic cylinder, but it has the dis-advantage that it's numerical evalution is difficult.

One of the best theoretical approach has been made by Fock[16]. In Fock's work, it was assumed that the wavelength characteristics of the incident field is small compared with the relevant dimensions of the scatterer as well as the radii of curvature of it's surfaces. From a detail investigation with the integral equation, Fock concluded that surface current has a local character in a penumbral region near to and including shadow boundary. This he called" principles of local field". Under this assumption he defined a " Universal function" for current and then produced to determine the current in the vicinity of the shadow boundary of a paraboloid of revolution located with it's axis perpendicular to the magnetic field of incident plane wave. Basic draw bakes of the Fock's theory was that, until than it appears to be mathematically intractable. Later in 1965 Negubaur and Backyniski[17] made a new approach to the problem by model[17] experiment in the laboratory and by the derivation of a modified theory based on Fresnel diffraction integral.

1.3 CONTENT OF THE THESIS (Part-I):

Upto this the diffraction of electromagnetic waves by one or more obstacles have been discussed . In all theoretical developments mentioned above, the directional pattern of the incident wave was not considered i.e. it was assumed that the transmitting antenna was an omnidirectional one. In practice, the case is quite different, most of the antennas used in communication system have highly directional pattern. In this thesis, a modification of the original theory has been developed incorporating the effects of directivity of the antennas. It has been observed that the theoretical results conforms more closely with the experimental results than obtained previously. (Using original Fresnel Kirchoff diffraction theory).

Recently, in microwave communication system, another interesting problem which encountered is diffraction of electromagnetic waves by skyscrapers in modern cities. In this thesis, both theoretical and practical investigation have been made on diffraction of electromagnetic waves over such obstacles. As it has already been observed that the physical shape of the obstacle influence the nature of the diffraction to some extent, hence a theoretical experssion has been developed considering the building to be a perfectly conducting flat-top double-edged obstacle. Numerical results have been obtained with the help of digital computer(IBM-360). Since, field experiment is very difficult for various practical limitations a model experiment, simulating the building obstacle was performed in the laboratory. The use of scalemodel technique greatly simplified many practical problems that could be encountered in the field-study.

1.4 HISTORICAL REVIEW: PART-II

Part II of the thesis deals with the measurement of dielectric constant of Bangladesh soil under various natural conditions. Main objects of this experiment was to prepare a complete radio-data for Bangladesh soil. Due to inadequate facilities and meger resources available at the disposal of the department for such a national problem, a limited number of soil samples from a few places of Bangladesh have been tested. Soil has been treated as a lossy dielectric and a procedure have been adopted for measuring this dielectric constant. Many experimental investigations supported by suitable theories[18] have been performed for measuring the dielectric constants at microwave frequencies, by various research workers[19]. One of the most important procedure is the method based on the measurement of VSWR. In this method, a section of wave-guide filled with the dielectric sample is treated as a four-pole network. Information about the equivalent network parameters gives a measure of the property of the medium of the wave-guide-section. This view point has been adopted in the actual measurement of the dielectric constant of soil samples.

The method of measuring the dielectric constant of a wave-guide medium based on principle of four-pole network is a very common approach. It's validity has been recognised independently by a number of writers, including Westphal[20] and J. Brown ... ..., but it's implication have heretofore not been fully exploited. Perhaps most well-known procedures using the above theory which employs an open and a short Ckt. termination. This method was published independently first by the British [21] and then by the American [(22)] authers. These-methods, based on specific output termination, utilize the four-pole view point in only a relatively narrow sence, since , no attempt has been made to incorporate any of the more highly developed aspects of four-pole measurement techniques. Later, A Olina and Altschules [23] published a method, in which they developed a relation between the dielectric constant and the determinant representing the admittance of the dielectric sample. This the measuring procedure has been reduced to finding the parameters of an equivalent net-work characteri zing it. When the dielctric constant is assumed to be purely real or when loss tangent-tanδ - is so small that can be measured independently, then the equivalent four-pole network may be considered as lossless and "tangent relation method"[26] may be used. If the dielectric sample is dessipative, geometrical method(given by Deschamps[24]) may be applied.

Upto this a brief description on the basic principles of the measuring techniques have been discussed. Main object of this experimental was to determine the electrical properties(dielectric constant and conductivity) of the soil at micro-wave frequencies. A Knowledge of the electrical properties of the earth surface is of considerable importance in Physics and electrical engineering as well as radio-communication. As for example, in radio-communication the electrical properties of the earth enter directly into the design of the transmitting installation. Further, the conductivity and dielectric constant of the ground are dominating factors in determining the effective service area of the broadcasting station, in which the bulk of the communication is effected by the electrical waves travelling along the surface of the earth. Finally, the efficiency of the receiving station is dependent upon the good conductivity of the ground upon which it is erected.

Much pionaeer work in the study of the transmission of electrical waves through earth has been performed. After it has been demonstrated that electrical waves could be transmitted to appreciable distances over the earth's surface attention was devoted by several investigators to the effect of the earth in wireless communication. Sir Oliver Lodge in 1899[25], demonastrated the application of classical electromagnetic theory to this problem, while Brylinsky and W. Burstyan[26] later studied the penetration of alternating currents in to soil and sea water. Confirmation of the fact that the earth played a part in the propagation of wireless waves was provided by the experiment of J.S. Sacho[17] in 1905[17] who found that radiation from a transmitter increased as the areal was raised above the earth's surface.

A mathematical investigation of the propagation of electric waves along the earth's surface was published by A Sommerfied [28] in 1909, and this paper still remains the most complete theoretical treatment of the subject. In order to reduce sommer-field's formulae to numerical quantities, attempts were made to obtain measurements of the conductivity of the soil material at audio frequencies by several workers, notably H. Lowy and K. Uller[29] in 1917[29].

A description of some direct measurement of the electrical properties of soil carried out at radio frequencies was published by J.A. Ratchiffe and F.G.W. White in 1930[30]. In this case the soil under examination formed the dielectric between the plates of cylindrical condenser and resistance of this condenser were measured at various radio-frequencies upto about 4 MC/sec. It has been reported that the apparent dielectric constant of the soil would decrease with the increase of frequency from 40 at 200 KHz to about 12 at 3 MHz under various moisture condition.

1.5 CONTENTS OF THE THESIS (Part-II)

A brief historical review regarding the measurement of the electric properties has been given in the previous section. The methods of measurement depends on various factors such, as, availability of instruments, financial assistance and limitation of "time". Considering all these factors, in this thesis the measurement at the dielectric constant of the soil have performed by two different methods. In the first method namely "The free space propagation method"--electromagnetic waves were transmitted towards a large block of soil sample and the reflected waves were received by a receiver. From the strength of the received signal and a knowledge of the type of polarization of the transmitted signal the effective dielectric constant was measured. The accuracy of the results obtained by this method was very sensitive to the angle of incidence of the transmitted signal, nature of the reflecting surface and accurate determination of the strength of the received signal as well as the polarization of the transmitted wave. In the second method, soil samples were prepared and a part of a wave-guide was loaded with the samples. Then by measuring the strength of the VSWR and the shift in the position of the maxima and minima of the field strength in the unloaded wave-guide section, the dielectric constant was measured. The measurement as performed for soil samples with varying moisture contents and densities. The mathematical theory behind the experiment has also been discussed.

CHAPTER 2

GENERAL SURVEY ON MICROWAVE DIFFRACTION

2.1 <u>INTRODUCTION:</u>

This chapter describes a brief description on the diffraction of electromagnetic waves over natural obstacles and some basic concepts on the diffraction phenomena. The basic concepts of electromagnetic diffraction [redacted] has been developed from optical diffraction theory. Numerical experimental evidences have been established in support of the above diffraction theory, which is known as Hygen's wavelet principle[31]. Although it is often thought that electromagnetic waves travel along the line of sight path but in practice electromagnetic waves propagates some what below this line due to existance of atmospheric refraction. Experiments have shown that waves may reach further into the geometric shadow region which can not be account by the principle of refraction. Hygon's principle explains that phenomena. According to this principle wave reflections do not occur only at one point but from the entire surface of the earth that is electromagnetically illuminated. Wavelets reradiates there in all directions from the multitude of elementary radiation centers of the earth surface, receiving incident electromagnetic wave energy. However, this diffraction phenomena is also dependent on the frequency of radiation as will be discussed later. It is also known that, the longer the wavelength the more pronounced are the diffraction effects, but the less significant are the refraction effects.

2.2 <u>BASIC-CONCEPTS OF DIFFRACTION:</u>

Diffraction is a phenomena accompanying all forms of wave motion, it's effect being more marked as the wavelength relative to the obstacle dimension increases. Diffraction effects differ from refraction effects in as much as ray bending due to refraction may occur in obstructed space. But we deal with variation from straight line course when partially cut off by an obstacle, such as an electromagnetic wave passes near edges of an opening(wedge shaped mountain) or a hole that may cause wave interference. Wave propagation behind the horizon (in the geometric shadow region) may partially due to diffraction.

In optics, it is known from experiment, as well as confirmed by theory, that when a monochromatic light is passed through a narrow operture and then allowed to incident on another screen behind the first one produces a blurred wider image or several bright or dark images of the slit. Such effects can be explained by Huygen's wavelet concept, modified by Fresnel by means of interference between component waves.

2.3 HUYGEN'S WAVELET PRINCIPLE & ITS MODIFICATION BY FRESNEL (INTERFERENCE EFFECT):

According to Chritian Hygens, the wavefront of a wave may be considered to be consists of many point source radiation which may be referred as "wavelet radiators" as shown in fig 1

To establish the proper diffraction theory for electromagnetic radiation, the boundary conditions, as for example when a wave meets another medium, such as at the surface of obstacles, must be satisfied. Again, instead of a single wave function, there are two function namely, that of electric field 'E' and that of magnetic filed 'H' Owing to thes boundary conditions, the wavefront passing through an opening of an obstacle must become perturbed because of what happens at the boundary. This means that at the inner surface of an opaque screen with an aperature, we generally have wave reflections as well as absorptions unless special provisions are met. For the sake of presenting well- known fundamentals, a single wave function W is chosen and it is assumedthat $w = 0$ at the inner surface of the screen and the normal derivatives $\partial w/\partial n = 0$, so that for the surface of an aperture, the wave condition is identical with the incident unperturbed wave. In Fig. 2 point T is taken as a radiation centre of primary surface of spherical waves. The full-line circles are wave crests and the dash circles are the troughs. The full-line outer circle is considered as a wave front containing Hygen's wavlet sources such as A, B, C.

These secondary radiation centers are all on a surface of equal phase Each one of these wavelet centers starts out spherical waves about A, B, and C , so that, wave energy also reaches to portions like point P of the geometrical shadow region. Space point P is a receiption centers of three arriving wave trains. The paths of rays AP, BP and CP are r, r +BB' and r + Cc' if arc AB'C' is a circle with radius 'r' about the center. In Fig. 2 the length r is taken an integral multiple of wavelet λ. This means that the wavelet originating at the Hygen's centere A must cause a wave crest at reception point P. Expressing the path differences BB' and Cc' by d and d', the corresponding phase delays are $\delta = Bd$ and $S = Bd'$ for $\beta = 2\pi/\lambda$. If s were exactly equal to half-wavelength, the crest of train AP would meet a through of the BP wave train at P. For the distance r containing many wavelength, we have the inverse relation $1/r \simeq 1/(r+d)$. Therefore, at reception center P, the arriving A wavelet effect will cencel the arriving B wavelet effect. The field AP can then be due only to the C. Wavelet which for a wave-function w yields, for the initial value W of w,

$$w = \frac{W}{d} \exp i[\omega t - B(r + d)]$$

generally, such ideal conditions do not occur and the three wavelets arriving at point 'p' with their effects also cause wave inferference all along the imaginary plane of reception.

Therefore, as far as the reception effect is concerned, the basis of the Hygens-Fresnel wavelet effect is that we deal not directly with the original source but with a multitude of secondary radiation centers located in the wave front of the primary wave. However, the diffraction is less pronounced around edges as the waves become shorter, but the diffraction effect in many cases cannot be ignored.

2.4: PHYSICAL EXPLANATION OF DIFFRACTION FROM A SHARP EDGE:

(optical-straight edge approximation)- upto this the diffraction phenomena and it's basic concepts have been discussed. In this article, diffraction of electromagnitic waves by sharp edge obstacle will be discussed. The Fig. 3 shows what happens when a plane wave

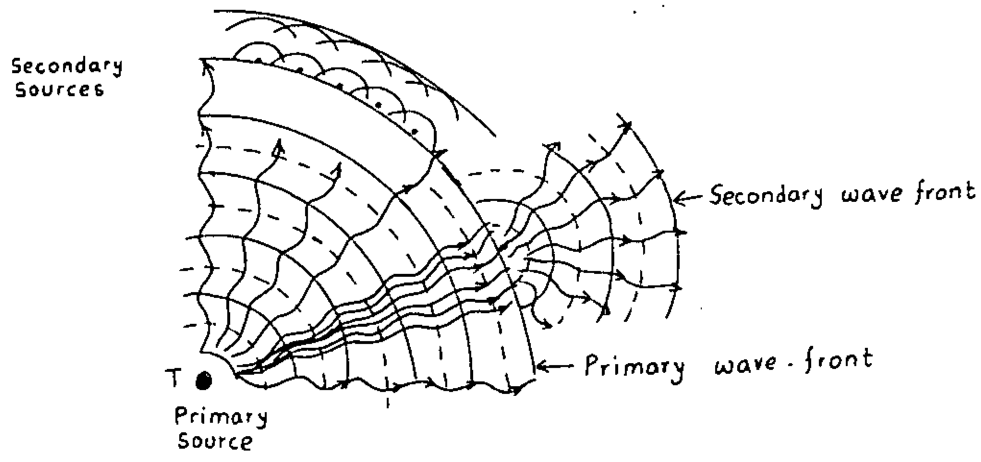

FIG NO. 1 a PRIMARY WAVE EXPANSION & HYGEN'S WAVELET

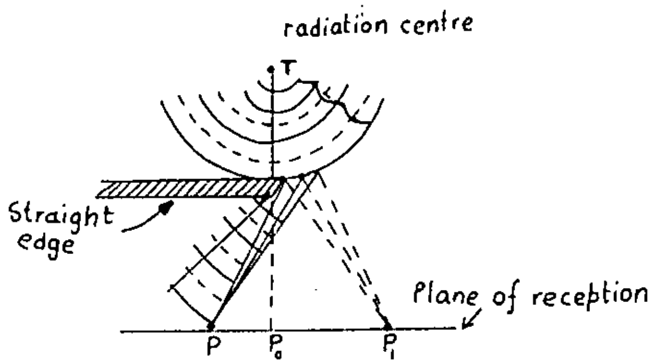

Fig. 1b Figure shows how a primary wavefront ABC originating from the primary source's acts as a multitude of secondary wavelets centers such as A, B & C.

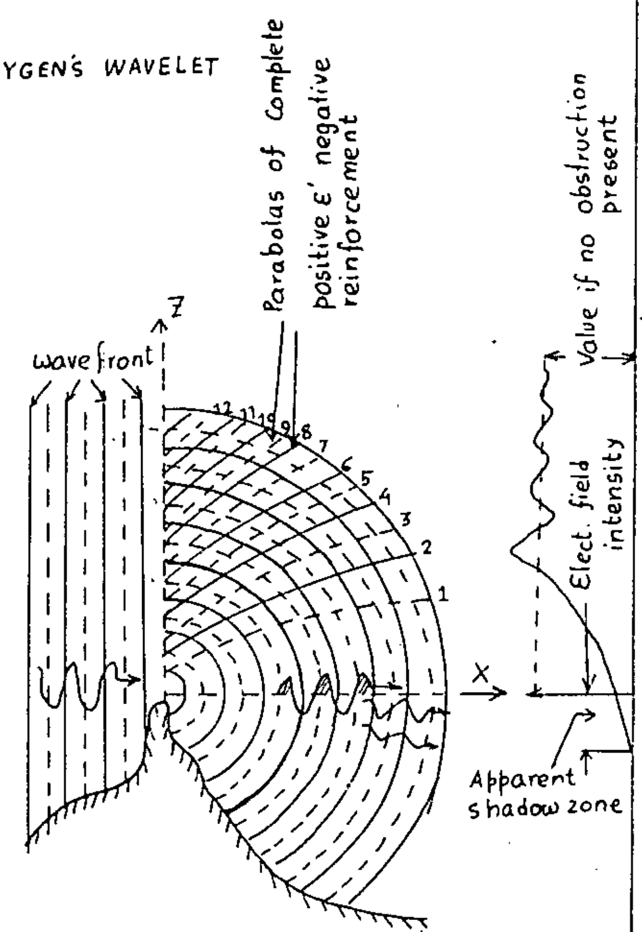

Fig. 1c Electromagnetic diffraction behind a sharp mountain wedge in the geometrical shadow-zone and in the unobstructed zone.

arrives at sharp edge at E normal to the XZ plane. The exaggerated diffraction pattern, whichaccording to sommafield, is a diffraction patten in the geometrical shadow region FG as well as in the unobstructed region FH. This explains the experimental optical obsérvztion that an edge E along Y -axis behaves like a linear light source, emitting cylindrical waves in the ± Z ± Y and ± X directions. The cylindrical wave procees below and behind the edge E, with a 1/ distance law, i.e. a small wave spread amplitude decreases, while in the unobstructed shape above and behind the edge E, wave interference between arriving plane waves and secondary spherical wave occur.

As a result the diffraction extends below and above the edge E. The wave spreads into the region below the E edges refers to a portion of the geometric shadow zone. The interference pattern between c ylindrical and plane wave yields paralolas. The maximum and minimum effects are represented by full drawn and dash -dash parabolas respectively. The waves radiated by the edge E decreases with 1/ distance. While there can be no space attenuation for the arriving plane waves, since there is no spread. The inverse squar - root law holds along a path of fixed diffraction but the amplitude does not change when the interference pätterns moves along the parabolic path, because the decrease of the angle of diffraction just off-sets the camplitude decays and causes an amplitude increases. The energy pattern as well either side of the edge can be explained by means of cornuspiral, as well as by Fresnel integrals.

2.5: MATHEMATICAL FORMULATION:

The basic idea of the Hygen - Fresnel theory is that the light disturbance at a point P arise from the superpostion of secondary waves proceed from a surface situated between this point and the light source. This concept is used in the electromagnetic diffraction phenomenon. This idea was put on a sounder mathematical cbasis by kirchoff, who showed that the Hygen's-Fresnel principle may be regarded as an approximate form of a certain integral theorem which expresses the solution of the homogeneous wave, equation of an arbitrary point in the field, in terms of the values of the solution and it's first derivations at all points on an arbitrany closed surface surrounding point P. At first considering a monochromatic wave,

$$V(x,y,z,t) = U(x,y,z)\, e^{-jwt} \quad \ldots\ldots\ldots\ldots\ldots\ldots\ldots (2.1)$$

In vacuum the space dependent part satisfies the time independent wave equation,

$$(\nabla^2 + R^2)\, U = 0 \quad \ldots\ldots\ldots\ldots\ldots\ldots\ldots (2;2)$$

where, $k = w/c$,

Eq- 2.2 is known as " Helmholtz" equation.

Let V be the volume bounded by a closed surface S; and let P be any point within it as shown in Fig. 4. We assume that U posses continuous first and second-order partial derivatives within and on this surface. Let U' is any other function which satiesfies the same continuity requirements as U, we have by greer's theorem;

$$\iiint_V (U \nabla^2 U' - U' \nabla^2 U)\, dv = -\iint_S \left(U \frac{\partial U'}{\partial n} - U' \frac{\partial U}{\partial n} \right) ds \quad ..(2.3)$$

where $\partial/\partial n$ denotes differentiation along inward normal to S. In particular, if U' also satisfies the time-dependent wave equation i.e. if,

$$(\nabla^2 + k^2)\, U' = 0.$$

the it follows at once that integrand on the left of eq. 2.3 vanishes at every point of V and consequently, *

$$\iint_S \left(u \frac{\partial u'}{\partial n} - u' \frac{\partial u}{\partial n} \right) ds = 0$$

et $u'(x,y,z) = e^{iks}/s$ where 's' is the distance from 'P' to the point (x,y,z). Now serrounding 'P' by a sphere of radius 'ε' nd extending integration between S' and S'' of this sphere we get, $\iint_S + \iint_{S'} \left[u \frac{\partial}{\partial n}\left(\frac{e^{iks}}{s}\right) - \frac{e^{iks}}{s}\frac{\partial u}{\partial n} \right] ds = 0$

ince integral over S is independent of ε, we may replace this integral by the limiting value of the ntegral as $\varepsilon \to 0$. Considering this fact into account and then after simplification the solution is ound as follows, $u(P) = \frac{1}{4\pi}\iint \left\{ u \frac{\partial}{\partial n}(e^{iks}/s) - (e^{iks}/s)\frac{\partial u}{\partial n} \right\} ds$ - - - - - - - - - - - (2.5)

This is known as one form of integral theorem of Helmholtz and Kirchoff. This theorem embodies the basic idea of the Hygen-Fresnel principles, the laws governing the contribution from different

$$* \iint \left(u \frac{\partial u'}{\partial n} - u' \frac{\partial u}{\partial n} \right) ds = 0$$

elements of the surface are more complicated than Fresnel assumed. Kirchoff showed, however, that in may cases the theorem may be reduced to an approximate but much simpler form which is essentially equivalent to the formulation of Fresnel, but which in additon arives an explicit formula for the inclination factor that remained indetermined in the Fresnel theory.

Considering an electromagnetic wave, from a point source P_0 propagated through an opening in a plane opaque screen, and let P' be the point at which the wave disturbance is to be determined, as shown in Fig. 4C.

To find the disturbance at P, the Kirchoff integral over a surface S formed by (eq...1) the opening A (2) a portion B, the non-illuminated side and (3) a portion $\mathcal{C}$ of a large sphere of radius R, centered at P which togather with A, B form a closed surface.

This integral equation become,

$$U(P) = \frac{1}{4\pi}\left[\iint_A + \iint_B + \iint_{\mathcal{C}}\right]\left\{U\frac{\partial U}{\partial n}\left(e^{iks}/S\right)-\left(e^{iks}/S\right)\partial u/\partial n\right\} ds \quad ..(2.6)$$

The difficulty is encountered that the values of U and $\partial u/\partial n$ on A, B, C which should be substituted in the above expression is never known exactly, However, it is reasonable to suppose that every where on A, except in the immediate vicinity of the rim of the opening, U and $\partial u/\partial n$ will not appreciably differ from the vvalues obtained in the absence of the screen and that on B there quantities will be approximately zero, Kirchoff accordingly set,

$$\text{on A}: \quad U = U^{(i)}, \quad \frac{\partial u}{\partial m} = \frac{\partial u^{(i)}}{\partial n}$$
$$\text{on B}: \quad U = 0; \quad \frac{\partial u}{\partial n} = 0 \quad ....(2.7)$$

where,

$$u^{(i)} = \frac{Ae^{ikr}}{r}, \quad \frac{\partial u^{(i)}}{\partial n} \quad \frac{Ae^{(ikr)}}{r}\left[ik-\frac{1}{r}\right]\cos\,(n,r)$$

The approximate eq. (2.7) are called the Kirchoff's boundary conditions and are the basis of Kirchoff diffraction theory.

Now, it remains to consider the contribution from ths sphe-

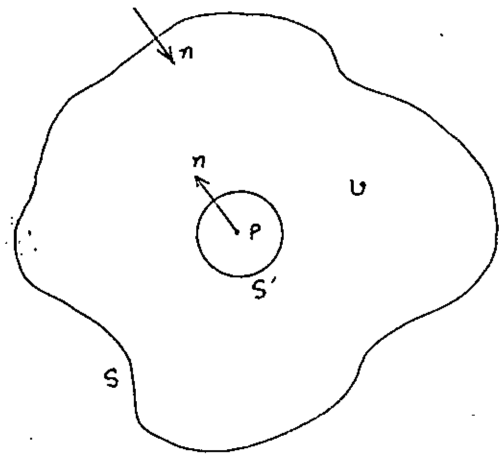

Fig 3 a

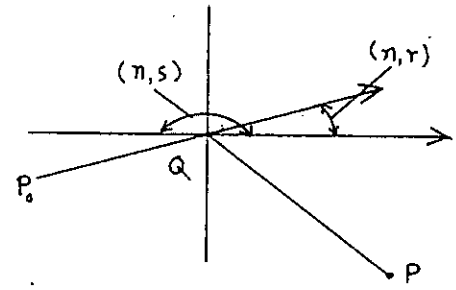

Fig 3 b

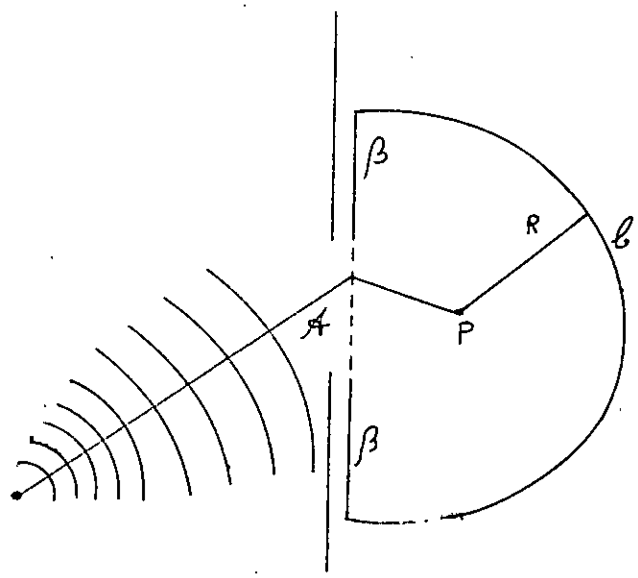

Fig 3 c

DIAGRAM SHOWING THE DIFFRACTION THROUGH THE APPERTURE OF SCREEN rical portion b. However, it may be shown that in the limit of the radius R growing very large, the disturbance at P is considered no contribution from could have reach point P.

Thus finally on substituting in eq. 2.6. and neglecting the normal derivatives of the terms $1/r$ and $1/S$ in comparison with R, we obtain

$$U(P) = -\frac{iA}{2\lambda}\int_{-h}^{\infty}\int_{A\,-\infty}^{\infty}\frac{e^{ik(r+s)}}{rs}\left[\cos(n,r)-\cos(n,s)\right]ds$$

This is known as Fresnel-Kirchoff diffraction theory. In the above case, the diffraction phenomena has been studied, when the wave is passed through an aperture of area A. For diffraction by the sharp-edge conducting half-plane, the surface integration shown above should be extended from the edge of the obstacle to infinity i.e. the complete surface along the half-plane but above the obstacle should be included. If cartesian co-ordinate system is considered, such that Z - axis has along the line of the edge and Y - axis is situated vertically upward, than the above equation for shapr-edged obstacle becomes,

$$U(P) = \frac{-iA}{2\lambda}\int_{-h}^{\infty}\int_{-\infty}^{\infty}\frac{e^{ik(r+s)}}{rs}\left[\cos(n,r)-\cos(n,s)\right]dx\,dy$$

where h represents the distance from the edge of the obstacle to the Z axis of the co-ordinate system.

CHAPTER 3

INTRODUCING THE EFFECT OF ANTENNA DIRECTIVITY IN THE FRESNEL KIRCHOFF DIFFRACTION THEORY

3.1 INTRODUCTION:

The original formulation of the Fresnel-Kirchoff integral equation does not consider the effect of antenna directivity. The transmitting and the receiving antennas are approximated as isotropic radiators. However, for all practical purposes, the results obtained by such approximation agree fairly well with the measurement values. If a very precise evaluation of the received field strength is required then the effect of the directivity of the receiving and the transmitting antenna should be considered. A modification to the original Fresnel-Kirchoff integral is incorporated to account for the directivities of the antennas. Theoretical calculations are made from these modified Fresnel-Kirchoff integral and it was also observed that these results agree more precisely with the practical measurements.

3.2 MATHEMATICAL FORMULATION OF THE PROBLEM:

The basic approach to the problem begins by considering the nature of the standard solution which is known as Fresnel-Kirchoff Integral equation when a sharp knife-edge is placed in between the transmitting and the receiving system, the received power is given[32] by the expression below:-

$$P_R = \frac{P_T}{192000\,\pi^2}\left\{\left[\int_{h}^{\infty}\int_{-\infty}^{\infty} g\left(\sqrt{x^2+y^2}\right)\cos\left(ax^2+ay^2\right)dx\,dy\right]^2 + \left[\int_{-h}^{\infty}\int_{-\infty}^{\infty} g\left(\sqrt{x^2+y^2}\right)\sin\left(ax^2+ay^2\right)dx\,dy\right]^2\right\}$$

where,

$$g\left(\sqrt{x^2+y^2}\right) = \frac{\sqrt{D_T D_R}}{d_T d_R}\left(1+\cos\theta_R\right)\cos^{\frac{1}{2}}\theta_T$$

$$a = \frac{\pi}{173.2}\;\frac{r_T + r_R}{r_T\, r_R}$$

r_T = Distance of the obstacle from the receives.

r_R = Distance of the obstacle from the transmitter.

d_T = Horizontal distance of the obstacle from the receiver.

d_R = Horizontal distance of the obstacle from the transmitter.

θ_T = Angle obtained by the line joining the obstacle and the transmitter with the axis of propagation.

θH =

PR = Received power.

PT = Transmitted power

X = axis = Horizontal axis, along the axis of propagation.

Y - axis = Vertical axis, placed just above the obstacle.

To evalute the values of the above integrals, the function $g(\sqrt{x^2 + y^2})$ was considered to be constant. The integrals were then simplified and the expression involved Fresnel-integral. But in the actual case the function $g(\sqrt{x^2 + y^2})$ does not remain constant. [redacted] For extensive study, the evaluation of the integral may be re-examined. From the fact that all zones in a given family of Fresnel zones have the same area, it may be concluded that all zones contributed equally to the magnitude of a given integral. If there were no variation in $g(\rho)$ with ρ, the expression for P_R would simply oscillate with constant amplitude as the upper limit of integral over was extended to infinity. The monotonic decrease in $g(\rho)$ with ρ prevents this from happening, however, for it causes the oscillation to be damped. The limit to which the aamplitude converges as the oscillation ceases is half the integral over the first zone alone for the same reason that the sum of an infinite geometric alternating series approaches half the first term when the absolute value of it's common ratio approaches unity.

Next, considering the effect of the variation of D_T and D_R with ρ on the integrals. Since, the variation of $g(\rho)$ with θ_T, θ_H d_T and d_R is already such as cause $g(\rho)$ to decrease monotonically with the increasing ρ, it follows that D_T and D_R can effect the integral to an appreciable extent only if their variation occur at small enough ρ_p values so that $g(\rho)$ still has appreciable magnitude. This however, could occur only for antennas having directivity patterns so narrow as to place their entire main lobes within the first

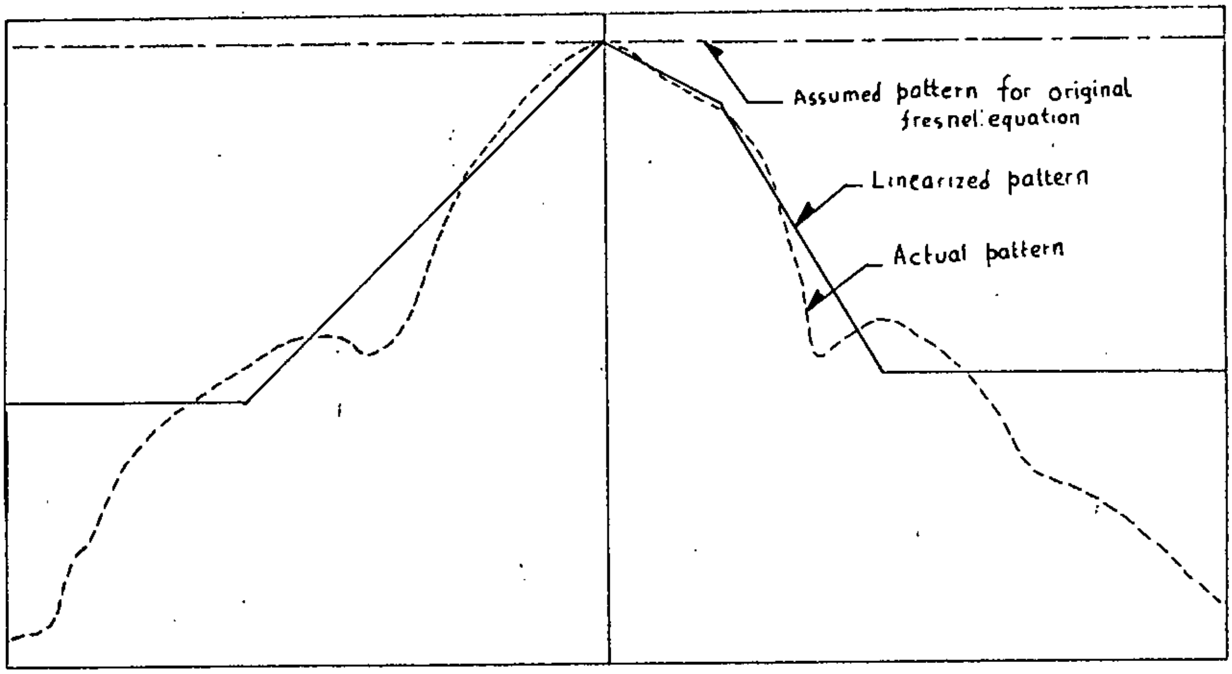

APPROXIMATE PATTERN FOR CASE-I & III
FIG NO. 4a

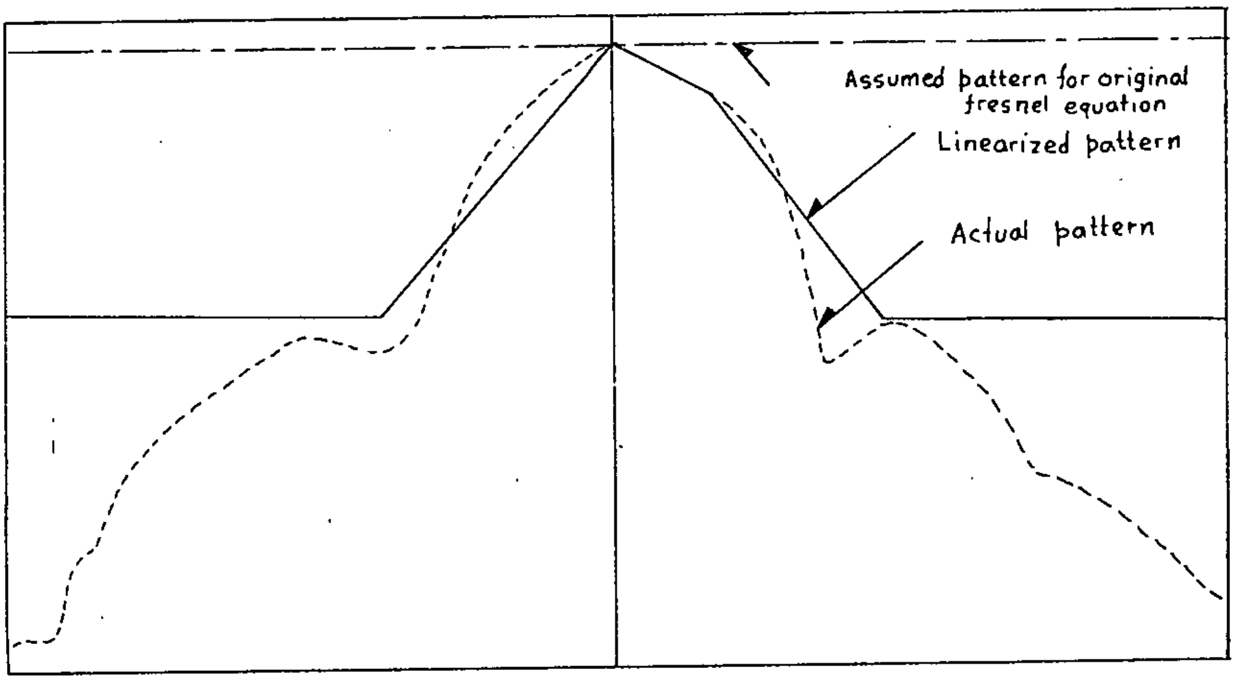

APPROXIMATE PATTERN FOR CASE-II
FIG NO. 4b

few Fresnel zones. As was pointed out earlier that this does not happen with practical antennas in line of sight microwave links. It may therefore be concluded that detailed shape of the directivity patterns of the antennas can influence the received signal only to a minor extent.

In this section, the effect of the variation of D_T and D_R with ρ has been theoretically studied. For this purpose, the directivities of the antennas used in the experiments were considered. The antenna patterns are given in the original hand-book. It was found that the antennas were of high directivities. The antenna patterns are shown in figure (4a). The patterns are approximated and linearized as shown in figure(4b).

From the approximated radiation pattern of the two antennas it was found that variation of the directivity could be assumed to vary linearly with the variation along y-axis, when $-h \leqslant y \leqslant o$ and $o \leqslant y \leqslant y_1$. The slope being considered to be m_{1T} and m_{2T} respectively for the transmitting antenna. For the receiving antenna those (slopes) are m_{1R} and m_{2R} respectively. The rest of the pattern i.e. for $y > y_1$ was assumed to be constant. The directivity at that region was very low and remained more or less same. For this reason there values were neglected. Considering all these factors, the variation of the directivity may be written as follows,

1. For $-h < y < o$

$$\sqrt{D_R D_T} = (D_{oT} + m_{1T} y)^{\frac{1}{2}} (D_{oR} + m_{1R} y)^{\frac{1}{2}}$$

$$= \sqrt{D_{oT} D_{oR}} (1 + m_{1T} y / \sqrt{D_{oT}})^{1/2} (1 + m_{1R} y / \sqrt{D_{oR}})^{\frac{1}{2}}$$

$$= \sqrt{D_{oT}/D_{oR}} + \frac{1}{2}\left(m_{1T}\sqrt{\frac{D_{oT}}{D_{oR}}} + m_{1R}\sqrt{\frac{D_{oR}}{D_{oT}}}\right) y + m_{1T} m_{1R} y^2 / 4\sqrt{D_{oT} D_{oR}}$$

$$\simeq \sqrt{D_{oT} D_{oR}} + K_1 y$$

where $K_1 = \frac{1}{2}(m_{1T}\sqrt{D_{oT}/D_{oR}} + m_{1R}\sqrt{D_{oR}/D_{oT}})$

2. For $o < y < y_1$

$$\sqrt{D_R \; D_T} = (D_{PT} - n_{2T}\, y)^{\frac{1}{2}} \, (D_{PR} - n_{2R} y)^{\frac{1}{2}}$$

$$\simeq \sqrt{D_{PT} \; D_{PR}} - \tfrac{1}{2}\left(n_{2T1} \sqrt{D_{PT}/D_{PR}} + n_{2R}\sqrt{D_{PR}/D_{PT}}\right) y$$

$$+ \left(n_{2T}\, n_{2R} \; / \; 4\sqrt{D_{OT}\, D_{OR}}\right) y^2$$

$$\simeq \sqrt{D_{PT}\, D_{PR}} - K_2 y$$

where, $K_2 = \frac{1}{2}\left(n_{2T}\sqrt{D_{PT} / D_{PR}} + n_{2R}\sqrt{D_{PR} / D_{PT}}\right)$

3. For, $y_1 < y$

$$\sqrt{D_T \; D_R} = \sqrt{D_{3T} \; D_{3T}}$$

These values of D_T and D_R is putted in the original expression. The two integrals are then considered saparately for each region of y.

1. for the region, $-h < y < o$ the expression becomes,

$$\int_{-h}^{o}\int_{-\infty}^{\infty}\left[\frac{c}{r_T \;\; r_R}\left(\sqrt{D_{OT}\, D_{OR}} + K_1 y\right)\right]\cos\left(ax^2 + ay^2\right)\; dx\, dy$$

Let, $\frac{CK1}{r_T \; r_R} = a1$; $\frac{c}{r_T \; r_R}\sqrt{D_{OT} D_{OR}} = a_{o1}$

Hence, the expression becomes,

$$\int_{-h}^{\infty}\int_{-\infty}^{\infty} a_{o1} \;\cos\left(ax^2 + ay^2\right) dxdy + \int_{-h}^{\infty}\int_{-\infty}^{\infty} a_1 y \cos(ax^2 + ay^2)\; dx\, dy$$

$$= \frac{a_{o1}}{a}\sqrt{\frac{\pi}{2}}\,\sqrt{\frac{2\pi}{2}}\left[c(h') - S(h')\right] + \frac{a_1}{2a}\sqrt{\frac{\pi}{2_a}}\left[1 - (\sin ap + \cos ap)\right]$$

$$= \frac{a_1 \pi}{2a}\left[c\,(h') - S(h')\right] + \frac{a_1}{2a}\sqrt{\frac{\pi}{2_a}}\left[1a\;(\sin ap + \cos ap)\right]$$

2. Considering the region $o < y < y_1$

$$\int_{o}^{y_1}\int_{-\infty}^{\infty}\left[\frac{c}{r_T r_R}\left(\sqrt{D_{OT}\,D_{OR}} - K_2\,y\right)\right]\cos\left(ax^2 + ay^2\right)\,dxdy$$

$$= \int_{o}^{y_1}\int_{-\infty}^{\infty}(a_{o2} - a_2\,y)\cos\left(ax^2 + ay^2\right)\,dx\,dy$$

where, $a_{o2} = \frac{c}{r_T\,r_R}\sqrt{D_{OT}\,D_{OR}}$

$$a_2 = \sqrt{\frac{cK_2}{r + r_R}}$$

$$= \int_{o}^{y_1}\int_{-\infty}^{\infty} a_{o2}\cos\left(ax^2 + ay^2\right)\,dxdy - \int_{o}^{y_1}\int_{-\infty}^{\infty} a_2 y\cos\left(ax^2 + ay^2\right)\,dxdy$$

$$= \frac{a_{o2}\,\pi}{2a\,a}\left[c\,(u_1) - s\,(u_1)\right] - \frac{a_2}{2a}\sqrt{\frac{\pi}{2a}}\left[\cos ap_1 + \sin ap_1 - 1\right]$$

3. Lastly in the region, $y_1 < y$, the expression becomes,

$$\int_{y_1}^{\infty}\int_{-\infty}^{\infty}\sqrt{D_{3T}\,D_{3R}}\,\cos\left(ax^2 + ay^2\right)\,dxdy$$

$$= \int_{y_1}^{\infty}\int_{-\infty}^{\infty} a_3\cos\left(ax^2 + ay^2\right)\,dxdy.$$

where, $a_3 = \sqrt{D_{3T}\,D_{3R}}$

$$= \frac{a_3\pi}{2a}\left\{\left[c\,(\infty) - c\,(u_1)\right] - \left[s\,(\infty) - s\,(u_1)\right]\right\}$$

Let us consider the 2nd integral in the original fresnel equation, considering the variation of directivity.

1. For the region $-h < y < o$, the integration becomes;

$$\int_{-h}^{o}\int_{-\infty}^{\infty} a_{o1}\sin\left(ax^2 + ay^2\right)\,dx\,dy + \int_{-h}^{o}\int_{-\infty}^{\infty} a_1 y\sin\left(ax^2 + ay^2\right)\,dxdy$$

$$= \frac{\pi a_{o1}}{2a}\left[S(h') + c(h')\right] + \frac{a_1}{2a}\sqrt{\frac{\pi}{2a}}\left[\cos(ap) - \sin(ap) - 1\right]$$

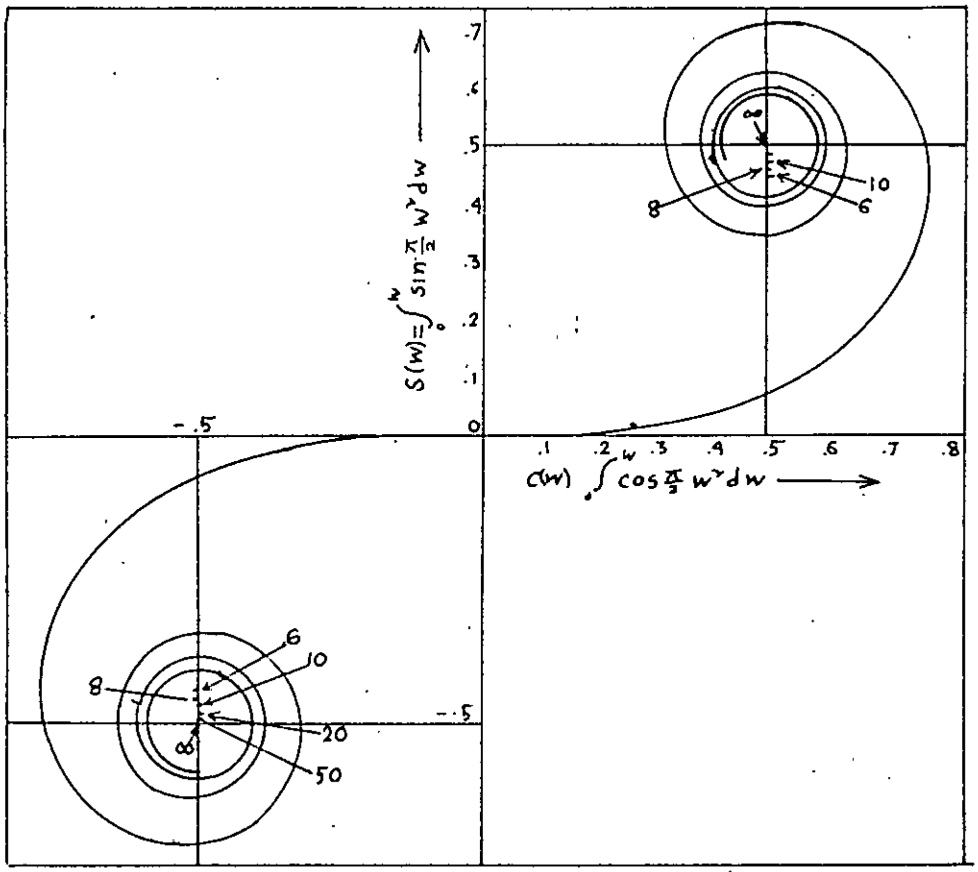

CORNU SPIRAL SHOWING THE VALUES OF THE INTEGRALS

FIG NO. 5

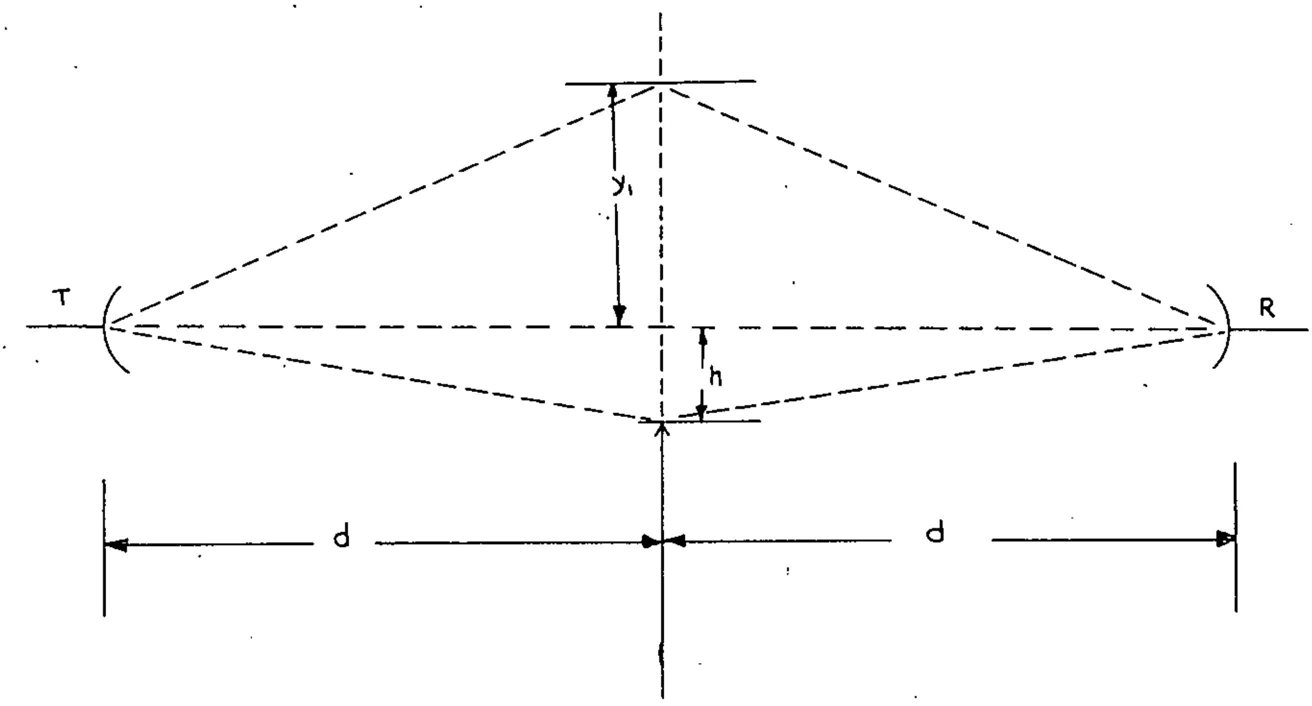

FIG NO. 6

Schematic diagram showing knife-edge diffraction (case-I)

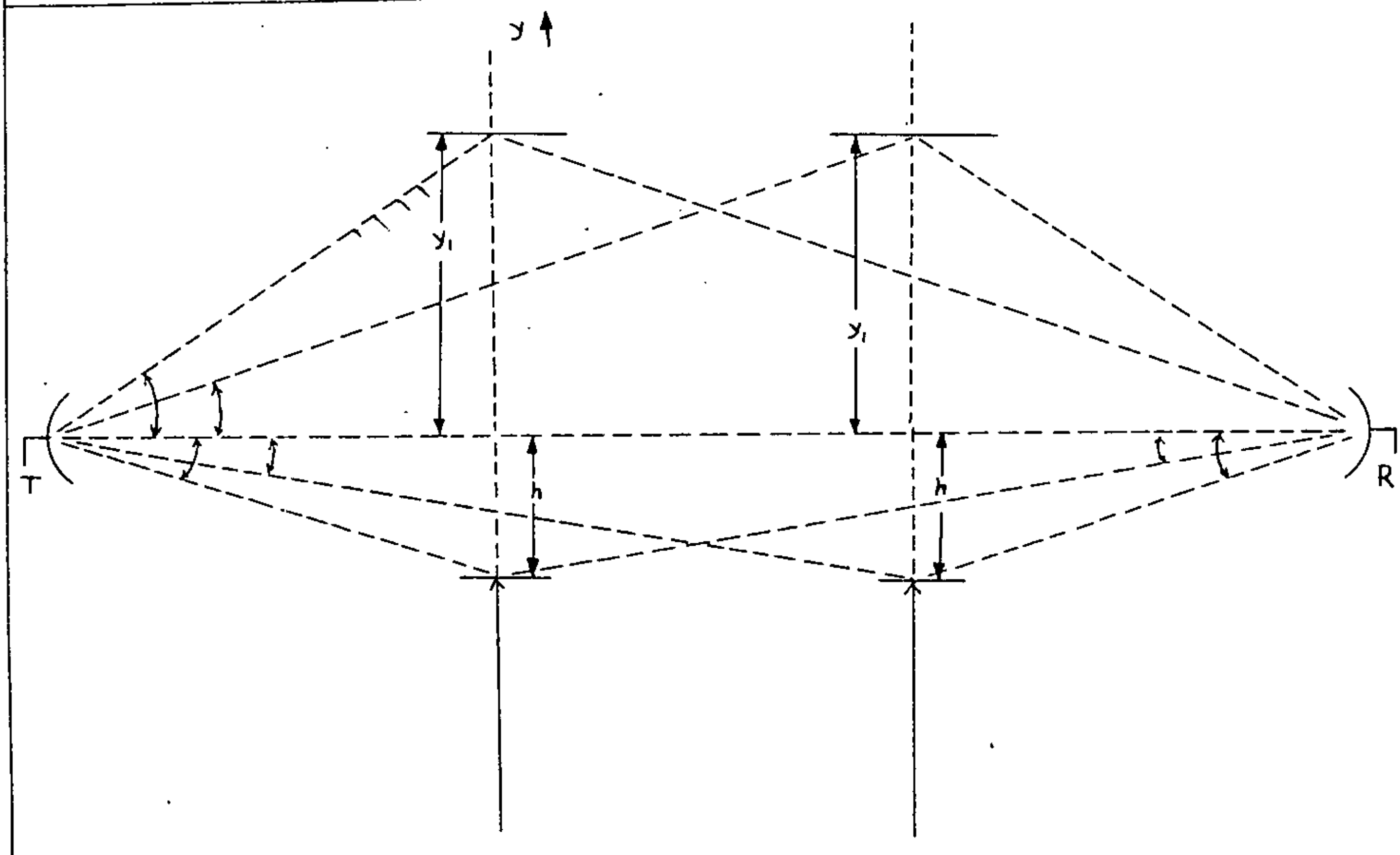

FIG NO. 7

Schematic diagram showing Knife edge diffraction (case I & III)

2. Next for the region $0 \leqslant y \leqslant y_1$

$$\int_0^{y_1}\int_{-\infty}^{\infty} a_{01} \sin (ax^2 + ay^2) \, dxdy + \int_0^{y_1}\int_{-\infty}^{\infty} a_1 y \sin (ax^2 + ay^2) \, dxdy$$

$$= \frac{a_{01}\pi}{2a} \left[s (y_1') + c (y_1') \right] + \frac{a_1}{2a}\sqrt{\frac{\pi}{2a}} \left[1 + \sin ap_1 - \cos ap_1 \right]$$

Where, $y_1' = \sqrt{a}\, y_1$

$p_1 = y_1^2$

3. Lastly for the region, $y_1 \leqslant y \leqslant \infty$

$$\int_{y_1}^{\infty}\int_{-\infty}^{\infty} a_3 \sin (ax^2 + ay^2) \, dxdy$$

$$= \frac{a_3\pi}{2a} \left[\left\{ S(\infty) - S(y_1') \right\} + \left\{ c(\infty) - c(y_1') \right\} \right]$$

3.3 NUMERICAL SOLUTION:

Case- I:

At first the numerical values of the slopes n_{1T} and n_{2T} is to be found. From the radiation pattern of the antenna, it is seen that, the radius of the first fresnel zone produces an angle of 6.2°($\tan^{-1} \frac{9.78}{91} = 6.2^\circ$ where $F_1 = 9.78$") and at that angle the directivity of the antenna is 4 db less than that of along the main axis.

Let, X_1 be the db reading along the main-axis

$(X_1 - 4)$ " " " " Ist fresnol

Let, X_1 Corresponds to P_1 watts of power

$(X_1 - 4)$ " " P_2 " " "

So, $X_1 = 10 \log P_1$

$X_1 - 4 = 10 \log P_2$

or $4 = 10 \log (P_1 / P_2)$

or $P_2 / P_1 = 10^{-.4}$

$$D_T = D_{OT} + n_{1T}(-h)$$

$$\text{or,} \quad n_{1T} = \frac{1 - 10^{-.4}}{h} \quad \frac{1-.4}{.823} = .73$$

Similarly n_{1R} is the slope where the receiving antenna produces such an angle at the first fresnel zone, the angle is found to be, $\tan^{-1} \frac{9.78}{251} = \tan^{1} .039 = 2.2^{\circ}$

Here the directivity is 1.5 db below ;

$$\text{hence,} \quad n_{1R} = \frac{1 - 10^{-15}}{.823} = \frac{1 - .694}{.823} = .37$$

Now, the directivity at the transmitting and receiving antenna at a distance y_1 is 7 db below, than the directivity at the main-axis.

$$\text{Hence,} \quad n_{2T} = \frac{1-10^{-.7}}{y_1} \quad \text{where}$$

$$= \frac{.8}{1.33}, \quad \frac{y_1}{91} = \tan 10^{\circ} = .176$$

$$= .606 \qquad \text{or } y_1 = 1.33 \text{ ht.}$$

Similarly, for n_{2R} ;

$$\frac{y_1}{251} = \frac{1.33 \times 12}{251} = .065$$

$$\text{or } \tan^{-1} .065 = 3.7^{\circ}$$

i.e. 2 db below the main axis.

$$\text{So,} \quad n_{2R} = \frac{1-10^{-.2}}{1.33} \quad \frac{.33}{1.33} = .28$$

Let us calculate the values of K_1 and K_2

$$K_1 = \tfrac{1}{2}\left(n_{1T}\sqrt{\frac{D_{OR}}{D_{OT}}} + n_{1R}\sqrt{\frac{D_{OT}}{D_{OR}}} \right)$$

$$= \frac{1}{2} (.7 + .73) = .55$$

$$K_2 = \frac{1}{2} \left(n_{2T}\sqrt{\frac{D_{OR}}{D_{OT}}} + n_{2R}\sqrt{\frac{D_{OT}}{D_{OT}}} \right)$$

$$= \frac{1}{2} (.28 + .606) = .443$$

Now, $$a = \frac{\pi}{173.2 \lambda} \quad \frac{r_T + r_R}{r_T \, r_R}$$

$$= \frac{\pi \times 5280 \times 12 \times 342}{173.2 \times 3.75 \times 251 \times 91} = 4.59$$

$$y'_1 = y\sqrt{\frac{2a}{\pi}} = 1.33 \times 1.709 = 2.56$$

$$h' = h\sqrt{\frac{2a}{\pi}} = .823 \times 1.709 = 1.40$$

$$h^2 = p, \quad y^2 = p_1$$

$$\frac{a_0 2\pi}{2a} = .428 \times 10^{-2} ; \quad \frac{a_1}{2a}\sqrt{\frac{\pi}{2a}} = \frac{\sqrt{2\lambda}\, K_1}{r \quad r_T \, r_R} = 1.83 \times 10^{-5}$$

$$- \frac{a_2}{2a} = \gamma \frac{-}{2a}$$

$$\frac{a_3 \pi}{2a} = (.428 \times 10^{-3})$$

Putting these values in the previous expression derived. The first integral is as follows;

a) For, $-h \leq y \leq o$

$$.428 \times 10^{-2} \left[c(h') - s(h') \right] + 1.83 \times 10^{-5} \left[-1(\sin ap + \cos ap) \right]$$

$$= .428 \times 10^{-2} \left[.55 - .71 \right] + .71 + 1.83 \times 10^{-5} \left[1 - (\sin 3.1 + \cos 3.1) \right]$$

$$\simeq -.068 \times 10^{-2}$$

b) For $o \leq y \leq y_1$

$$.428 \times 10^{-2} \left[c\,(y') - s\,(y') \right] - 1.93 \times 10^{-5} \left[\cos ap_1 + \sin ap_1 - 1 \right]$$

$$= .428 \times 10^{-2} \left[.41-.57\right] - 1.93 \times 10^{-5}\left[\cos 10^{\circ} + \sin 10^{\circ} - 1\right]$$

$$\simeq -.068 \times 10^{2}$$

c) For $y_1 \leqslant y \leqslant \infty$

$$.428 \times 10^{-3}\left[(.5-.57)-(.5-.41)\right]$$

$$\simeq -.068 \times 10^{-3}$$

Next the values of the 2nd integral is evaluted,

For $-h \leqslant y \leqslant o$

a) $$.428 \times 10^{-2}\left[s(h') + c(h')\right] + 1.83\times10^{-5}(\cos ap - \sin ap - 1)$$

$$= .428 \times 10^{-2}\left[.55 + 725\right] + 1.83 \times 10^{-5}\left[\cos 3.1 - \sin 3.1 - 1\right]$$

$$\simeq .539 \times 10^{-2}$$

b) For $0 \leqslant y \leqslant y_1$

$$.428 \times 10^{-2}\left[s(y') + c(y')\right] + 1.93 \times 10^{-5}\left[1 + \sin ap_1 - \cos ap_1\right]$$

$$= .428 \times 10^{-2}\left[.41 + .57\right] + 1.93 \times 10^{-5}\left[1 + \sin 10^{-10} - \cos 10\right]$$

$$\simeq .419 \times 10^{-2}$$

c) For $y_1 \leqslant y \leqslant \infty$

$$.428 \times 10^{-3}\left[(.5-.57) + .5 - .41)\right]$$

$$= .008 \times 10^{-3}.$$

Hence, the value of the total integral becomes,

$$I_1^2 + I_2^2 = \left[(-.068 - .068 - .0068) \times 10^{-2}\right]^2 + \left[(.539 + 419) \times 10^{-2}\right]^2$$

$$= .02 \times 10^{-4} + .918 \times 10^{-4}$$

$$= .938 \times 10^{-4}$$

So, the expression for received power becomes,

$$P_R = c\,(I_1^2 + I_2^2)$$

Where 'C' is a constant to be evaluted. Since, it was not possible to find the mismatching of the system, So, the effect of this mismatching is to be considered in the value of C. which should be same for both case(received power with and without the knife-edge), The reading was taken with the knife-edge removed and all other conditions remaining same. It was found to be 23.6 db. From the calibration of the I.F. amplifier shown in Fig-33, it corresponds to .00092 mw i.e. .92 μw. Now, the expression for received power is,

$$P = 2c\left(\frac{\lambda}{r}\right)^2 \left[S(\infty) \quad s + (\infty)\right]^2 + \left[c(\infty) + c(\infty)\right]^2$$

$$\text{or} \quad c = 2 \times c \times (.428 \times 10^{-2}) \times 2$$

$$\text{or} \quad c = \frac{.00092}{4 \times (.428 \times 10^{-2})^2} = 12.56$$

Now, the received power becomes,

$$P = c\left[I_1^2 + I_2^2\right] = 12.56 \times .938 \times 10^{-4} \ \text{mw}$$

$$= 1.178 \ \mu\text{w}.$$

To compare the results with that of the original theory,

$$P_{R_\phi} = c \times 2 \times (.42 \times 10^{-2})^2 \left\{\left[c(\infty) + (h')\right]^2 + \left[s(\infty) + s(h')\right]^2\right\}$$

$$= 1.20 \ \mu\text{w}$$

Experimentally the received power was 1.16 μ w.

Case - II:

Let us consider the case when the knife-edgeobstacle was placed at the centre i.e. $r_T = r_R = 171"$

From the Fig-3 it is seen that,

$$\tan\theta_T = \tan\theta_R = \frac{h}{r_T} = \frac{11.13}{171} = .065$$

where, $h = F_1 = \sqrt{\dfrac{r_T\, r_R}{r_T + r_R}} = 11.13 = .93$ ft.

i.e; $\theta_T = \theta_T = \theta_H \simeq 3.75^\circ \simeq 4^\circ$

From , the linearized pattern it is found to be 2 db below than the gain at the main-axis;

$$\text{Hence } n_{1T} = n_{1R} = \frac{1 - 10^{-.2}}{.93} = .399$$

'y_1' is the distance such that the angle ,

$\theta_H = \theta_T = 10.5^\circ$. Hence, from the radiation pattern

$$n_{2T} = n_{2R}\ \frac{1 - 10^{-.8}}{y_1} \quad ; \tan 11^\circ = .185 = \frac{y_1}{171}$$

$$= \frac{.84}{2.64} = .319 \qquad \text{or, } y_1 = 2.636 \text{ ft.}$$

now, to find the value of D_3, as previously from the radiation pattern is 18 db below,

$$\text{So, } \frac{P_1}{P_3} = 10^{1.8}$$

$$\text{or, } D_3 = 10^{-1.8} = .159$$

From these results, the following constant may be calculated as follows:

$$K_1 = \tfrac{1}{2}\,(n_{1T} + n_{1R}) = .399$$

$$K_2 = \tfrac{1}{2}\,(n_{2T} + n_{2R}) = .319$$

$$a = \frac{\pi \times 5280 \times 12 \times 342}{173.2 \times 3.75 \times 171 \times 171} = 3.58$$

$$h' = h\sqrt{\frac{2a}{\pi}} = .93 \times 1.15 = 1.4$$

$$y' = 2.636 \times 1.51 = 400$$

Now, the numerical results of the Ist integrals becomes,

For $-h \leqslant y \leqslant 0$

a) $.428 \times 10^{-2}[c(h') - s(h')] + 1.83 \times 10^{-5}[1-(\sin ap+\cos ap)]$

$= .428 \times 10^{-2} [.55 - .71] + 1.83 \times 10^{-5} [1- (\sin ap + \cos ap)]$

$\simeq - .068 \times 10^{-2}$

b) For $o \leqslant y \leqslant y_1$

$.428 \times 10^{-2} [c(y') - s(y')] - 1.93 \times 10^{-5}[(\cos ap_1 + \sin ap_1 - 1)]$

$= .429 \times 10^{-2} [.5 - .45] - 1.93 \times 10^{-5} [\cos ap_1 + \sin ap_1 - 1]$

$\simeq .02 \times 10^{-2}$

c) For $y_1 \leqslant y \leqslant \infty$ $\quad \frac{a 3\pi}{2a} = .766 \times 10^{-3}$

$.766 \times 10^{-3} (.5 - .5) - (.5 - .45)$

$= -.06 \times 10^{-3}$

Similarly the value of the 2nd integral becomes;

a) For $-h \leqslant y \leqslant o$

$.428 \times 10^{-2} [s(h') + c(h')] + 1.83 \times 10^{-5}[\cos ap - \sin ap - 1]$

$= .428 \times 10^{-2} [.55 + .71] + 1.83 \times 10^{-5} [\cos ap - \sin ap - 1]$

$= .539 \times 10^{-2}$

b) For $o \leqslant y \leqslant y_1$

$.428 \times 10^{-2} [c(y') + s(y')] + 1.93 \times 10^{-5}(1+\sin ap_1 - \cos ap_1)$

$= .428 \times 10^{-2} [.5 + .45] + 1.93 \times 10^{-5} (1+\sin ap_1 - \cos ap_1)$

$= .406 \times 10^{-2}$

c) For $y_1 \leqslant y \leqslant \infty$

$.766 \times 10^{-3} [(.5 - .5) + (.5 - .45)] = +.06 \times 10^{-3}$

Now, $I_1^2 = (-.068 + .02)^2 \times 10^{-4} = .0023 \times 10^{-4}$

$I_2^2 = (.539 + .406)^2 \times 10^{-4} = .893 \times 10^{-4}$.

Hence; $I_1^2 + I_2^2 = (.893 + .0023) \times 10^{-4} = .895 \times 10^{-4}$

Now, to find the value of the constant as calculated before. The free-space reading with the obstacle removed was found to be 23.4 db that corresponds to .0008 mw . From this value, the expression become;

$$P_R = 2c\left(\frac{\lambda}{r}\right)^2 \left\{ \left[s(\infty) + c(\infty) \right]^2 + \left[c(\infty) + s(\infty) \right]^2 \right\}$$

$$c = 10.93$$

So, the theoretically received power become,

$$P_R = 10.93 \times .895 \times 10^{-4}$$

$$= .978\ \mu w$$

The calculated received power from the original expression become,

$$P_R = 2c\left(\frac{\lambda}{r}\right)^2 \left\{ \left[s(\infty) + s(h') \right]^2 + \left[c(\infty) + c(h') \right]^2 \right\}$$

$$= 2c \times (.428 \times 10^{-2})^2 \times (.5+.71)^2 + (.5+55)$$

$$= 1.024\ u\ w.$$

Experimentally received power is .97 μw.

Case -III:

In this case $r_T = 251''$ $r = 91''$

From the fig. it is seen that,

$$\tan \theta_T = \frac{9.87}{251} = .039 \qquad \theta_T = 2.24^\circ$$

$$\tan \theta_H = \frac{9.87}{91} = .11 \qquad \theta_H = 6.3^\circ$$

here

$$F_1 = h = 9.87'' = .823\ ht.$$

From the radiation pattern,

$$m_{1R} = \frac{1-10^{-.5}}{.823} = .249$$

$$m_{1R} = \frac{1-10^{-.5}}{.823} = .83$$

To find y_1, let us take K_G $\theta'_H = 12^\circ$

So, $\tan 12^{\circ} = \frac{y_1}{91} = .208$

$y_1 = 18.15'' = 1.52$ ft.

$n_{2T} = \frac{1-10^{-.2}}{1.52} = .244$ (since, $\theta'_T = 4^{\circ}$)

$n_{2R} = \frac{1-10^{-.9}}{1.52} = .57$ (since, $\theta'_H = 12^{\circ}$)

Now, $K_1 = \frac{1}{2}(n_{1T} + n_{1R}) = .539$

$K_2 = \frac{1}{2}(n_{2T} + n_{2R}) = .41$

$\frac{a_1}{2a}\sqrt{\frac{\pi}{2a}} = \frac{K1\sqrt{2\lambda}}{r\sqrt{r_T\, r_R}} = 1.58 \times 10^{-5}$ where $r = r_T + r_R$

$\frac{a_2}{2a}\sqrt{\frac{\pi}{2a}} = 1.202 \times 10^{-5}$, $\frac{a_3\pi}{2a} = (.428 \times 10^{-3})$

As previously,

$h' = h\sqrt{\frac{2a}{\pi}} = .823 \times 1.709 = 1.406$

$y' = 1.52 \times 1.709 = 2.6$

Putting these numerical results in the Ist integral of the expression,

a) $.428 \times 10^{-2}\left[c(h') - s(h')\right] + 1.58 \times 10^{-5}\left[1 - (\sin ap + \cos ap)\right]$

$= .428 \times 10^{-2}\left[.55 - .71\right] + 1.58 \times 10^{-5}\left[1 - (\sin ap + \cos ap)\right]$

$= -.068 \times 10^{-2}$

b) For $0 \leq y \leq y_1$

$.428 \times 10^{-2}\left[c(h') - s(h')\right] - 1.202 \times 10^{-5}(\cos ap_1 + \sin ap_1 - 1)$

$= .428 \times 10^{-2}\left[.4 - .55\right] - 1.202 \times 10^{-5}(\cos ap_1 + \sin ap_1 - 1)$

$\simeq .064 \times 10^{-2}$

c) For $y_1 \leq y \leq \infty$

$.428 \times 10^{-3}\left[(.5 - .4) - (.5 - .55)\right]$

$= .06 \times 10^{-3}$

Similarly for the 2nd integral,

a) For $-h \leqslant y \leqslant 0$

$$.428 \times 10^{-2}\left[c(h') + s(h')\right] + 1.58 \times 10^{-5}(\cos ap - \sin ap - 1)$$

$$= .539 \times 10^{-2} + 1.58 \times 10^{-5}(\cos ap - \sin ap - 1)$$

$$= .539 \times 10^{-2}$$

b) For $0 \leqslant y \leqslant y_1$

$$.428 \times 10^{-2}\left[s(u') + c(u')\right] + 1.202 \times 10^{-5}(-\cos ap_1 + \sin ap_1 + 1)$$

$$= .407 \times 10^{-2} +$$

c) For $y_1 \leqslant y \leqslant \infty$

$$= .428 \times 10^{-3}\left[(5 - .4) + (.5 - .55)\right]$$

$$= .02 \times 10^{-3}$$

From the results calculated above, the values of the Ist and 2nd integrals becomes,

$$I_1 \simeq -(.068 + .064) \times 10^{-2}$$

or $$I_1^2 \simeq .017 \times 10^4$$

$$I_2 = (.539 + .407 - .002) \times 10^{-2}$$

or $$I_2 = .946 \times 10^{-2}$$

or $$I_2^2 = .895 \times 10^{-4}$$

To find the constant 'c', the free-space reading was such that it corresponds to .8 μw .

So,

$$.0008 = 2c\left(\frac{\lambda}{r}\right)^2\left\{\left[s(\infty) + s(\infty)\right]^2 + \left[c(\infty) + c(\infty)\right]^2\right\}$$

or, $c = 10.93$

So, the received power for the modified expression becomes,

$$P_R = c\left(I_1^2 + I_2^2\right) = 10.93 \times 10^{-4}(.895 + .017)$$

$$= .997\ \mu w$$

The received power can be found by using the original Fresnel expression,

$$P_R = 10.93 \times 2\left\{\left[s(\infty) + s(h')\right]^2 + \left[c(\infty) + c(h')\right]^2\right\}$$

$$= 1.24 \ \mu w.$$

Experimentally the received power was .98 μw

TABLE - 1

Exp. No.	Distance from Transmitter r_T	Distance from Receiver r_R	Theore Calculated received power		Experimental values	
			Standard Fresnel Kirchoff theory	Incorporating the effect of directivity	Transmitted Power P_T	Received Power P_R
Case -I	91"	251"	1.2 μw	1.178 μw	8 mw	1.16 μw
Case -II	171"	171"	1.024 μw	.978 μw	8 mw	.97 μw
Case-III	151"	91"	.997 μw	1.240 μw	8 mw	.98 μw

3.4 DISCUSSION:

Main object of this investigation was to study the percentage deviation of the received power between experimentally found values and theoretically calculated values (using original Fresnel -Kirchoff equation and modified Fresnel-Kirchoff equation). A comparison between the two sets of percentage deviations (one is between the experimental values and theoretically calculated results from original Fresnel-Kirchoff equation and the other is between the experimental values and theoretically calculated results from modified Fresnel-Kirchoff equation) gives an idea about the results obtained from the modified Fresnel-Kirchoff equation. From the results shown in the table-1 it is seen that the average deviation of the results obtained from the original Fresnel-Kirechoff expression to that of the experimental results are small. In this case the percentage deviation can be calculated as follows;

$$\text{Error in\%} = \frac{P_{R\,(theo)} - P_{R(exp)}}{P_{R\,(exp)}} \times 100$$

where, $P_{R(Theo)}$ = Theoretically calculated received power

$P_{R(exp)}$ = Experimentally found received power.

From the table ,

Case- I $\quad \mathcal{E}_1 = \frac{1.2-1.16}{1.16} \times 100 = 3.5\%$

Case-II $\quad \mathcal{E}_2 = \frac{1.024-.97}{.97} \times 100 = 5.56\%$

Case-III $\quad \mathcal{E}_3 = \frac{1.024-.98}{.98} \times 100 = 4.48\%$

So , the average error in percent is given by,

$$\mathcal{E}_{av} = \frac{1 + 2 + 3}{3}\% = 4.51\%$$

From the above result it is seen that the percentage deviation is not much for our practical purpose. However, the error should be much less. The scale model technique used was not perfect and as a result the antenna diameter was quite comparable to the first Fresnel radius, As a result, the edge of the first Fresnel zone could not be specified properly. Again, when the antennas have high directive property i.e. when most of the powers are connoentrated in the first few Fresnel zones, then the accuracy fails. The antennas used were of high directive patterns. The percentage error could be improved by avoiding all these difficulties. Next, considering the percentage deviation between the experimental values and theoretically calculated results using modified Fresnel-Kirchoff Theory, it can be seen that the error has decreased much. From the table -1 , the percentage deviation is,

Case- I $\quad \mathcal{E}_1 = \frac{1.178 - 1.16}{1.16} \times 100 = 1.55\%$

Case-II $\quad \mathcal{E}_2 = \frac{.978 - .98}{.98} \times 100 = .82\%$

$$\text{Case- III} \quad \mathcal{E}_3 = \frac{.997 - .98}{.98} \times 100 = 1.72\%$$

The average percentage error is given by,

$$\mathcal{E}_{av} \frac{1 + 2 + 3}{3} = 1.36\%$$

From the above results it is seen that the percentage error has been improved quite appreciably. However, one important point which is to be mentioned here is that, the antenna pattern was considered along X - Y plane only. Due to mathematical complicacy the three-domensional variation of the radiation pattern of the antennas were not considered. However, one can easily guess that the percentage error could be more less if the three dimensional antenna patterns would be considered.

CHAPTER 4

DIFFRACTION FROM MOUNTAINS & BUILDINGS

4.1 INTRODUCTION:

Much has been discussed about knife-edge diffraction of electromagnetic waves. In this chapter a detail discussion on the theoretical and experimental investigation that has been carriedout to study the diffraction phenomena of electromagnetic waves in the presence of a double-knife-edged flat top conducting obstacle will be made. The theoretical approach has been performed by using the concept of four-ray theory. Numerical results were obtained with the help of digital computer (IBM -360).

Main object of this investigation was to study the diffraction of microwaves by skyscrapers in cosmopolitan cities. This was performed in the laboratory by using scale-model technique. A conducting structure having double knife-edge with a flat top has been used as a model of the 'Building Structure'. This technique (scale-model technique) have been developed whereby the effect of various practical obstacles on the propagation of electromagnetic waves over the surface of the earth can be investigated within the laboratory.

The major advantage of the scale-model technique is the ease with which control can be exercised over the pertinent parameters, such as obstacle shape, geometry of the propagation link, frequency, polarization etc. Further more model experiments are relatively inexpensive, considering all these factors, this scale-model techniques have been utilised in this investigation. Detailed theoretical formulation and a complete description of the experiment with the results compared mutually have been discussed in the following section.

4.2 FORMULATION OF THE PROBLEM FOR DIFFRACTION BY MOUNTAIN:

For theoretical formulation of the problem of diffraction by a flat -top double edged obstacle, the basic knife-edge diffraction theory and the diffraction of electromagnetic waves by smooth cylindrical mountains will be reviewed.

4.2a KNIFE-EDGE DIFFRACTION:

The scalar theory of knife-edge diffraction by a conducting

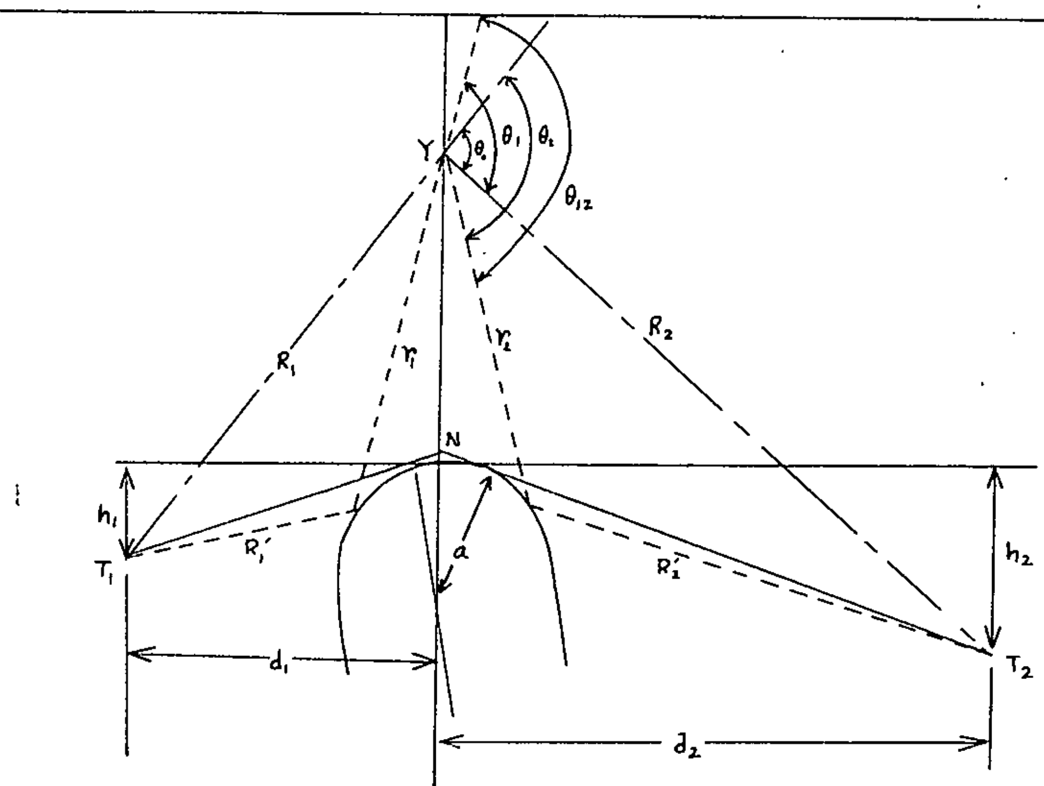

FIG NO. 8

FOUR RAY THEORY FOR MOUNTAIN WITH SMOOTH CREST

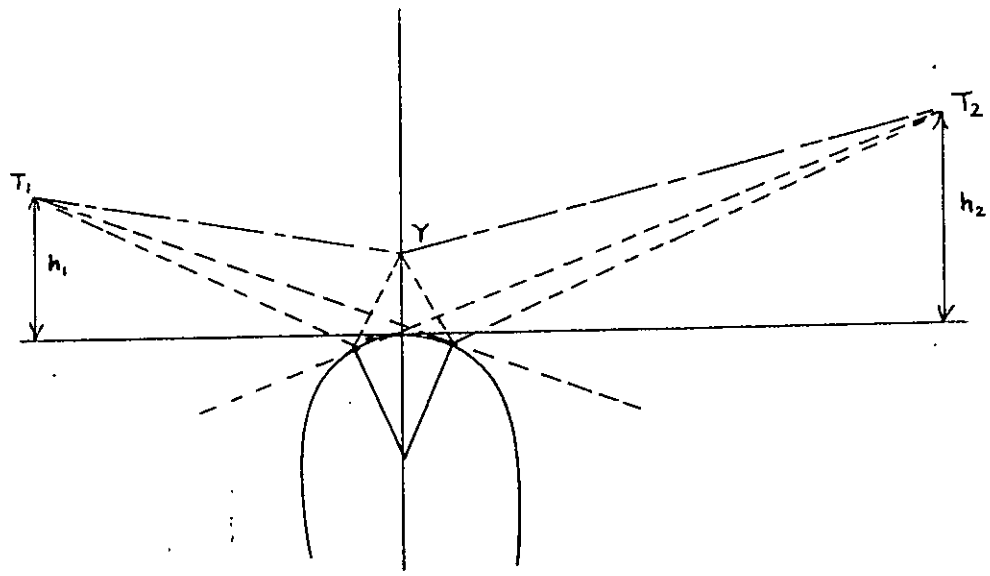

FIG NO. 9

STATION ABOVE THE MOUNTAIN

half-plane is based on ,

$$E = (JK/2\pi) \int_{y=0}^{\infty}\int_{z=-\infty}^{\infty} (1/R_1R_2) \exp\left[-jk(R_1 + R_2)\right] \cos\theta \; dz dy \quad \text{--(4.1)}$$

E is the field at receiver T_2(Fig- 7) when a spherical wave $(1/R_1)\exp\left[-jk(R_1 - Ct)\right]$ is transmitted from T_1. The present treatment differs stightly from the usual one in that the integration is carried out over the half-plane AC which is not in general the continuation of the plane AB of the obstacle. The plane B'AC goes through the edge A of the obstacle and devides angle T_1AT_2 into equal parts.

The scattering angle ψ_1 and ψ_2 has been assumed to be small, so that the following approximation can be considered to be valid.

$$d_1 \simeq D_1, \quad d_2 \simeq D_2$$

Another consequence of the assumption of small scattering angles is that the directional patterns of the transmitter and receives could be neglected in equation 4.1.

The integration with respect to z is carriedout in the usual manner leading to,

$$E = \frac{e^{j\pi/4}}{2d_1d_2}\sqrt{\frac{Kd}{\pi}}\int_0^{\infty} e^{-jk\left[R_1 + R_2\right]}\cos\theta \; dy$$

where, $2/d = 1/d_1 + 1/d_2$

4.2b DIFFRACTION BY CYLINDRICAL MOUNTAIN :

The case of diffraction by a mountain with a smooth crest is illustrated by Fig- 8 and 9 . It is assumed that the mountain (which is drawn like a wall by thickness 2a with parallel sides) is topped by a half-cylinder of radius 'a' with it's axis through point M. The tangents to the cylinder through T_1 and T_2 intersect at N, MANC is the plane of reference and of integration in the same sense as in the knife-edge case. The scattering angle $2\psi_0 \simeq \psi_1 + \psi_2$ is assumed to be small and $d_1 \simeq D_1$, $d_2 \simeq D_2$.

The effects taking place in the case of Fig-8,9 are the following,

1) Radiation travels from T_1 to Y where it acts as a source of secondary wavelet which irradiates T_2. The scattered radiation is exactly the same as in the case of a knife-edge mountain.

2) Radiation travels from T_1 to S_1 and is reflected towards point Y where it causes another secondary wavelet which also irradiates T_2.

3) The radiation from both secondary wavelets mentioned in (1) and (2) is reflected at S_2 to reach T_2 via path YS_2T_2.

Hence there are four different paths along which radiation can travel from T_1 to T_2 viz $T_1 Y T_2$, $T_1S_1YT_2$, $T_1YS_2T_2$ and $T_1S_1YS_2T_2$. The total scattring field at T_2 can be obtained when the integral in equation 4.2 is replaced by the four integrals.

$$E = \frac{e^{J\pi/4}}{2d_1d_2}\sqrt{\frac{kd}{\pi}}\left\{\int_{y_0}^{\infty} \exp\left[-Jk(R_1+R_2)\right]\cos\theta\, dy\right.$$
$$+\rho\int_{y_0}^{\infty} \mathrm{Div}(s_1)\exp\left[-Jk(R'_1+r_1+R_2)\right]\cos\theta\, dy$$
$$+\rho\int_{y_0}^{\infty} \mathrm{Div}(s_2)\exp\left[-Jk(R_1+r_2+R'_2)\right]\cos\theta_2\, dy$$
$$\left.+\rho^2\int_{y_0}^{\infty} \mathrm{Div}(s_1)\,\mathrm{Div}(s_2)\exp\left[-Jk(R'_1+r_1+r_2+R'_2)\right]\cos\theta_{12}\, dy\right\}$$

This equation requires two explanation,

1) The factor indicates change of phase and / or intensity on reflection. It may be shown that for perfect conductor $= +.7$ for vertical polarization and $= -1.0$ for horizontal polarization.

2) The intensity of a beam which is reflected by a curved surface is reduced due it's energy being spread over a wider angle. The divergence factors $\mathrm{Div}(s_1)$ and $\mathrm{Div}(s_2)$ representing these intensity losses for reflections at s_1 and s_2 are given by,

$$\mathrm{Div}(s_i) = 1\Big/\sqrt{1 + \frac{2\sec\alpha_i}{a(1/R'_i + 1/r_i)}}$$

Where α_1 and α_2 are the angles of incidence.

4.3 DIFFRACTION BY SKYSCRAPERS USING SCALE MODEL TECHNIQUE:

4.3a FORMULATION OF THE PROBLEM:

So far, the diffraction by a mountain with smooth cylindr-

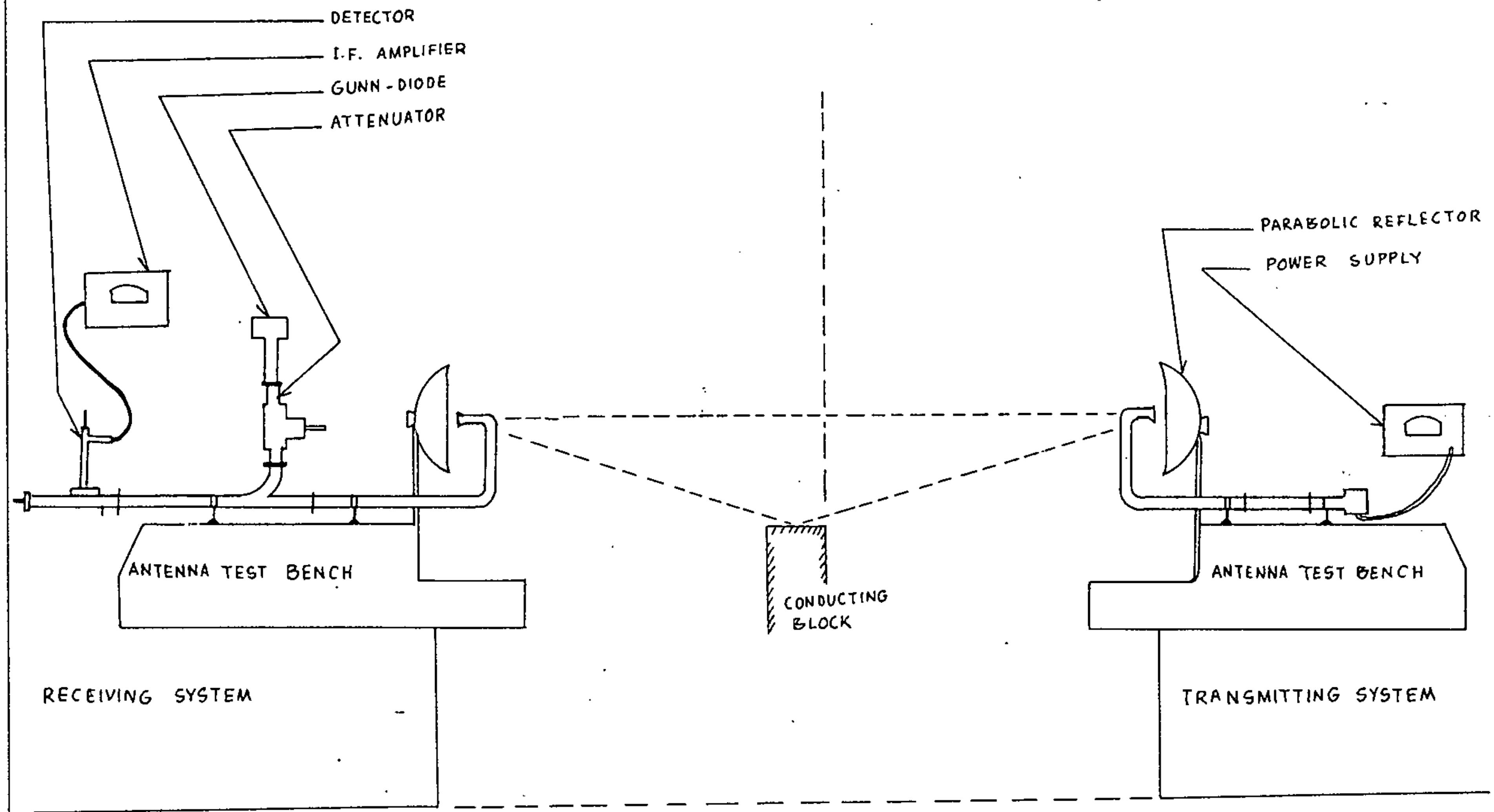

FIG NO. 10

EXPERIMENTAL SET UP FOR DIFFRACTION MEASUREMENT DUE TO CONDUCTING BLOCK

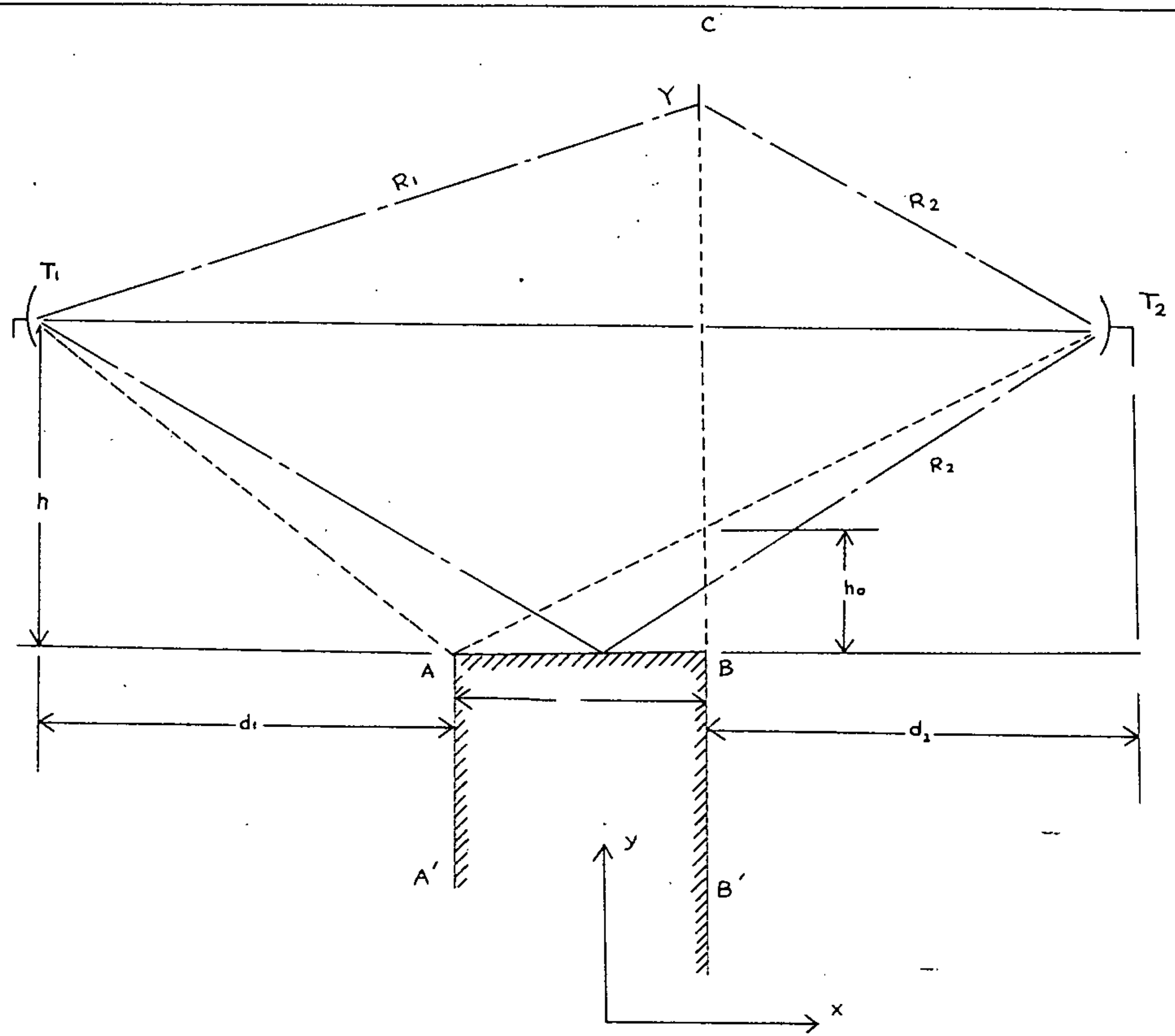

FIG NO. 11

SCHEMATIC DIAGRAM OF DIEFRACTION DUE TO A CONDUCTING OBSTACLE

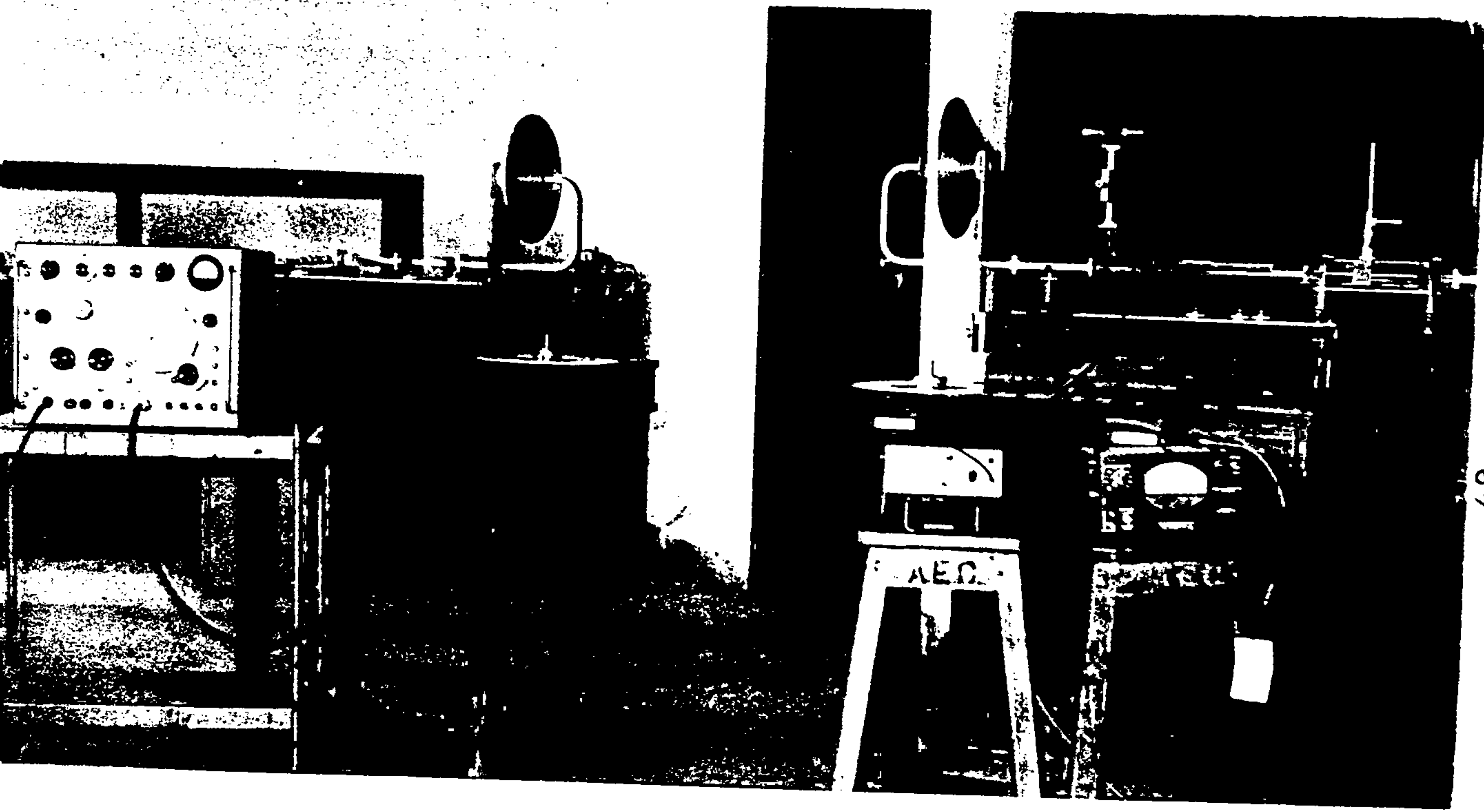

Experimental Setup for studying 'Diffraction Phenomena' ical crest have been discussed. The diffraction by the above mentio ned conducting obstacle(a model structure of building) will be discussed now. The fig-10 illustrate the diffraction phenomena. It is assumed that the conducting obstacle has two edges with a flat top surface between them. The length of the flat top surface being infinitely extended along the plane passing between the transmitter and receiver system. The width being four inches i.e. the edges may be considered to be separated by four-inches distance(about four λ).

The conducting obstacle has two vertical sides e.g. the surface A A', B B'. The plane Y BB' lying along the surface BB' had been assumed to be the plane of reference and of integration in the same sense as in the knife-edge case. The scattering angle was assumed to be small i.e. $d_1 \simeq D_1$; $d_2 \simeq D_2$.

The effects taking place can be explained as below, from Fig-10,11

1) Radiated wave travels from the transmitter T_1 to Y (the point is on the plane of reference) where it acts as a source of secondary wavelets which irradiates T_2. This scattered radiation is similar to case of a diffraction cause by a knife-edged obstacle.

2) The radiation travelling from the transmitter T_1 towards the edge A is diffracted by the edge, where it acts as a source and irradiates the reference surface YBB' .Here, again they act as Hygen's sources that irradiates the receiver T_2.

3) In the third case, the radiation travels from T_1, towards the flat top surface of the obstacle. The wave is reflected and acts as a secondary source lying in the plane of reference. These secondary wavelets than irradiates the receiver T_2.

Hence, the three different paths along which the radiation can travel from T_1 to T_2 are as follows,

(1) $T_1 Y T_2$, (2) $T_1 A Y T_2$ (3) $T_1 XS T_2 [-h$ to $-(h-h_o)]$

From the above four-ray concept and the ray paths as described, the expressions for received electric field can be written as similar to the previous case(diffraction by smooth cylindrical mountain)). However, it will be shown later that the contribution for the rays travelling along the path $T_1A\ YT_2$ will be negligible. The detail analysis of this approximation will be given later. So, under the above assumptions the integrals can be written as follows,

$$E = \frac{e^{j\pi/4}}{2d_1\ d_2}\sqrt{\frac{kd}{\pi}}\left\{\int_{-h}^{\infty}\exp\left[-jk\ (R_1+\ R_2)\right]\cos\theta_0 dy + \rho\int_{-h}^{-(h-h_0)}\exp\left[-jk\ (\ r'_1+r'_2+\ R_2\ )\right]\ \cos\theta_2\ dy\right\}$$

In the above expression the diffraction from the edge at A has been neglected. This approximation can be explained from the 'energy' point of view. In the ideal case, the edge at A is a straight line along the z-axis. The power that is diffracted by the edge A must be less than the incident power at the edge. Again the incident power depends on the surface area on which the power is being incident. In the limit, the edge at A is a straight line, the total incident power will also very small. Hence, the diffracted power will be much less. Considering the above mentioned fact, the diffraction due to this edge will be neglected.

The first integral represents the scattered field at T_2, due to the diffraction by the edge at B and due to waves propagated through the unobstructed region.

The 2nd integral requires some explanations. This integrals represents the field at the receiver, for the rays those are reflected by the flat-top surface of the obstacle. The factor ρ indicates change of phase and/or intensity on reflection. For a perfect conductor $\rho= +.7$ for vertical polarization(electric vector perpendicular to the flat top surface) and $\rho= -1.0$, for horizontal polarization(electric vector parallel to the flat top surface).

The limit of the integration has been imposed from $(-h)$ to $-(h-h_0)$. The justification of this limit may be explained as follows. The plane of reference on which the "Hygen's source has been considered is the plane YBB'. The ray coming from the transmitter T_1 and incident on the flat-surface at the point just to the next of the edge A will be reflected and appears at the point 'P' on the reference plane. Here, this can be considered to be a secondary wavelet which irradiates receives T_2 . The rest of the rays incident on the flat conducting surface and than reflected by the surface also serve as a secondary wavelet on the reference plane that irradiates the receives T_2. But all these points are below the point 'P' .Hence the sources that have been appeared in the plane YBB' due to the reflection from the flat-top surface must lie below the point P. So, the limit of the integration should be confined from $-h$ to $-(h-h_o)$ where $BP = h_o$.

To express the integrand in term of variable y only, let us consider a general case. Let a ray from T_1 incident on the flat-top surface at a point X(Fig. 11,) and is reflected by the surface. It acts as a Hyger's source at point S from which the secondary wavelets irradiates the receiver T_2. The ray traversed along the path r'_1 and r'_2. The point X is at a distance x from the point B. From the above discussion the following relation can be written fig- 11.

$$r'_1 = \sqrt{(d_1 + d - x)^2 + h^2}$$
$$r'_2 = \sqrt{x^2 + (y + h)^2}$$

The relation between x and y can be found as follows at the point X,

$$\frac{d_1 + d - x}{h} = \frac{x}{h + y}$$

$$\text{or,} \quad \frac{d_1 + d - x}{x} = \frac{h}{h + y}$$

$$\text{or,} \quad x = \frac{h + y}{2h + y} (d_1 + d)$$

4.3b: <u>TRANSFORMATION OF INTEGRALS:</u>

The first integral of the equation may be evaluted as in the knife-edge case. The behavior of this integral may be analysed. It is seen that at large values of 'Y' the exponent oscillates very rapidly Again at higher values of y the angle cos Θ increases very sharply. So, we may expect that main contribution of the integral comes from small values of Y. Under this approximation the path length R_1 and R_2

can be approximated to be $(d + d_1 + y^2/2(d_1 + d))$ and $(d_2 + y^2/2d_2)$. But this approximation can not be permitted in the second integral. Here the path length $r_2 = \sqrt{d^2 + (y + h)^2}$ can not be approximated as before. Since, main contribution of the integral comes from small values of y, at which values $(y + h)$ is quite comparable to that of 'd', So, the evalution becomes difficult.

Again, as in all the integrals, main contribution of the integrals comes from small value of y, so the consine term can be neglected.

For, the problems encountered in the evalution of the integrals, the expression have been solved with the help digital computer(IBM-360).

Under the approximation assumed above, the final expression can be written as follows,

$$R_1 = \sqrt{(d_1 + d)^2 + y^2} \simeq (d_1 + d) + y^2/2(d_1 + d)$$

$$R_2 = \sqrt{d_2^2 + y^2} \simeq d_2 + y^2/2d_2$$

$$r_1 = \sqrt{d_1^2 + h^2}$$

$$r'_1 = \sqrt{(d_1 + d - x)^2 + h^2}$$

$$r'_2 = \sqrt{x^2 + (y + h)^2}$$

$$x = \frac{h + y}{2h + y}(d_1 + d)$$

Using the above relations, the final expression for electric-field received at T_2 becomes,

$$E = \frac{e^{j\pi/4}}{2d_1 d_2}\sqrt{\frac{kd}{\pi}}\left\{\int_{-h}^{\infty} \exp\left[-jk\left\{(d_1+d) + y^2(d_1+d) + d_2 + y^2/2d_2\right\}\right]dy\right.$$

$$+\rho \int_{-h}^{-(h-h_0)} \exp\left[-jk\left\{\left[\left(d_1 + d - \frac{h+y}{2h+y}(d_1+d)\right)^2 + h^2\right]^{\frac{1}{2}} + \left[(y+h)^2 + \left(\frac{h+y}{2h+y}(d_1+d)\right)^2\right]^{\frac{1}{2}} + d_2 + y^2/2d_2\right\}\right] dy \quad \text{------ (4·1)}$$

where, h is the radius of the first Fresnel-zone, where the obstacles were placed to determine the obstacle gain.

4.3c NUMERICAL SOLUTION (COMPUTER AIDED):

Since the equation 4.1 can not be put into any standard form so the expresion was solved with the help of digital computer(IBM-360). To compare the results with the experimentally found values, the integrals were evaluted for three different values of h, d_1 and d_2, corresponding to the three positions, where the obstacle was placed during experiment. In eachacase, the obstacle was place at the edge of first Fresnel radius to observe the obstacle gain.

Let us consider the evalution of the first integral of equation 4.1, where the range of integration have been imposed from -h to ∞. Examining the exponential function, it is observed that, due to the presence of the y^2 term, the frequency of oscillation of the function increases as the value of y increases. As a result, the oscillation of the exponential function increases and the function, cramps at higher values of y. For this reason, the exact value of the integral cannot be evaluted with the help of the computer. However, the problem was solved by using graphical method. For the purpose, different values of the integral at higher values of y were printed. When they were plotted with real and imaginary values along two perpendicular axis, cornu-spirals were obtained. Now, the centre of the spiral gives the value of the integral at infinity. Thus the final values of the integrals were obtained from Fig 12 and Fig. 13.

For evaluation of the second integral no such difficulties has arisen, since the limit of integrations were of finite values.

The results of the computer programming have been given below. For completeness a sample computer program for the above problem has been included in the appendix - .

The received power is calculated from the results obtained with the help of digital computer. Three different cases are described separately for three different positions of the obstacle placed between the receiver and the transmitter set;

COMPUTER RESULTS

Numerical results of Ist Integral

d_1 = 247," 87"

d_2 = 291", 251"

Real Values	Imaginary values	Values of Y(in inches)
-0.87345686 E 01	-0.76212530 E 01	30.00
-0.86021433 E 01	-0.73566065 E 01	30.00
-0.83472490 E 01	-0.72064209 E 01	30.60
-0.80518179 E 01	-0.72205257 E 01	30.90
-0.77133141 E 01	- 0.76736755 E 01	31.49
-0.77868052 E 01	-0.79599094 E 01	31.79
-0.80095606 E 01	-0.81539707 E 01	32.09
-0.83031845 E 01	- 0.81858463 E 01	32.39
-0.95614519 E 01	-0.80427322 E 01	32.69
-0.86884985 E 01	-0.77763023 E 01	32.99
-0.86354799 E 01	-0.74860172 E 01	33.29
-0.84214449 E 01	-0.72830057 E 01	33.59
-0.81287308 E 01	-0.72470894 E 01	33.89
-0.78729506 E 01	-0.73936968 E 01	34.09
-0.77576141 E 01	-0.76649189 E 01	34.49
-0.78310251 E 01	-0.79502630 E 01	34.79
-0.80633256 E 01	-0.81307039 E 01	35.09
-0.83582726 E 01	-0.81289730 E 01	35.39
-0.85877361 E 01	-0.79446020 E 01	35.69
-0.86512032 E 01	-0.76572599 E 01	35.99
-0.85193071 E 01	-0.73943233 E 01	36.28
-0.82505379 E 01	-0.72749939 E 01	36.58
-0.79676714 E 01	-0.73550386 E 01	36.88
-0.78027840 E 01	-0.75982933 E 01	37.18
-0.78348341 E 01	-0.78903151 E 01	37.48
-0.80495806 E 01	-0.80906439 E 01	37.78
-0.83429785 E 01	-0.81007566 E 01	38.08
-0.85697737 E 01	-0.79145012 E 01	38.38
-0.86152296 E 01	-0.76246710 E 01	38.68

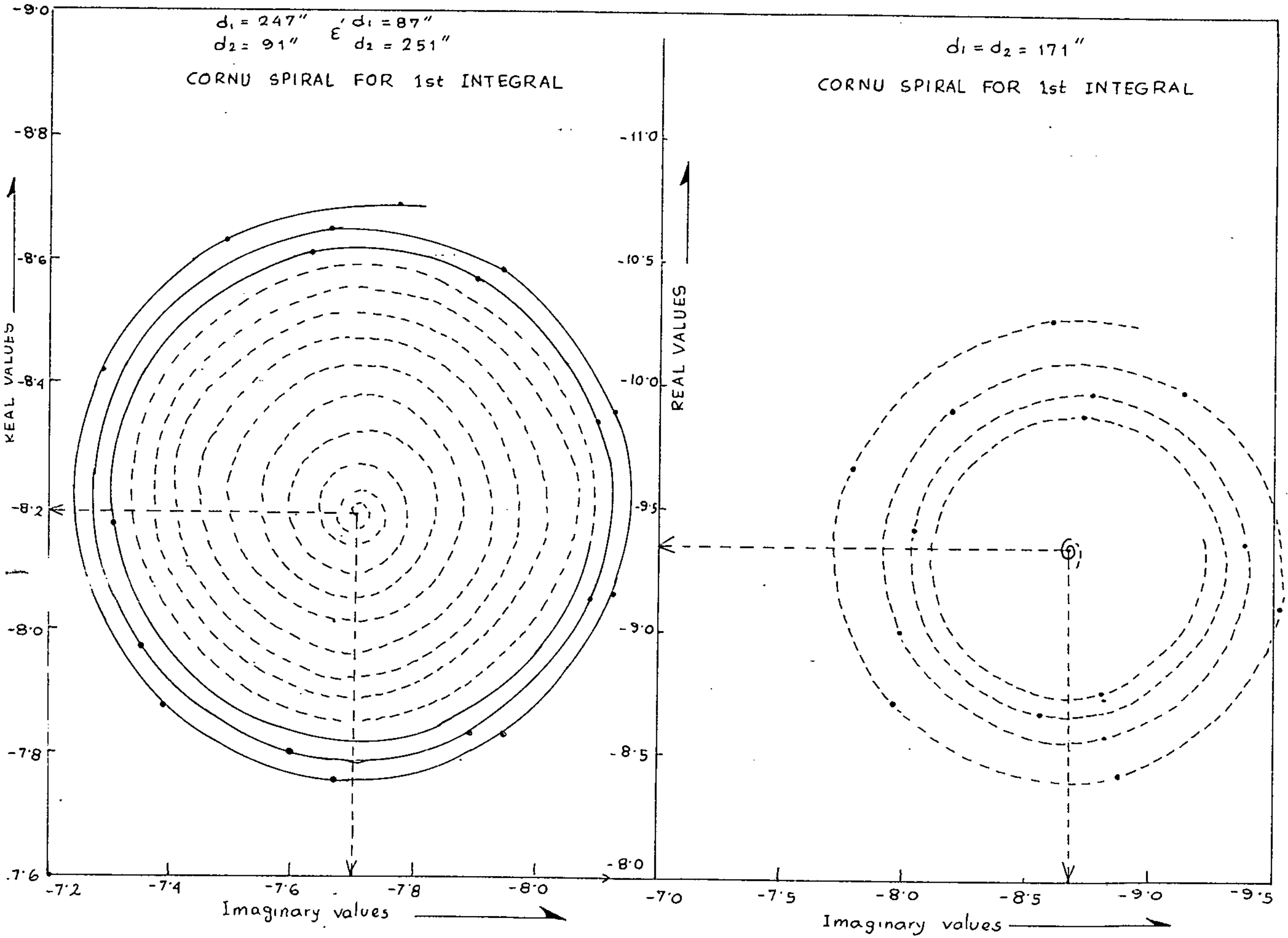

d₁ = 247″ d₂ = 91″
ε′ d₁ = 87″ d₂ = 251″
CORNU SPIRAL FOR 1st INTEGRAL
REAL VALUES
Imaginary values
-9·0
-8·8
-8·6
-8·4
-8·2
-8·0
-7·8
·7·6
-7·2
-7·4
-7·6
-7·8
-8·0
d₁ = d₂ = 171″
CORNU SPIRAL FOR 1st INTEGRAL
REAL VALUES
Imaginary values
-11·0
-10·5
-10·0
-9·5
-9·0
-8·5
-8·0
-7·0
-7·5
-8·0
-8·5
-9·0
-9·5

Case – I $d_1 = d_2 = 171''$

a) Calculation of the received power in the presence of the obstacle:

$$E = \frac{e^{j\pi/4}}{2d_1d_2}\sqrt{\frac{kd}{\pi}}\left\{(-9.35 - j\,8.7) + \cdot 7(-2.55 + j.253)\right\}$$

$$= c_1\,(-11.14 - j8.5)$$

where, $c_1' = \frac{e^{j\pi/4}}{2d_1d_2}\sqrt{\frac{kd}{\pi}}$

Since, the received power is proportional to EE^*,

Hence,

$$P_1 = C''_1\,EE^* = C'_1\,(11.14^2 + 8.5^2)$$

$$= C'_1 \times 196.35$$

b) Calculation of the received power under free-space condition:

When the obstacle was removed, then the limit of integration of the Ist integral should be extended from $-\infty$ to $+\infty$ since, the function is an even one, so it is only necessary to find the value of the integral having limit from 0 to ∞. Hence the received electric field under this condition becomes,

$$E = \frac{e^{j\pi/4}}{2d_1d_2}\sqrt{\frac{Rd}{\pi}}\left\{2 \times \int_0^{\infty}(\exp\left\{-jR\,(R_1 + R_2)\right\}\;dy)\right.$$

$$= C_1 \times 2\,(-3.9 - j\,3.7)$$

So, the received power $P_2 \propto EE^* = C'_1 \times 4\,(3'o^2 + 3.7)$

$$= c'_1 \times 115.56$$

Case-II: $d_1 = 87''$, $d_2 = 251''$

a) Calculation of the received power in the presence of obstacle:

The received electric-field strength is given by,

$$E = C_2 \left\{ (-8.2 - j7.7)+.7(-1.9+.41) \right. = C_2(9.53-j7.4)$$

The received power $P_2 \propto EE^* = C'_2(9.53^2 + 7.4^2) = C'_2 \times 145.56$

b) <u>Calculation of the received power under free-space propagation:</u>

The received electric field strength is given by,

$$E = C_2 \times 2x \int_0^{\infty} \exp\left[-jk\,(R_1 + R_2)\right] dy$$

$$= C_2 \times 2\,(-3.35 - j3.64)$$

$$P_2 \propto EE^* = C'_1 \times 4 \times (3.35^2 + 3.64^2) = C'_1 \times 97.88$$

<u>Case No- III:</u> $d_1 = 241''$, $d_2 = 91''$

a) <u>Calculation of the power received in the presence of obstacle:</u>

The received field-strength is given by,

$$E = C_3 \left\{ (-8.2 - j7.7) + .7(-1.98 + j.159) \right.$$

$$= C_3\,(-9.59 - j7.59)$$

$$P_1 \propto EE^* = C_3\,(9.59^2 + 7.59^2) = C_3 \times 149.58$$

b) <u>Power received under free-space propagation:</u>

Similarly, electric field is given by,

$$E = C_3 \left\{ 2x \int_0^{\infty} \exp\left[-jk\,(R_1 + R_2)\right] dy \right\}$$

$$= C_3 x 2x\,(-3.35 - j3.64)$$

The received power P_2 is given by,

$$P_2 \propto EE^* = C_3 \times 4\,(3.35^2 + 3.64^2) = C_3 \times 97.88$$

4.4 RESULTS AND DISCUSSIONS:

To find the obstacle gain i.e. power gain over the free-space propagation condition, the ratio of P_1 to P_2 is to be determined. This ratio gives the obstacle gain for three different positions. To compare the results with that of the experimental values, both results (theoretical and experimental) are tabulated in table No-2.

TABLE – 2:

No. of cases	Experimental				Theoretical		
	Free Space reading in db	Reading in presence of obs in db	Obstacle gain in db	Obstacle gain	Field strength in free space	Field strength in presence of obstacle	Obstacle gains
	P_2	P_1	10 log P_1/P_2	P_1/P_2	P_2	P_1	P_1/P_2
Case- I	30 db	32.9	2.9db	1.95	C_1x115.56	C_1x196.35	1.7
Case-II	30 db	32.5	2.5db	1.75	C_2x97.88	C_2x145.56	1.49
Case-III	30 db	32.5	2.5db	1.75	C_3x97.88	C_3x149.58	1.53

From, the above table one can easily observe that, theory and experiment conforms more or less fairly. There is however small discrepencies. The probable reasons for this discrepencies are discussed below.

Perhaps one of the major cause of this discrepencies, is the negligence of the diffraction due to the edge A. It has been pointed out that the diffraction due to this edge was neglected for mathematical complicacy. It is probably that the scattered electromagnetic waves from the edge A adds in phase with the direct received field-strength resulting an increase of overall gain.

The second probable cause of this discrepencies was the finite dimension of the conducting obstacle. It was assumed that the conducting obstacle was infinitely extended along transverse-direction. But in practice the conducting obstacle was about six-feet long along the transverse-direction.

The end edges of the diffracting obstacle might act as a diffracting edge and scattered electromagnetic waves might add in phase at the receiver resulting an increase of over all gain.

Among other causes of the discrepencies, the basic optical approach might be one of them. It has already been mentioned that, this approach is an approximated and simplified approach. It does not consider the characteristics of the diffracting edge. When a diffraction due to a sharp-edge was found, it is immaterial whether the edge is a conducting edge or an insulated one. But in practice, the case is not so simple. When there is a conducting edge, the upper-side of the conducting sheet is excited by the induced current which radiates electromagnetic waves. This radiation from the penumbral region of the conducting -sheet is completely neglected in the optical-theory. In this problem also, similar radiation from the vertical side of the conducting obstacle facing the receiving antenna might occur.

CHAPTER 5

AN ALTERNATIVE APPROACH BASED ON FOUR-RAY THEORY

5.1 INTRODUCTION:

The expression in equation 4.1 has been deduced on the basis of some simplifying assumption mentioned earlier. In this section an attempt was made to deduce a comparatively more accurate expresion. In the previous approach, the diffraction due to the edge A was neglected. The justification of this approximation has also been described before. The present attempt is also based on the Fresnel-Hygen's principle. In this case, two reference surfaces have been considered in place of a single reference surface as in the former case.

5.2 BASIC APPROACH TO THE PROBLEM :

It is assumed that electromagnetic wave transmitted from the primary source T_1 (transmitter) reaches the surface -1, (Fig- 12) which is a vertical surface just above the edge 'A' . Here, they acts as a secondary source and radiates wavelets in all directions. All points on this surface acts as a source. Part of the radiation travels directly to the surface -2 which is a vertical surface just above the edge B and part of the radiation travels towards the flat-conducting surface and then after being reflected from the conducting surface irradiates the surface-2. From surface-2 they radiates secondary (tertiary) wavelets which irradiates the receiver T_2. The approach is more accurate than the formerone, since no approximation to the diffracting edge has been considered. The mathematical formulation of the above view point is described below;

The conducting surface has two vertical sides. The side AA' and side BB' (Fig- 12) are the two reference surfaces over which the sources are considered. The effects taking place can be explained as follows (Fig- 12)

1) Radiation travels from the transmitter T_1 to Y' (the point on the surface-1) where it acts as a source of secondary wavelets which irradiates all the points on the surface-2. For present purpose, at first only one point Y will be considered on the surface-1 which have received radiation from Y'. This point Y again acts as a

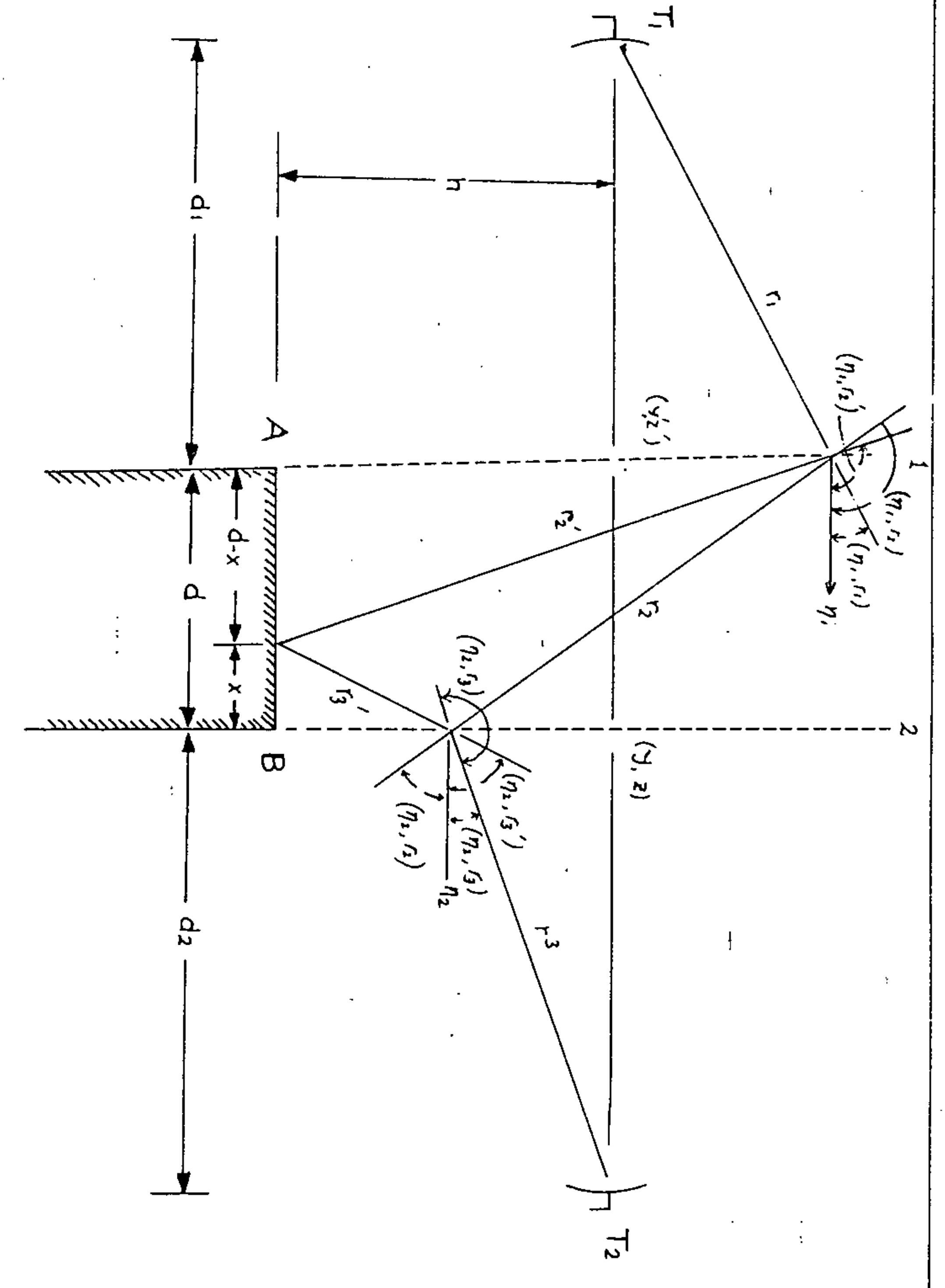

Fig-12

SCHEMATIC DIAGRAM SHOWING DIFFRACTION BY THE OBSTACLE source of radiation which then irradiates the receiver T_2. The point Y receives scattered radiation from all points on the surface- 1.

2) In the next case, radiation travels from the transmitter T_1 to Y' and then radiates secondary wavelets towards the flat conducting surface of the obstacle where it is reflected towards the point Y lying in the surface-2 where it again acts as a source of radiation that irradiates the receiver T_2.

Hence, there are two different paths along which the radiation can travel from T_1 to T_2. The paths are as follows,

1) T_1Y' YT_2
2) T_1Y' X YT_2

From the above concept of four-ray theory and the ray paths as described, the received electric-field can be found from the following expression using the Fresnel-Kirchoof diffraction theory. The integrals can be written as follows:-

$$E = \int_{-h}^{\infty}\int_{-\infty}^{\infty}\int_{-h}^{\infty}\int_{-\infty}^{\infty}\left\{\frac{1}{r_1 r_2} \exp\left[-jk\,(r_1+r_2)\right]\left[\cos\,(n_1,r_1)-\cos(n_1,r_2)\right]\right\}$$

$$\frac{1}{r_3}\cdot \exp\left[-jk\,r_3\right]\left[\cos\,(n_2,r_2)-\cos(n_2,r_3)\right] dZ'\,dY'\,dz\,dy.$$

$$+\,\rho\int_{-h}^{\infty}\int_{-\infty}^{\infty}\int_{-h}^{\infty}\int_{-\infty}^{\infty}\left\{\frac{1}{r\,(r_1'+r_2+r_3')}\exp\left[-jk(r_1+r_2'+r_3')\right]\left[\cos(n_1,r_1)-\cos(n_1,r_2')\right]\right.$$

$$\frac{1}{r_3}\;\exp\left[-jkr_3\right]\left[\cos\,(n_2,r_3)-\cos(n_2,n_3)\right]dZ'\,dy'\,dz\,dy \quad \text{----(5.1)}$$

The above integrations need some explanation. The first integral represent the received field strength due to direct transmission of the waves passing over the obstacle. The term within the 2nd bracket of the ist integral represents the field-strength received at point Y (on surface-2) due to secondary radiation from a point Y'(on surface -1). The rest of the term represents the field strength-received at receiver T_2 from the point Y. But, the point Y receives radiation from all points of the surface-1. The received field-strength at T_2 depends also on the inclination factor at Y i.e. the receiving field-strength at T_2 also depends on the direction in which the point Y receives signal from it's source which are points lying on the surface -1. So, in order to evalute the integral, one can not perform the integration of the function within 2nd bracket independently, because in that case it is not possible to determine the direction in which the point Y receives signal from the point Y'. In order to avoid this confusion, the evalution of the integration should be such that at first the received signal due to radiation from different points of Y which has been enerzised by a single point of Y' should be calculated. Then the similar procedure is repeated for different point of Y' i.e. mathematically the integration with respect to y and z should be performed first and then the integration with respect to Y' and Z' should be performed.

Same, treatement also hold for evaluation of the 2nd integral.

<u>Evaluation of the Integral:</u>

In order to evalute the integrals, all variables inside the integration sign should be expressed interms of independent variables y, z, y' and z' where y' and y are the vertical axis lying in the surface-1 and 2 respectively and z' and z axes are perp. to the plane of the paper. From the geometrical confugaration the following relations can be established:-

$$r_1 = (d^2_1 + y'^2 + z^2)^{\frac{1}{2}}$$

$$r_2 = \left\{d^2 + (y-y')^2 + (z - z')^2 \right\}^{\frac{1}{2}}$$

$$r_3 = (d_2^2 + y^2 + z^2)^{\frac{1}{2}}$$

$$r_{3'} = \left[(y + h)^2 + (z-z')^2 \frac{x^2}{d^2} + x^2 \right]^{\frac{1}{2}}$$

$$r'_2 = \left[(y' +h)^2 + (z-z')^2 \frac{(d-x)^2}{d^2} + (d-x)^2\right]^{\frac{1}{2}}$$

$$x = d(y+h)/(y+y'+2h)$$

$$\cos (n_1, r_1) = \frac{d_1}{r_1} = \frac{d_1}{(d_1{}^2 + y'^2 + z^2)^{\frac{1}{2}}}$$

$$\cos(n_1, r_2) = -\frac{d}{r^2} = -\frac{d}{\left\{(d^2 + (y-y')^2 + (z-z)^2\right\}^{\frac{1}{2}}}$$

$$\cos(n_2, r_2) = \frac{d}{r_2} = \frac{d}{\left\{d^2 + (y-y')^2 + (z-z')^2\right\}^{\frac{1}{2}}}$$

$$\cos(n_2, r_3) = -\frac{d_2}{r^3} = -\frac{d_2}{(d^2{}_2 + y^2 + z^2)^{\frac{1}{2}}}$$

$$\cos(n_2, r'_2) = -\frac{(d-x)}{r'_2} = -\frac{(d-x)}{\left\{(y'+h)^2 + (z-z')^2 \frac{(d-x)^2}{d^2} + (d-x)^2\right\}^{\frac{1}{2}}}$$

$$\cos(n_2, r'_3) = \frac{x}{r'_3} = \frac{x}{\left\{(y+h)^2 + (z-z')^2 \frac{x^2}{d^2} + x^2\right\}^{\frac{1}{2}}}$$

Putting the above relation in equation (5.1) the equation takes very complicated form. The expression can not be expressed in terms of any standard form. However, the integration may be performed with the help of digital computer.

CHAPTER 6

THEORETICAL BACK-GROUND OF THE MEASUREMENT OF DIELECTRIC CONSTANT OF SOIL

6.1 INTRODUCTION:

There are various methods for measurement of dielectric constants at microwave frequencies[30]. The choice of method depends to a large extent upon the type of work contemplated, method which is satis -factory in research is sometimes not workable for routine measurement, and conversely. Again, another fact which is to be considered about the preparation of the sample, an operation which often takes more time that the actual process of measurement is not suitable for a series of measurement. Thus a method requiring rod-shaped samples is almost impossible to use with certain type laminates, which are ordinarily supplied in sheet form, but on the other hand, free space methods which require fairly large sheets are inconvenient when the temperature and humidity are to be controlled or when the material is not available in appreciable quantity. The choice of method is likewise influenced by the properties of the material itself, apart from it's form or availablity; for example, those with losses are not always conveniently treated by the methods used for low loss materials. Another most important item influencing the utility of a given method is the cost and availability of the instruments.

Considering all these factors two different methods have been adopted for the measurement of dielectric constant of soil. The first of this methods is the "Measurement by transmission in free-space". The accuracy of the results obtained in this method is very much sensitive to the precise measurement of the strength of the reflection signal from the sample and also on the nature of polarization of the waves. The second method is based on the principle of wave-guide measurement. In this method informations about the strength of the standing wave-ratio and shift of the field strength maximum or minimum are necessary for complete description of the real and imaginary parts of the dielectric constant of the material filling the wave guide section.

6.2 MATHEMATICAL THEORY OF THE MEASUREMENT:

2a: Measurement by Free-space propagation

Among the two methods discussed above, the theory of the first method i.e. "Measurement by transmission in free-space" will be discussed first. The basic theory behind this measuring techni--que is the well-known Fresnel-reflection Theory.

In this procedure, a transmitted waves is allowed to incident on a large block of dielectric (to be measured) having sufficient thickness (since dielectric is considered to be lossy), so that no wave can penetrate very deep in to the dielectric slab. The wave is allowed to incident on the sample at a finite angle, the reflected wave is then received with a receiving system and the strength of this signal is measured. From, the measurement of the transmitted and received signal strength the dielectric constant was calculated.

When the reflecting surface is plane, the magnitude of the electric field vector 'E_r' of the reflected wave is related to the corresponding magnitude of incident electric field vector 'E_i' through the Fresnel formulas as follw [30].

Horizontal polarization,

$$E_h = \frac{u_t \sin\theta_t \cos\theta_i - u_i \sin\theta_i \cos\theta_t}{u_t \sin\theta_t \cos\theta + u_i \sin\theta_i \cos\theta_i} E_i \quad \text{--------}$$

vertical polarization,

$$E_r = \frac{u_t \sin\theta_t \cos\theta_i - {}_i \sin\theta_i \cos\theta_t}{{}_t \sin\theta_t \operatorname{Cost}\theta_i + \sin\theta_i \cos\theta_t} E_i \quad \text{--------}$$

Where, θ_i and θ_t denote angles of incidence and refraction respectively, μ and ϵ are the permeabilities and permittivity with 'i' and 't' identifying quantities as measured in the media containing the incident and refracted wave respectively. Using the Snell's law of reflection we know,

$$|K_i| \sin \theta_i = |K_t| \sin \theta_t$$

Putting these values in the above expressions for E_r and simplifying. We find,

Horizontal polarization,

$$E_r = \frac{\mu_t |k_i| \cos \theta_i - \mu_i \sqrt{|k_t|^2 - |k_i|^2 \sin^2 \theta_i}}{\mu_t |k_i| \cos \theta + \mu_i \sqrt{|k_t|^2 - k_i^2 \sin^2 \theta_i}} E_i$$

Vertical polarization,

$$E_r = \frac{\epsilon_t |k_i| \cos\theta - \epsilon_i \sqrt{|k_t|^2 - |k_i|^2 \sin^2\theta_i}}{\epsilon_t |k_i| \cos \theta_i + \epsilon_i \sqrt{|k_t|^2 - |k_i|^2 \sin^2\theta_i}}$$

For our present purpose μ_i and μ_t can be considered to be same and equal to μ_0, the free-space value. In the above two experiment there are two unknowns ϵ_t and k_t. Knowing the values of E_r/E_i for both types of polarization, we can easily solve for ϵ_t and K_t. So, the problem of finding the dielectric constant reduces to find the ratio of electric fields (Reflected/ incident) for both types of polarization.

6.2b: MEASUREMENT BY VSWR TECHNIQUE:

In the second method a section of the wave-guide is loaded with a proper dielectric sample. The sample may be tapered for matching purpose. However, when the sample is a lossy one, then using sufficiently long sample is an obvious solution to this problem. It was observed that the soil samples when sufficiently long prevents any type of mismatching problem. Now, the reflection co-efficient(magnitude and phase) was measured for the system. From this measured value, the dielectric constant was calculated. So, the problem of finding dielectric constant reduced to find a relation between the reflection co-efficient(both magnitude and phase) and the dielectric constant. The theory is described below:-

The boundary conditions that are to be satisfied at the surface of a discontinuity in the properties of the medium are that the tangential components of the electric and magnetic fields must be continuous. Supposing a discontinuity in a wave-guide such that the plane of the discontinuity is perpendicular to the axis of the guide. The power flow down the guide is $P = \frac{Re(Zw)}{2} H_t^2 ds$, where the integral is taken over the cross-section of the guide. Nowe, H_t must be continuous accross the interface of the two dielectrics; whereas the wave impedence Z_w will change discontinously. Therefore, it is clear that there must be a reflected wave at the interface and this will be sufficient to satisfy the conditions at the boundary. Moreover, the equivalent impedance that correctly describe this reflection should be chosen proportional to the wave-impedance. Hence, the equivalent circuit representing the discontinuity is simply that shown in Fig-A

The standing wave ratio 'r' is the ration of the impedance taken in such a way that $r > 1$. The value of the wave-impedance for E and H modes are given as below:-

$$Z_H = \frac{j\omega\mu}{\gamma} \quad , \quad Z_E = \frac{\gamma}{j\omega\mu} \qquad \text{...........(6.1)}$$

For the case of no loss i.e. in medium (1) this reduces to

$$Z_H = \frac{\lambda g}{\lambda}\xi \quad ; \quad Z_E = \frac{\lambda}{\lambda_g}\xi$$

where λ is the wavelength in the medium and ξ is $\sqrt{\mu/\epsilon}$

When the dielectric material i.e. medium (2) is lossy as in this case, then wave impedance becomes complex. It's value can be calculated from the complex dielectric constant $(\epsilon' - j\epsilon'')$ as follows:-

From Equation (6.)

$$Z_H = \frac{j\omega\mu}{\alpha + j\beta} \quad \text{where complex propagation constant } \gamma = \alpha + j\beta$$

or,
$$Z_H = \frac{\omega\mu\beta}{\alpha^2 + \beta^2}\left(1 + j\frac{\alpha}{\beta}\right)$$

$$= \frac{\omega\mu}{\beta + \frac{\omega^4 \epsilon''^2 \mu^2}{4\beta^3}}\left(1 + j\frac{\omega\epsilon''\mu}{2\beta^2}\right)$$

$$Z_E = \frac{\beta}{\omega\epsilon^2 + \omega\frac{\epsilon''^2}{\epsilon'}}\left[1 + \frac{\omega^2\epsilon''\mu^2}{2\beta^2\epsilon'} - j\left(\frac{\omega^2\epsilon''\mu}{2\beta^2} - \frac{\epsilon''}{\epsilon'}\right)\right]$$

However, the above expressions for Z_E and Z_H can be transformed to a some-what more useful form in the following way (since, we are con-cerned with . Only TE-mode, only Z_H will be discussed here):

$$Z_H = \frac{\lambda_g}{\lambda}\sqrt{\frac{\mu}{\epsilon'}} \quad \frac{1 + j\frac{1}{2}\tan\delta\left(\frac{\lambda_g}{\lambda}\right)^2}{1 + \frac{1}{4}\tan^2\delta\left(\frac{\lambda_g}{\lambda}\right)}$$

Normalising this impedance with that of medium (1)

$$Z_H(n) = \sqrt{\frac{\epsilon_0}{\epsilon'}}\, \frac{1 + j\,\frac{1}{2}\tan\delta\,(\lambda_g/\lambda)^2}{1 + \frac{1}{4}\tan^2\delta\,(\lambda_g/\lambda)^2}$$

where, $\tan\delta = \frac{\epsilon''}{\epsilon'}$

Again putting, $\lambda_g/\lambda_g = \frac{1}{\sqrt{(1 - p)}}$ where $P = \left(\frac{\lambda}{\lambda_c}\right)^2$

the experssion becomes,

$$Z_H(n) = \frac{1}{\sqrt{k}} \quad \frac{1 + j\,\frac{1}{2}\tan\delta\left(\frac{1}{1-p}\right)}{1 + \frac{1}{4}\tan^2\delta\left(\frac{1}{1-P}\right)} \qquad \dots\dots\dots\dots(6.2)$$

where, $k = \epsilon'/\epsilon_0$ = Real part of the dielectric constant.

To express the equation (6.2) interms of measurable quantities i.e. re-flection co-efficient. We use the following relation,

$$r = \frac{Z_H(n) - 1}{Z_H(n) + 1} = \frac{\left[1 + j\frac{1}{2}\tan\delta\left(\frac{1}{1-p}\right) / \sqrt{k}\left\{1 + \frac{1}{4}\tan^2\delta\left(\frac{1}{1-p}\right)\right\}\right] - 1}{1 + j\frac{1}{2}\tan\delta\left(\left(\frac{1}{1-p}\right) / \sqrt{k}\left\{1 + \frac{1}{4}\tan^2\delta\left(\frac{1}{1-p}\right)\right\}\right) + 1}$$

Now, for practical purpose, considering the material to be such lossy so that $\tan^2\delta$ can be neglected. After simplification the relative di-electric constant (real part) can be found as follows,

$$k \simeq \frac{(1 + r_i)^2 - 4r_i p}{(1 - r_i)^2} \quad \text{where} \quad r_i = |r|$$

$$\tan\delta \simeq \frac{k - 1}{k} / \sqrt{\frac{k - p}{1 - p}} \; \tan \; r_i' \quad \text{where} \; r_i' = r$$

CHAPTER 7

MEASURING TECHNIQUE

7.1 METHOD -1, FREE-SPACE MEASUREMENT:

7.1a: EXPERIMENTAL SET-UP

The experimental setup for measuring the dielectric constant by free-space measurement is shown in Fig-14. For this purpose, two horn-fed parabolic antennas were used. The antennas were mounted on wooden frames with an arrangement such that they could be focussed in different directions along vertical plane i.e. the axis of rotation was horizontal.

In the transmitting system gunn-diode was used as a signal-generator. The gunn-diode was connected with the horn by means of a co-axial cable through an attenuator. The attenuator was used to separate the generator from the antenna. A frequency-meter was also used to measure the transmitted frequency. The transmitted frequency was found to be 8 GHz and the output power was 10 mw.

In the receiving system, the received signal was fed to a directional coupler while the other input terminal of the coupler was fed by a local-oscillator(gunn-diode). The output of the directional coupler was fed to a crystal detector for tuning purpose, from which the detected tuned signal was fed to a I-F camplifier-having intermediate frequency of 30 MC/S. Thus the reading of the I-F camplifier was proportional to the received signal strength.

7.1b: BASIC PRINCIPLE OF THE MEASUREMENT:

The basic principles of measurements used were as follows. At first the two antennas were placed at a distance of about 160 inches. The received signal strength was observed for direct transmission as shown in Fig. 13. Next, the sample was placed on a tray having 6ft. by 6ft. sides and six-inches deep. The trays was placed at the centre. The transmitting and the receiving antennas were focussed towards the sample as shown in Fig. 14. Then, both the antennas were adjusted (focussed) properly for optimum readings. The experiment was repeated for both types of polarization(Horizontal and vertical). The polarization of the transmitted wave was changed by rotating the feeder

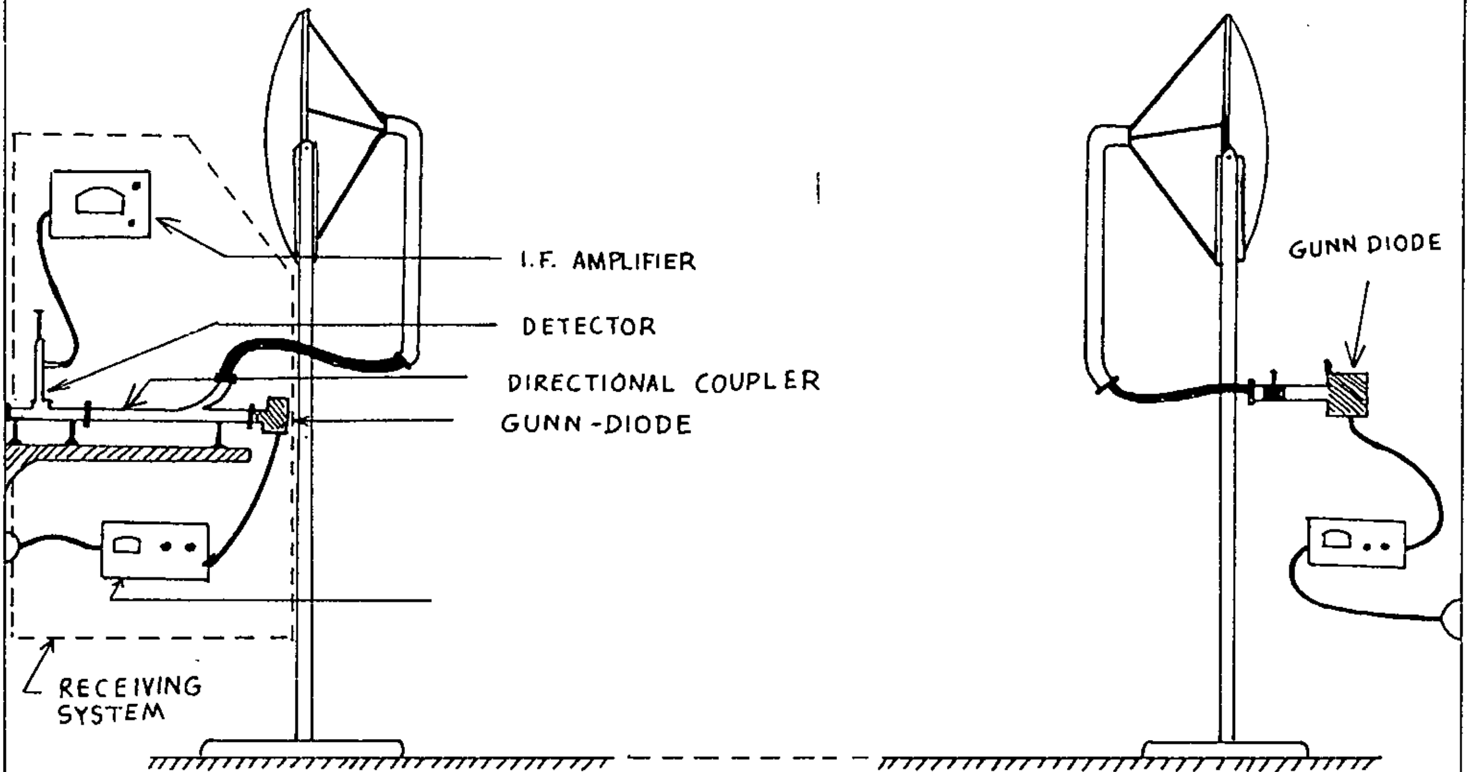

FIG NO. 13 SETUP FOR DIRECT TRANSMISSION

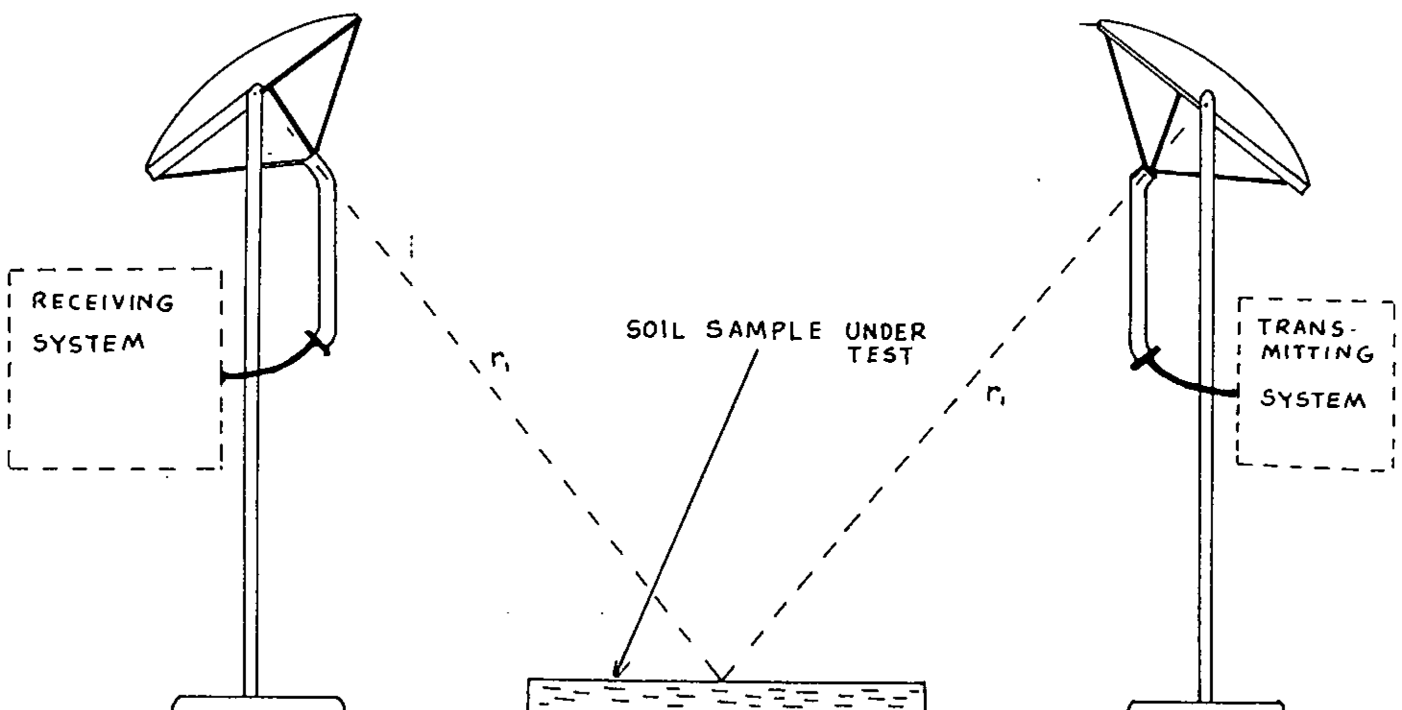

FIG. NO. 14 SETUP FOR TRANSMISSION THROUGH REFLECTION (horn-antenna) of the transmitting antenna through 90° degrees. From the difference between the two readings, the ratio E_r/E_i (for both types polarization) was calculated . Since, only the difference between the two readings are needed, mismatch of the antennas with the signal generators, scattering phenomena and transmitter-receiver coupling effects etc. are cancelled out in both cases. However following assumtion were necessary for the measurement.

1) Since, main object of this investigation was to find the effective dielectric constant of the sample, so the existance of any surface roughness of the sample that causes scattering will be considered as absorption due to surface and will be included in the dielectric constant.

2) The sample thickness was of six-inches. It was assumed that the most of the incident wave was reflected by the surface of the sample and the rest of the waves that are transmitted through the sample was not reflected back by the metallic surface of the tray at the botton but absorbed completely while travelling through the sample. The assumption was quite reasonable. Thus skin depth penetration was calculated with a typical value of the sample, and it was found that the transmitted signal strength decays very rapidly before they reach the botton of the tray.

3) The shading-effects due to horns of the two antennas were neglected. As this effect was same for both types of readings (direct and reflected) so the effects cancelled out.

4) To find the reflection-coefficient E_r/E_i, both the incident and reflected fields should be measured on the surface of the sample or the measurements should be such that the direct and the reflected fields should travel same distance from the surface of the sample to the point of measurement. The assumption is quite reasonable, as it is a known and accepted fact that both E_r and E_i decreases as the inverse of the distance traversed. So, the ratio (Er/E_i) measured just at the surface of the sample and the ratio measured at a finite distance from the surface should yield same result. The assumption

made above can be proved analytically.

Let,

E_{ir1} = The signal strength at a point 'r_1' from the transmitter

E_{i2r1} = " " " " " '$2r_1$' " " "

E_{ir} = " " " " " r " "

E_{rr1} = " " " just on the surface of the sample after reflection.

E_{r2r1} = The reflected signal strength after travelling distance 'r_1' from the sample.

In the fig- , let r be the direct distance between the transmitter and receiver. If the incident ray could travel the distance '$2r_1$,' thus the signal strength was given by,

$$E_{i2r_1} = \frac{r}{2r_1} E_{ir}$$

Now, for validity of our assumption, the following relation are to be proved;

<u>Reflected wave measured after travelling 'r'_1 from the sample:</u>

Incident signal measured after travelling distance '$2r_1$' from the transmitter:

$$= |\rho| = \frac{E_r}{E_i}$$

The left-hand side of the equation- can be written as follows,

$$\frac{E_{r2r1}}{E_{i2r1}} = \frac{\frac{2r_1}{r_1}}{\frac{2r_1}{r_1} E_i r_1} = \frac{|\rho| E_i r_1}{E_i r_1} = |\rho| \quad \text{(approved)}$$

Under these assumptions, the reflection coefficients for both type of polarized wave was measured. Then the Fresnel relation for reflection was used to calculate the dielectric constant. The experiment was also performed for measuring the dielectric constant of water under various salinity condition. Finally, the dielectric constant of soil was measured.

The table-shows the dielectric constant of water under various salinity condition.

TABLE – 3:

Quality	Salinity in dc μυ	Horizontal polarization Free space	Horizontal polarization Water reflector	Vertical polarization Free space	Vertical polarization water reflector	ϵ_r
Fresh		46.5 db	44.2 db	47.0 db	43.7 db	43.4
Water		31,6 db	29.21db	23.65db	20.50db	70.0
Saline Water	8,600 μυ	32.9 db	30.6 db	33.8 db	30.6 db	67.22
Saline		26.9 db	25.25db	30.6db	26.4 db	
		26.8 db	25.50db	30.2db	28.2 db	
		26.8 db	25.7 db	33.8db	28.8 db	
Water	20,000 μυ	28.0 db	26.2 db	32.0 db	30.3 db	
		28.0 db	25.9 db			67.02
		28.4 db	26.2 db			
		27.2 db	23.0 db			
		max -readings are listed				
		28.4 db	26.2 db	33.8 db	30.3 db	

The experiment was then repeated for measuring the dielectric constant of the soil. The experimental datas are tabulated in table- 4.

TABLE – 4:

Quantity	Material	Horizontal Polarization Free-space	Horizontal Polarization Soil reflected	Vertical Polarization Free-space	Vertical Polarization Soil reflected	ϵ_r
Loose Packed	Dry Soil	32.7 db	24.7 db	24.6 db	15.0 db	1.39
Loose packd	Dry soil	34.3 db 30.5 db 32.0 db	26.3 db 25.4 db 25.4 db	33.5 db	15.0 db	1.56
Loose packed	Dry soil	36.9 db	27.4 db	34.0 db	18.0 db	1.314

7.1C DISCUSSION:

The results measured for water was more or less satisfactory. It was observed that as the salinity of the water increased, the dielectric constant decreased gradually. This is the general property of any material. Due to the lack of accuracy, the losses in water could not be measured. From the expression given in equation- it was found that the conductivity of water depends greatly on the reflection co-efficient. It may be shown that there may be 20 to 30% , variation in the result of conductivity when the reflection co-efficient for both polarization devices from the actual result of the order of .007. But the relative dielectric constant is not that much sensitive to the reflection co-efficient. This was the main draw-back of the procedure.

From, the results found for soil, it may be seen that the relative dielectric constant of the soil is much less than the standard one. This variation is due to loose packing of soil. Since, the soils were packed loosely, it acted as a porous medium and the reflection from the soil surface was much less .Again, due to surface roughness the reflected wave was scattered in different directions. All these factors results in a decreased field-strength in the receiver. As a result the relative dielectric constant has a tendency to proceed towards unity. So, the measured dielectric constant was much less than the typical values. These difficulties lied us to adopt another method described in the next section.

7.2a: EXPERIMENTAL SET-UP:

7.2 METHOD -II - WAVE-GUIDE MEASUREMENT:

The difficulties of the previous method lied us to adopt another method for accurate measurement of dielectric constant(of Bangladesh soil). In this procedure the soil was treated as lossy dielectric medium and a standard wave-guide section was loaded with the soil sample. The wave-guide was excited for propagation of TE_{10} mode. The reflection coefficient for the wave at the air dielectric interface was measured by wave-guide technique. The soil sample has been treated as a four-pole terminal. The output terminal has been considered to be terminated by a matched load having same impedance as that of the characteristic impedance of the wave-guide. This has been done in practice, by taking sufficient length of the soil sample. Since, the sample is a lossy one, so the wave is absorbed by the sample before it reaches the termination at the far-end.

Upto this the basic outline of the experimental procedure have been discussed. It is an accepted fact that the success of an experiment is solely dependent on the accuracy of the measurement. In this case, this accuracy is mostly dependent on the successful preparation of the soil samples. For this purpose, the samples should be collected from different places so that one can find the behavior of the different samples. Next, the techniques of preparing samples should be such that, the dependence of dielectric constant on various parameters of the samples can be studied extensively. As for example, soil densities from different samples should not vary widely. Because, if it happens so, one might be in a ambiguess position, since it would than be difficult to determine whether the variation of dielectric constant at a particular frequency was due to varying the types of soil or densities of soil. So, the techniques of preparing sample is an important fact to be considered. The method of collecting samples and technique of preparing samples suitable for wave-guide use have been discussed in the next section.

7.2b: COLLECTION OF THE SAMPLE:

Due to lack of adequate fund and transport facilities extensive sample collections as required for a complete investigation of such a topics was not possible. A few representative samples were collected from different places as discussed later.

It has already been mentionedbefore that, one of the main object of this experiment was to prepare a radio-data for Bangladesh soil at microwave frequencies(J & X-band). Since, statistical average is the main feature of this experiment, so the samples should be collected properly from different places. For measurement of soil characteristics of Dacca, soil samples from(1) Mirpur (2) Engineering University Campus (3) Joydevpur (4) Narayanganj, and (5) Tongi were collected. In each of these places samples were collected from three different spots and each of about two hundred yeards apart and mixed thoroughly to get the average soil characteristics.

Similarly, samples from three different places namely(1) Chittagong Hilly area(Chittagong Cantonment area) (2) Chittagong Port area (North potenga),(3) Chittagong City area (Chittagong New-Market area) were collected. Same procedures were adopted for collection of samples from each of these places.

Besides this, token samples were collected from Comilla, and Noakhali district. These were collected from Dowood-Kandi and Feni. The collected samples were prepared properly to pack them inside the wave-guide.

7.2C: TECHNIQUES OF PREPARING SAMPLES:

Special techniques were used to prepare the soil -samples for packing them into the wave-guide. At first, the soil samples from each places were mixed with known quantities of water to make them pasty. The percentage of water added(by weight) were maintained constant for all types of samples. The pasty samples were then placed in small polythelene bags. The polythene bags were prepared such that they had same-surface area, as the inner surface area of the waveguide. Then a smooth wooden piston was used to press the samples, so that the soils are packed properly inside the wave-guide. The density of the packed soil, off-course depends on the pressure delivered by the piston. The pressures were tried to maintain constant throughout the preparation of the samples. It has already been mentioned that the wave-guides were loaded with samples of sufficient length so as to avoid reflection from the termination of the wave-guide section. The front face of the samples were made as smooth and vertical as possible. The wave-guide section loaded with the samples was then fixed at the output terminal of the universal carriage. After the experiment being performed, the samples were then placed in the open atmosphere for sufficient time so as to avaporate all it's moisture. The samples were weighted again and then placed inside the wave-guide section for experiment. The transverse dimension of the samples shrinked due to

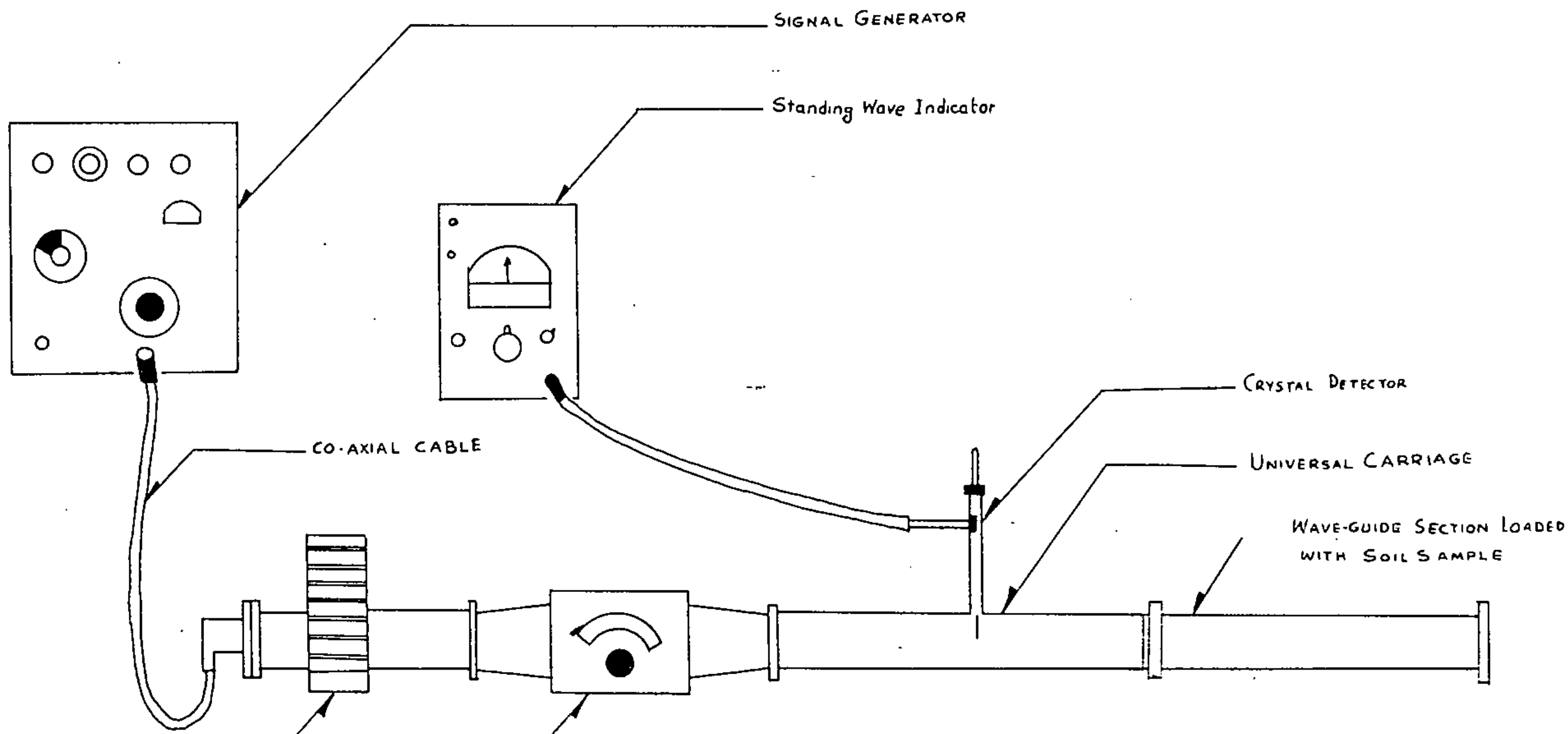

Fig – 15

EXPERIMENTAL SET UP FOR MEASURING DIELECTRIC CONSTANTS

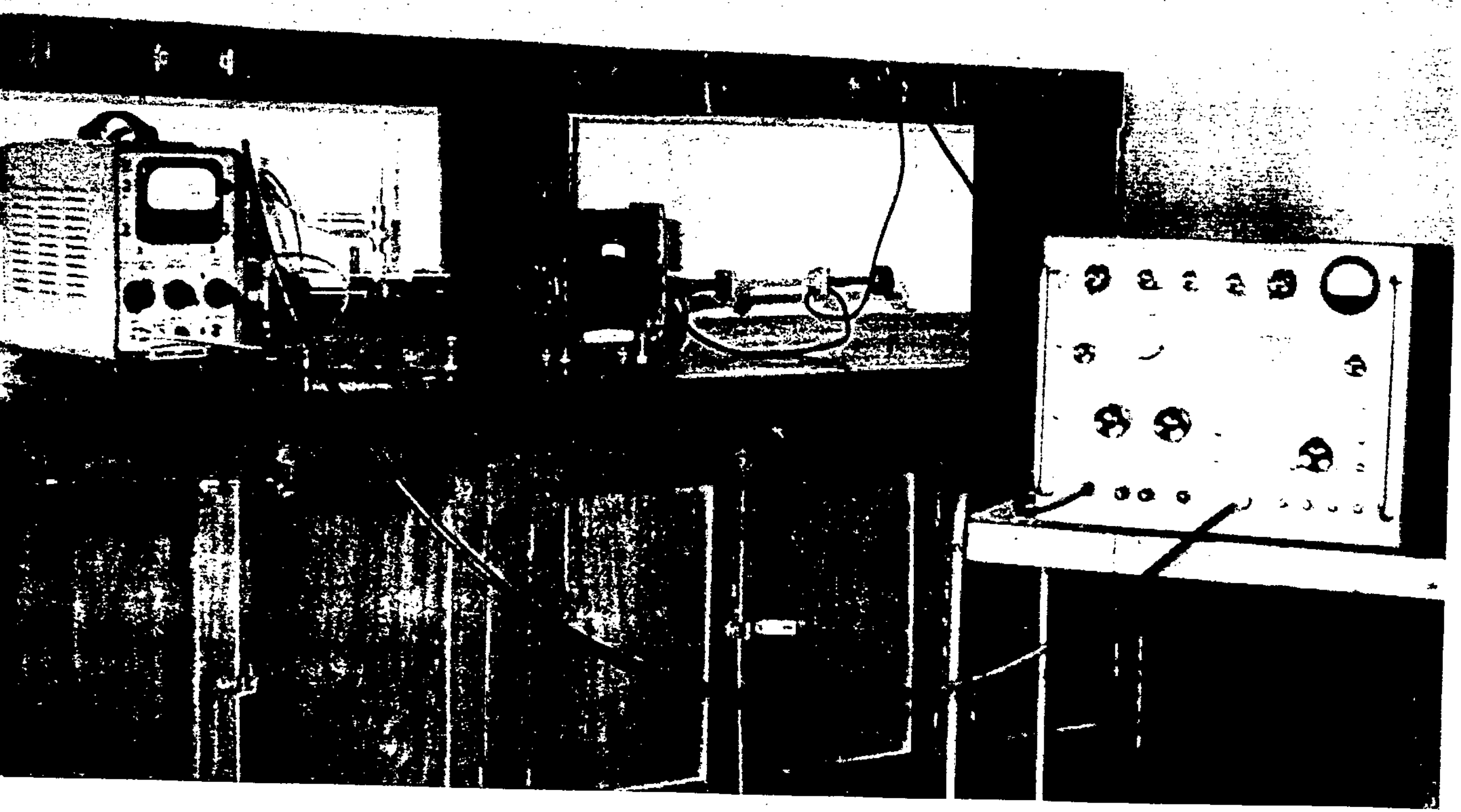

Experipental Setup for measuring Dielectric Constant of Soil (From Bangladesh) dryness. However, the change of dimension was not much. From, known weight, the densities and moisture contents of each samples were calculated. Thus knowing the percentage of moisture contents and densities of the samples, dependence of the values of dielectric constants on these parameters were plotted. The measurements were performed at different frequencies(X and J band).

7.2d: MEASURING SET UP AND EXPERIMENTAL PROCEDURE:

The experiment was performed in the laboratory of the department of electrical engineering. The procedure is known as "a general method depending on reflection". In this method the sample is placed inside the rectangular wave-guide sections. The length of the soil samples were sufficient to avoid reflection from the termination of the samples. To prevent any short of scraches and damages of the inner side of the wave-guide section, the soil samples were placed in thin polythene bags and then the wave-guides were loaded with these samples. Proper care was taken, so that sample-surfaces were perpendicular to the wave-guide. The input terminal of the wave-guide section was connected to a universal-carriage where metallic probe was used to measure the reflection co-efficient. The probe picked up the electric-field intensity and [redacted] after being detected by the crystal detector the signal was fed to a standard standing-wave indicator, to determine the standing wave ratio. Amplitude modulated signal was transmitted for this purpose. The input side of the universal carriage was connected to the signal generator through an adjustable attenuator and a frequency -meter. The whole experiments were repeated for complete J-band and X-band to observe the frequency dependence character of the samples. The experimental set-up is shown in fig. 15. For determination of the complex permittivity of the soil both the magnitude and position of the standing wave pattern was necessary. Unfortunately the position was not determined accurately. So, the imaginary part of the permittivity was not determined. This imaginary part is responsible for the conductivity of the material. For this reason, to get some idea about the conductivity of the material, the d-c conductivity of the soil samples were measured as shown in Fig- 16.

In this procedure, the sample was placed in a wooden frame. Two-sides of the sample was pressed by conducting copper-plates from which wires were connected to the input terminal of the wheat-stone bridge to measure the unknown resistance of the sample. Galvanometer was used to observe the null-point of the bridge-circuit. Now, from the relation $R = \rho l/A$, the resistivity was calculated, from which conductivity was found. The datas are tabulated in table no. 3.

7.2C : A FEW SOURCES OF ERROR:

Perhaps the most widely known of the wave-guide methods is that in which the standing-wave ratio is measured directly by standing wave indicator. Despite it's general acceptance this method has certain short comings. The possible sources of error are out line here.

DEVIATION FROM SQUARE LAW:

In the first place, it is assumed that the input of standing wave indicator i.e. r-f detectors obey square-law. But in practice, the detector obeys the square-law approximately and often the voltage V from the detector is;

$$V \propto E^{\alpha}$$

Where E is the electric-field in the r-f line. If $\alpha \neq 2$, such a relation never gives true proportionality of r-f power and receives reading and it is apparent that both the magnitude and the percentage error approach infinity with standing-wave ratio, no matter how small the deviation of α from the ideal value 2 may be. Nor is it easy to correct the error by evalution of α by some graphical methods, for α is likely to depend on field strength over the wide ranges encountered in the present application,. since a detector sufficiently sensitive to respond to the minimum is usually overloaded at the maximum. The error increases when high standing-wave ratio is to be measured.

However, the error can be minimized by the application of an attenuator to reduce the signal strength.

2) IMPURITY OF GENERATOR OUTPUT POWER:

It has been assumed throughout the foregoing discussion that only a single frequency is generated by the source of r-f power. The output power of modulated Klystron does not satisfy this condition, however, but some times has components at frequencies different from the fundamental. This behavior is the result of improper modulation of the generator, it is quite different from the normal presence of harmonics in the frequency spectrum of a pulse. It is of interest, however , to investigate the effect.

, A mathematical investigation can be made. As described in R-f-I , the r-f power is not present simultaneously at two frequencies, but rather one frequncy exists for alternate pulses of the modulator, or one frequency at one point of each pulse, a different frequency at a later point of the same pulse. For approximate qualitative computation, therefore, powers are added instead of amplitude, and the meter reading is assumed to be the sum of the values for two individual frequencies. With such an approach neither equal resonance of the cavity nor equal sensitivity of the receiving system need be assumed, and in addition, the power need not be equally devided between the two frequencies. If the load reflection is independent of frequency over the small variation in question, the,

$$\frac{1}{(SWR)^2_{measured}} = \frac{1}{(SWR)^2_{true}} + \frac{1}{1-\rho} \left(\frac{X \quad \lambda}{\lambda}\right)^2 \quad \frac{2\rho}{1+\rho^2} \left(\frac{\Delta f}{f}\right)^2$$

gives the measured standing-wave ratio at a distance X from the interface in terms of it's true values and the ratio ρ^2 of received powers at frequencies f, $f + \Delta f$. The aboveresult was obtained for direct measurement of the power standing -wave ratio as the ratio of maximum to minimum.

3) WALL-LOSSES:

Another type of error may be encountered during measurement, which is known as wall-loss. This is the loss introduced by the waveguide which has been neglected so far. This loss is not the same with the filled as with the empty guide, for not only are the energy relations changed by the presence of a dielectric, but the field in the sample is often a standing-wave field rather than the travelling-wave field formerly obtained. The error is accordingly not cancelled by the bridge procedure as would perhaps be expected and special composition is necessary. If the empty guide were completely loss less,

$$(\tan \delta_{measured}) = (\tan \delta_{sample}) + (\tan \delta_{wall})$$

Would be obtained when measuring the transmission of the sample contained in a piece of the actual lossy guide. The condition of the zero loss, for the empty guide may be simulated if the substitution is made,

$$t = t_{measured} \exp \left[\left(-\frac{\pi d}{\lambda} \right) (\tan \delta_{wall}) \sqrt{1-P} \right]$$

and hence wall losses may be readily corrected where as $\tan \delta_{wall}$ is known. To determine this parameter, 't' is measured with two widely different lengths of empty guide, where-upon the appropriate form of the equation,

$$\tan = -\frac{\lambda \sqrt{k - P}\ \tan t}{\pi k d} + O(\tan^2 \delta)$$

with $k = 1$ and t = ratio of transmission, gives the desired result. Since, the loss is of concern here rather than k, the large path difference used for finding $\tan \delta_{wall}$, with consequent magnification of the effect of frequency drift, causes no undue error in normal practice.

4. ERROR DUE TO CLEARENCE BETWEEN THE SAMPLE AND THE GUIDE:

Another sources of error is the clearence between the sample and the guide, which is necessarily present to some extent in all methods not carried out with the sample in free-space. Although the exact theoretical results are available for the situation illustrated in the Fig-7A , it suffices here to give the empirical equation,

$$k_{true} = (k_{measured} - 1) \frac{b}{b'} + 1$$

which has been experimentally varified in a number of ccases (Rf-4a). The stated dependence on b' is suggested by the uniformity of the E-field in the vertical direction; that the result is substantially independent of a' for small clearence, fallows from the fact that the field is zero at the sides of the guide. Corrections for clearence may be given in other cases, for example, for round or co-axial wave-guides, although it is usually necessary to assume that the sample is centered for an exact theoretical derivation. It must be mentioned that errors from clearence can be greatly reduced by use of a mode in which the E-field is tangential to the inner surface of the guide at all points. The field must then be nearly zero at the edge of the sample, and hence, for all dimensions, a reduction of error is obtained which is similar to that noted in connected with dimension a'. An example of such a mode is the TE_{10}-mode in circular wave-guide, which was suggested and actually used in (Rf Ba) as a neams of eliminating this source of error.

7.3: CLASSIFICATION OF THE NATURE OF SOIL SAMPLES:

So far, the measuring procedure and it's draw backs have been discussed. It has already been mentioned that, the variation of dielectric constant with respect to the frequencies have been observed, curves have been plotted having dielectric constant VS. frequency . It will be shown that some peculiar nature of these curves hayve been found. To explain the nature of these curves one should have at least some idea about the chemical composition of the soil-samples that have been investigated. For this reason, minenalogical datas of the soil-samples have been described.

So, before going into the detail discussion of the results, that have been achived, a brief mineralogical study report on which soil- classifications and soil-constituents of Bangladesh are based have been given. This report have been summerised from a paper published by H.C.J. Huizing(F AO Associate Export) in 1970 during a reconniaisance study of the mineralogy of sand fractions from Bangladesh sediments and soils.

Without going into detail discussion of the Bangladesh soil, a brief results of the mineralogial study will be presented here. Most of the sands appear to have been derived from a wide variety of rocks and in consequence, a high dose of percentage concentration of different minerals is found in the soil. To classify the types of soil, different minerals species have been grouped togather to forms, as far as possible, natural mineral groups. A short description of the textuaral classification and mechanical composition of the investigated soil has been given in table 4.

<u>TABLE - 5</u>

Code No.	Place of Collection	Parant Location and Physiography	Textural Classification	Colour	Mechanilal Composition			Soil Series
					Clay	Silt	Sand	
1	Tonti	Deeply weathered Modhupur Clay	City Clay	Strongly mottled red and gray	53%	30%	17%	
2	Mirpur Top soil	Moderately weathered , Modhupur clay		Mottled Pale brown & Grey	58%	25%	17%	
3	Joydevpur	Digraded Modhupur clay		Grey, weakly, mottled with brown & white.	28%	65%	7%	Chiata
4	Engg. Varsity	Deeply weathered Modhupur clay		Red-brown mottled with grey	53%	30%	17%	
5	Chittagong Hill area(cant)	Deposits of Deyn Tila formation	Fine sandy loan	Brown with some gray mottles	12%	15%	73%	Khadim Nagar
6	Chittagong Port Area.	Piedment alluvial plain	Fine Sandy loan	Grey, weakly mottled with brown	12%	30%	58%	Bijipur
7	Chittagong Town Area	Recent piedment alluvium	Loamy fine sand	Grey, weakly mottled brown loamy sand	8%	8%	84%	Hoanak
8	Feni(5 miles N.W. along DA-Trunk Rd	Old Meghna Estuarine flood plain	Silt loam	Grey	20%	70%	10%	Tippara
9	Dawood Kindi	Young Meghna Deposit, middle Meghna flood plain	Silt loam	Grey	25%	70%	5%	Fuldi
10	Narayanganj	Recent Brahmaputra deposit mixed with Modhupur Clay	Clay loam (loam of Brahmaputra alluvial + clay of Modhupur clay		35%	55%	10%	

The table shows the classification of the investigated soil-samples. This classification has been performed on the basis of some experiments done by the department of Bangladesh soil survey office under the supervision of Mr. Shahidul Islam(Asstt. Director, Bangladesh soil survey department). For convenience, a physiographic map of Bangladesh has also been shown in Fig-17 which indicates the various classes of soil described in the table-4.

On the basis of the above classification and a mineral-logical report published by H. C. J. Huizing (F A O Associate Expert), the mineralogical ingredients have been roughly estimated. The estimation have been shown in the table 6.

TABLE 6:

Code No. of sample:	Non trans-parent	Aggreg-ate	Heavy mineral	Mica	Alkali-field spar	Plagio-cb_u		Carbo-nate:
1, 2, 3, 4	11	.25	.8	1.1	4.25	2.0		-
5	7	1	1	2	12	4		-
7								-
8	6	1.8	5.6	10	13	11		-
9	4	1	2	71	2	3		-

*

From, the above table it is seen that in most cases, the largest component of the soil constituents are quartz and in some cases are mica. Among other constituents, non-transparent materials and alkali-fields-par are main. except these constituents there may be some gases which may normally be trapped in the perfor-ated soil samples. However, to explain the nature of the curves obtained, one should have a complete theoretical idea about the nature of the variation of permittivity of gases and solids with the applied frequency of the electromagnetic fields. For this reason, a brief discussion on the variation of the permittivity with frequency have been presented in the appendix-

* The results shown in the above Table are supplied by soil survey department (Bangladesh) and require some further clarification. Due to some inconveniences these could not be performed within our limited facilities.

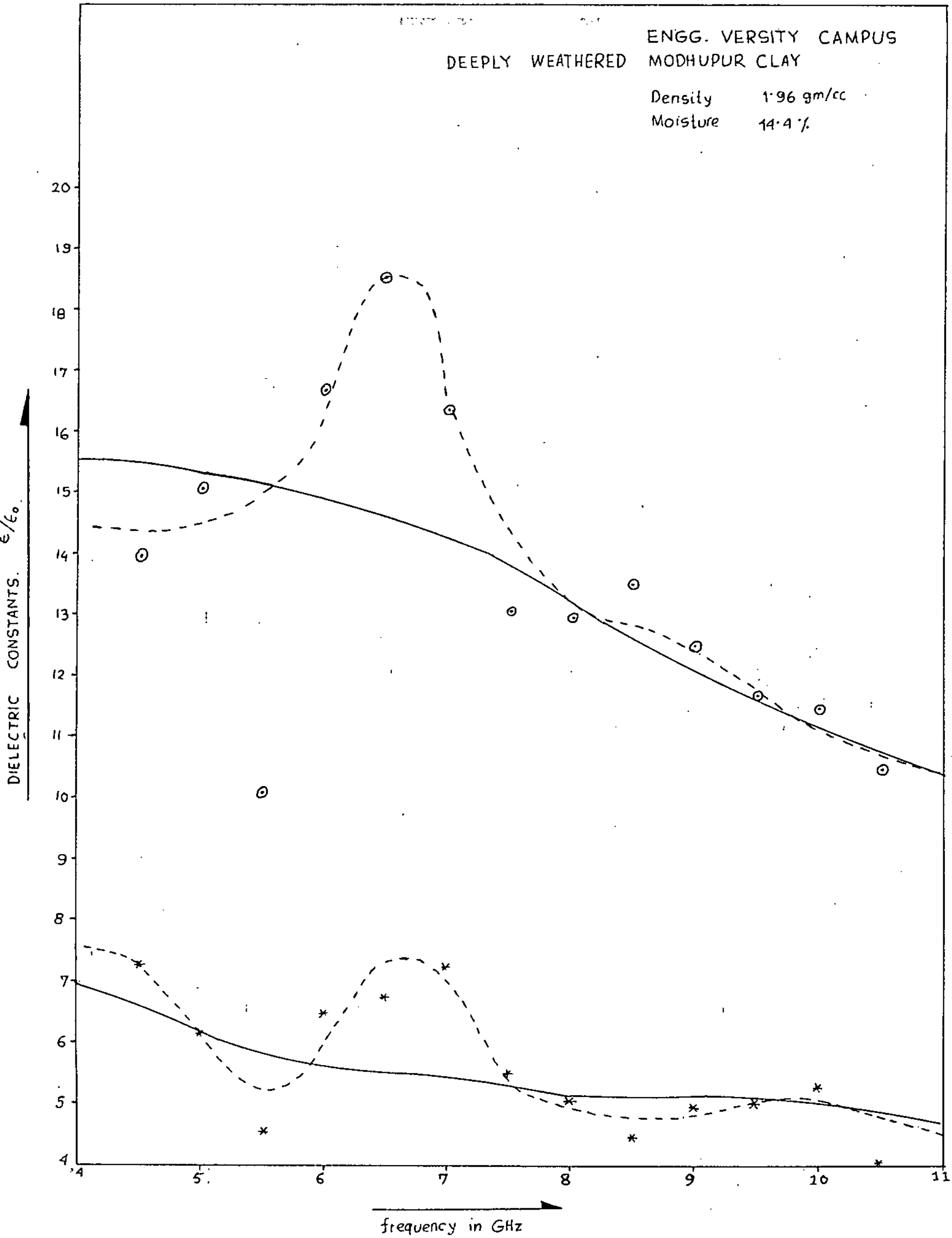
ENGG. VERSITY CAMPUS
DEEPLY WEATHERED MODHUPUR CLAY
Density 1·96 gm/cc
Moisture 14·4 %
DIELECTRIC CONSTANTS. ε′/ε₀
20
19
18
17
16
15
14
13
12
11
10
9
8
7
6
5
4
4
5
6
7
8
9
10
11
frequency in GHz

TABLE 1A

f in GHz	10·5	10	9·5	8·5	9·0	8·0	7·5	7·0	6·5	6·0	5·5	5·0	4·6
VSWR	4·3	4·4	4·5	5·8	5·0	6·4	7·2	5·2	5·48	5·9	5·9	8·1	10·0
	4·3	4·45	4·5	5·85	4·9	6·3	7·4	5·6	5·52	6·0	5·9	8·2	10·0
	4·3	4·45	4·5	5·8	4·9	6·3	7·3	5·6	5·38	6·05	5·9	8·2	10·1
	4·5	4·5	4·75	6·3	5·15	6·2	7·2	4·3	5·5	4·62	4·7	6·15	9·5
	4·45	4·6	4·8	6·2	5·2	6·2	7·3	4·5	5·6	5·4	4·75	5·8	10·0
	4·45	4·75	4·7	5·35	5·08	6·15	7·4	4·5	5·4	5·4	5·4	4·6	10·0
	4·5	4·75	4·73	5·38	5·18	6·15	7·3	5·6	6·3	6·2	4·2	7·3	10·5
	4·5	4·8	4·8	5·4	5·15	6·2	7·3	5·6	6·35	6·2	4·5	7·3	10·5
	4·55	4·8	4·8	5·5	5·2	6·2	7·2	5·5	6·3	6·2	4·5	7·35	10·8
	3·8	4·5	4·15	5·8	5·4	6·0	7·5	5·1	5·5	5·6	4·3	7·4	10·0
	3·75	4·55	4·15	5·9	4·9	6·0	7·4	5·0	5·5	5·6	4·3	7·4	10·0
AVERAGE													
S_{av}	4·06	4·4	4·46	5·72	5·086	6·12	7·36	5·14	5·71	5·74	4·87	7·23	10·05
ρ	·605	·63	·645	·702	·67	·72	·76	·67	·70	·703	·66	·76	·82
K	10·416	11·45	11·66	13·49	12·47	12·92	13·06	16·39	18·57	16·66	10·03	15·03	13·98

TABLE 1B (DRY)

VSWR	2·3	2·9	3·15	3·0	3·2	3·5	4·71	3·35	3·3	3·5	3·05	4·7	6·9
	2·5	2·9	3·15	3·0	3·15	3·7	4·7	3·4	3·45	3·6	3·25	4·55	7·1
	2·25	2·9	3·0	3·15	3·04	3·8	4·6	3·35	3·40	3·5	3·25	4·5	7·1
	2·6	3·0	2·92	3·55	3·08	3·85	4·5	3·4	3·3	3·5	3·1	4·8	7·0
	2·6	3·0	2·9	3·6	3·15	4·0	4·55	3·3	3·5	3·6	3·3	4·5	6·9
	2·55	3·05	2·95	3·58	3·07	3·9	4·5	3·35	3·4	3·55	3·25	4·5	7·1
AVERAGE													
S_{av}	2·47	2·96	3·01	3·13	3·12	3·79	4·59	3·36	3·39	3·54	3·2	4·59	7·02
R	·424	·495	·501	·516	·515	·582	·642	·541	·544	·559	·523	·642	·751
K	4·1	5·41	5·19	4·54	5·08	5·31	5·64	7·41	6·91	6·63	4·63	6·32	7·39
K_{cor}	4·02	5·29	5·08	4·46	4·97	5·20	5·52	7·24	6·75	6·48	4·53	6·18	7·22

ENGG. VERSITY SOIL

TABLE 1A → Moisture 14·4%
TABLE 1A → Density 1·96 gm/cc

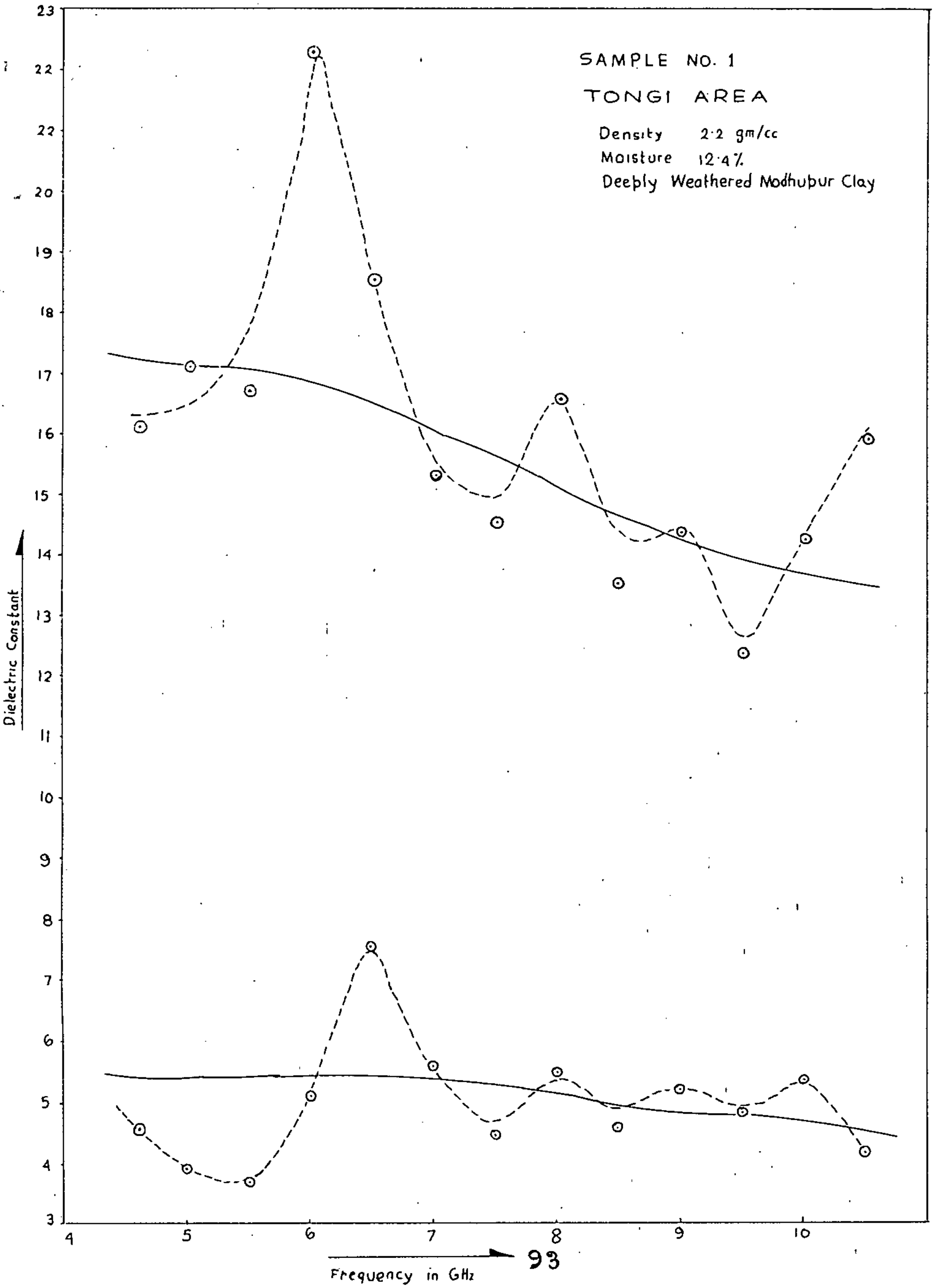
SAMPLE NO. 1
TONGI AREA
Density 2·2 gm/cc
Moisture 12·4%
Deeply Weathered Modhupur Clay
Dielectric Constant
Frequency in GHz
23
22
22
20
19
18
17
16
15
14
13
12
11
10
9
8
7
6
5
4
3
4
5
6
7
8
9
10

TABLE. 3A

f in GHz	4.6	5.0	5.5	6.0	6.5	7.0	7.5	8.0	8.5	9.0	9.5	10.0	10.5
VSWR	10.6	7.2	6.3	6.5	5.7	5.05	7.3	6.6	5.9	5.65	5.1	5.22	5.22
	10.8	7.7	6.2	6.5	5.8	5.1	8.6	7.0	5.6	5.7	4.8	5.23	4.8
	10.5	7.6	6.25	6.4	5.8	5.2	8.0	6.8	5.7	5.7	4.9	5.2	5.0
	10.7	8.2	6.7	6.8	5.6	4.8	7.4	6.8	5.4	5.4	4.4	4.75	5.3
	10.8	8.2	6.45	6.5	5.6	4.7	7.7	7.0	5.4	5.38	4.4	4.75	5.05
	10.6	8.2	6.6	6.6	5.6	4.75	7.7	7.1	5.6	5.5	4.3	4.75	5.05
	10.7	8.3	6.7	6.7	5.7	4.7	7.6	7.0	5.6	5.4	4.25	4.8	5.2

AVERAGE

S	10.67	7.9	6.46	6.57	5.69	4.9	7.76	6.9	5.6	5.53	4.59	4.96	5.08
ρ	.83	.775	.73	.74	.70	.66	.77	.75	.70	.69	.64	.66	.67
k	16.11	17.1	16.72	22.32	18.58	15.27	14.5	16.55	13.48	14.40	12.28	14.26	15.92

TABLE 3B (DRY)

VSWR	5.1	3.35	3.32	3.02	3.0	2.8	4.0	4.1	3.08	3.3	2.9	3.0	2.5
	5.2	3.25	3.35	3.15	3.0	2.9	3.95	4.15	3.1	3.4	2.9	3.0	2.5
	5.8	3.8	3.6	3.05	3.1	3.0	4.1	3.7	3.05	3.15	2.95	2.95	2.4
	5.4	3.7	3.4	3.1	3.0	2.9	4.1	3.71	3.08	3.13	3.0	2.9	2.5
	5.2	3.4	3.3	3.1	3.02	2.9	4.0	3.8	3.2	3.02	2.8	3.0	2.55
	5.1	3.1	3.2	3.06	3.05	3.0	4.0	3.85	3.1	3.0	2.9	3.0	2.5

AVERAGE

S	5.3	3.43	3.36	3.08	3.58	2.92	4.03	3.89	3.1	3.17	2.91	2.98	2.49
ρ	.683	.549	.541	.510	.563	.490	.602	.590	.512	.521	.488	.497	.427
K	4.61	3.93	3.73	5.16	7.7	5.71	4.52	5.55	4.63	5.26	4.88	5.46	4.16
K_c	4.51	3.85	3.66	5.05	7.52	5.58	4.43	5.43	4.53	5.15	4.78	5.34	4.08

SAMPLE FROM TONGI

TABLE A — Density 2.2 gm/cc; Moisture 12.04%

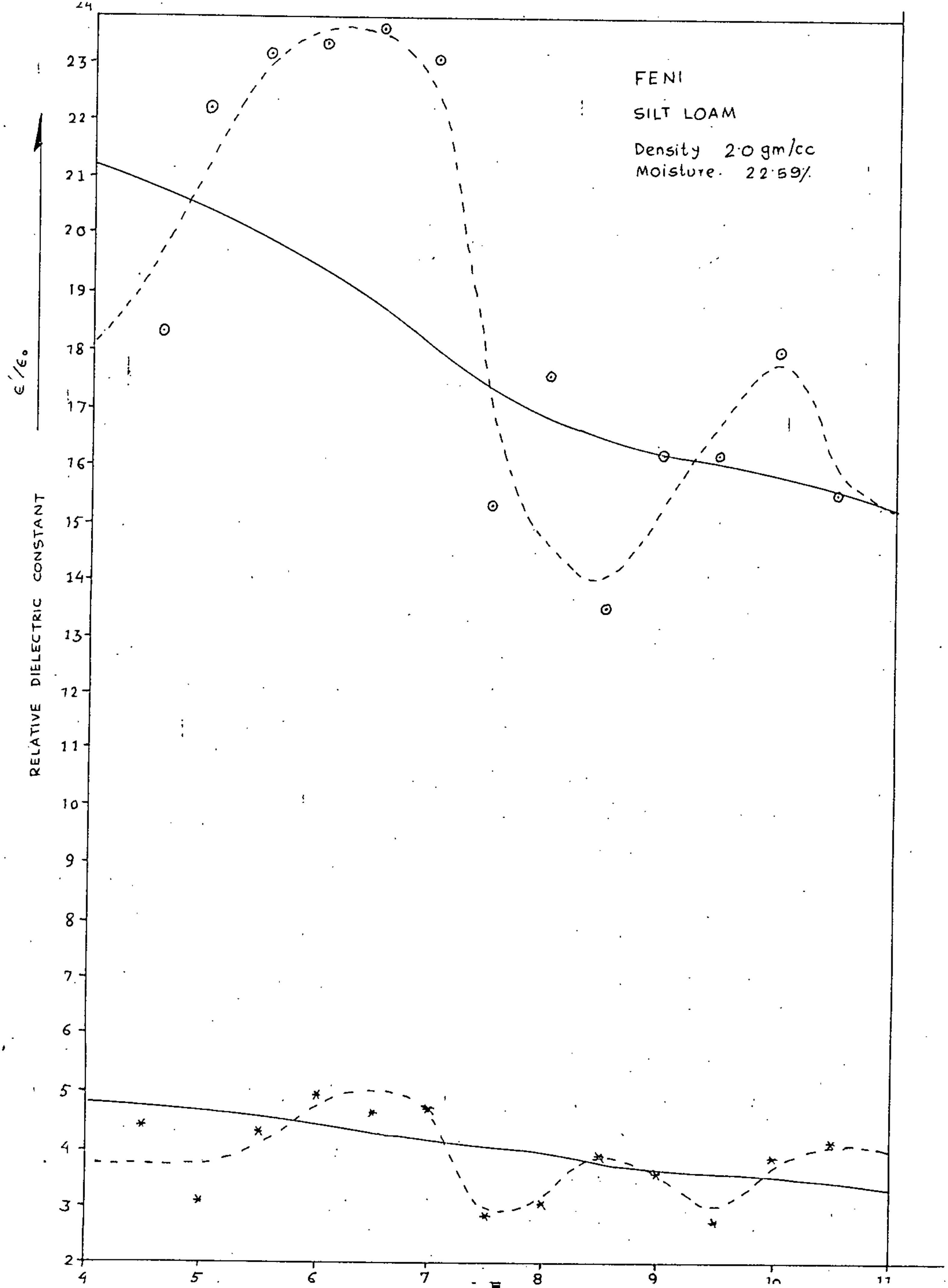
FENI
SILT LOAM
Density 2·0 gm/cc
Moisture 22·59%
RELATIVE DIELECTRIC CONSTANT
ε′/ε₀
24
23
22
21
20
19
18
17
16
15
14
13
12
11
10
9
8
7
6
5
4
3
2
4
5
6
7
8
9
10
11

TABLE 4 A

f in GHz	4·6	5·0	5·5	6·0	6·5	7·0	7·5	8·0	8·5	9·0	9·5	10·0	10·5
VSWR	11·2	8·3	7·5	6·7	6·2	5·9	8·3	7·4	5·9	5·8	5·6	5·7	5·0
	11·15	8·2	7·4	6·8	6·2	5·9	8·1	7·3	5·7	5·9	5·8	5·8	4·9
	11·8	9·6	7·6	6·8	6·5	5·8	7·5	7·0	5·5	5·8	5·3	5·4	5·0
	11·9	9·6	7·5	7·0	6·6	5·85	7·8	7·2	5·7	5·7	5·3	5·4	5·0
	11·6	9·5	7·7	7·0	6·35	6·0	7·9	7·1	5·6	5·8	5·4	5·5	4·95
	11·6	9·5	7·8	6·8	6·6	6·3	7·95	7·1	5·7	5·8	5·5	5·6	5·0

AVERAGE

S	11·54	9·12	7·6	6·85	6·41	5·96	7·93	7·18	5·68	5·8	5·48	5·57	4·975
ρ	·84	·80	·767	·745	·73	·713	·776	·756	·70	·705	·691	·695	·665
K	18·33	22·2	23·33	23·46	23·6	23·02	15·34	17·47	13·48	16·17	16·16	17·98	15·42

TABLE 4 B (DRY)

VSWR	5·4	3·0	3·2	3·0	2·8	2·6	3·0	2·8	2·9	2·5	2·1	2·45	2·4
	5·5	3·0	3·2	3·0	2·8	2·7	3·02	2·9	2·95	2·5	2·1	2·5	2·7
	5·3	3·1	3·35	3·1	2·8	2·8	3·06	2·6	3·05	2·8	2·05	2·55	2·6
	4·95	3·15	3·2	3·0	2·7	2·6	3·05	2·7	3·0	2·6	2·1	2·5	2·5
	5·2	3·0	3·25	3·2	2·8	2·7	3·04	2·8	3·0	2·7	2·15	2·45	2·5
	5·5	3·1	3·18	3·1	2·75	2·65	3·0	2·8	2·9	2·6	2·2	2·55	2·45

AVERAGE

S	5·31	3·06	3·23	3·07	2·78	2·68	3·03	2·77	2·97	2·62	2·12	2·5	2·53
ρ	·683	·507	·527	·509	·471	·456	·504	·469	·496	·448	·359	·429	·433
k	4·61	3·21	4·5	5·16	4·8	4·85	x4·89	3·16	4·13	3·75	2·82	3·99	4·28
K_c	4·42	3·09	4·31	4·94	4·60	4·65	2·79	3·04	3·96	3·60	2·72	3·83	4·11

SAMPLE FROM FENI RIVER COASTAL AREA

TABLE 4A → Density 2·0 gm/cc
→ Moisture 22·59%

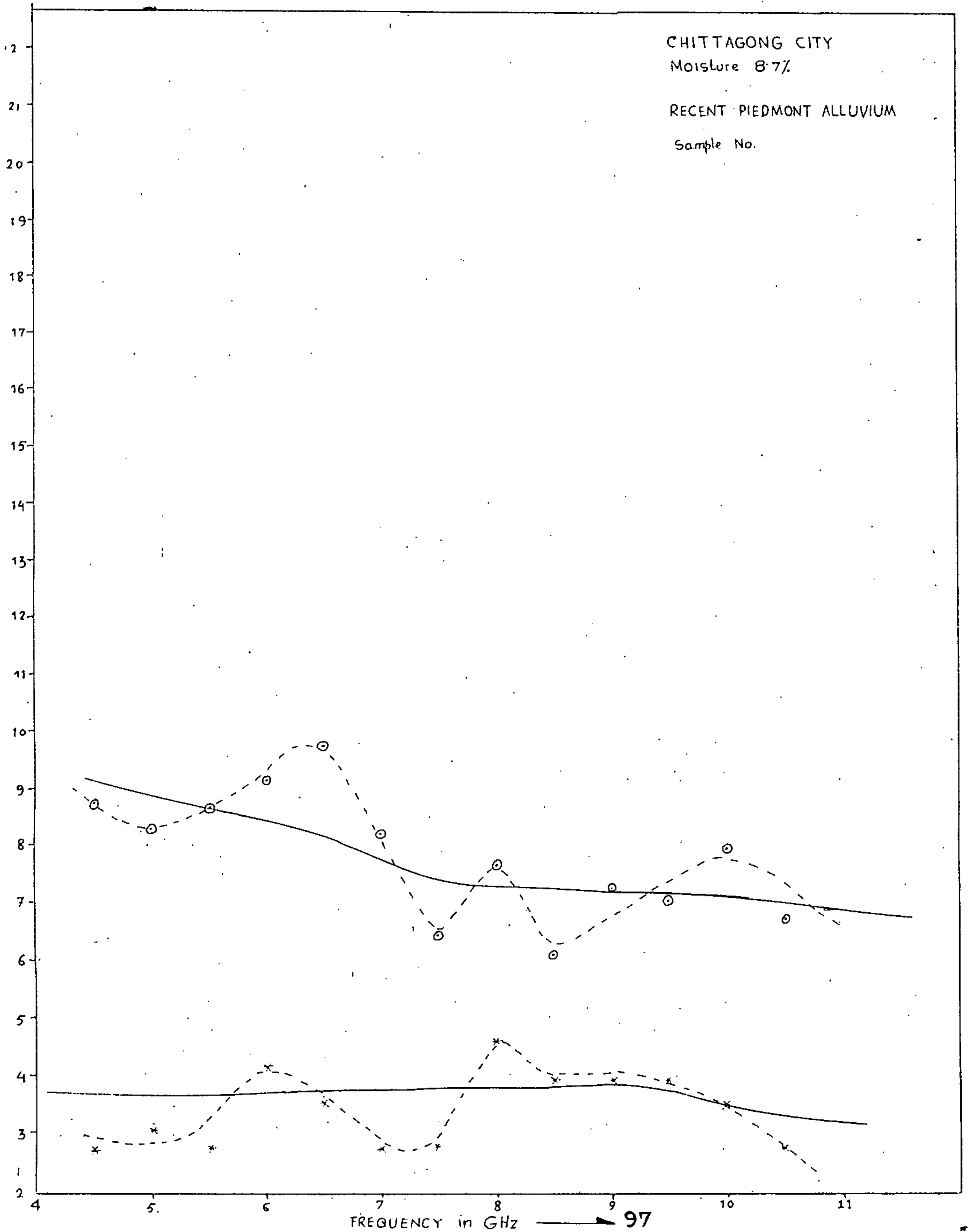
CHITTAGONG CITY
Moisture 8·7%
RECENT PIEDMONT ALLUVIUM
Sample No.
FREQUENCY in GHz

TABLE 6A

f in GHz	4·6	5·0	5·5	6·0	6·5	7·0	7·5	8·0	8·5	9·0	9·5	10·0	10·5
VSWR	8·0	4·8	4·5	3·85	3·83	3·38	4·8	4·5	3·72	3·8	3·75	3·8	3·5
	8·0	4·4	4·4	3·7	3·75	3·3	4·85	4·55	3·75	3·72	3·7	3·7	3·4
	7·5	5·6	4·5	4·4	4·0	3·5	5·1	4·65	3·65	3·8	3·5	3·65	3·38
	7·5	5·6	4·5	4·3	4·1	3·6	5·0	4·7	3·65	3·83	3·5	3·4	3·0
	7·7	5·8	4·6	4·5	4·0	3·7	5·0	4·65	3·8	3·8	3·4	3·8	3·0
	7·8	5·7	4·7	4·5	4·2	3·8	5·0	4·7	3·7	3·88	3·45	3·5	3·1

AVERAGE

S	7·75	5·32	4·53	4·21	4·06	3·55	4·96	4·63	3·71	3·80	3·55	3·64	3·23
ρ	·771	·684	·638	·616	·605	·560	·664	·645	·575	·583	·561	·569	·527
K	8·77	8·33	8·66	9·18	9·75	8·21	6·43	7·63	6·09	7·24	7·06	7·95	6·71

TABLE 6B (DRY)

VSWR	4·0	3·0	2·2	2·5	2·38	1·96	2·95	3·5	2·9	2·6	2·5	2·4	1·9
	4·0	3·0	2·19	2·6	2·4	1·9	3·0	3·4	2·8	2·6	2·5	2·3	2·0
	3·5	3·0	2·5	2·6	2·3	1·95	2·9	3·5	2·8	2·7	2·6	2·4	2·0
	3·55	3·0	2·55	2·6	2·3	1·9	2·95	3·4	2·7	2·6	2·55	2·3	1·9
	3·8	2·9	2·3	2·5	2·35	2·0	3·0	3·6	2·9	2·8	2·5	2·2	2·0
	3·9	2·9	2·35	2·6	2·38	2·05	3·0	3·5	3·0	2·7	2·6	2·4	2·05

AVERAGE

S	3·79	2·97	2·35	2·57	2·35	1·96	2·97	3·48	2·85	2·67	2·54	2·33	1·98
ρ	·582	·496	·403	·44	·403	·324	·496	·554	·481	·455	·435	·399	·329
K	2·75	3·05	2·78	4·16	3·56	2·77	2·8	4·61	3·87	3·87	3·88	3·51	2·76
K_c													

SAMPLE FROM CHITTAGONG CITY

Moisture 8·7%

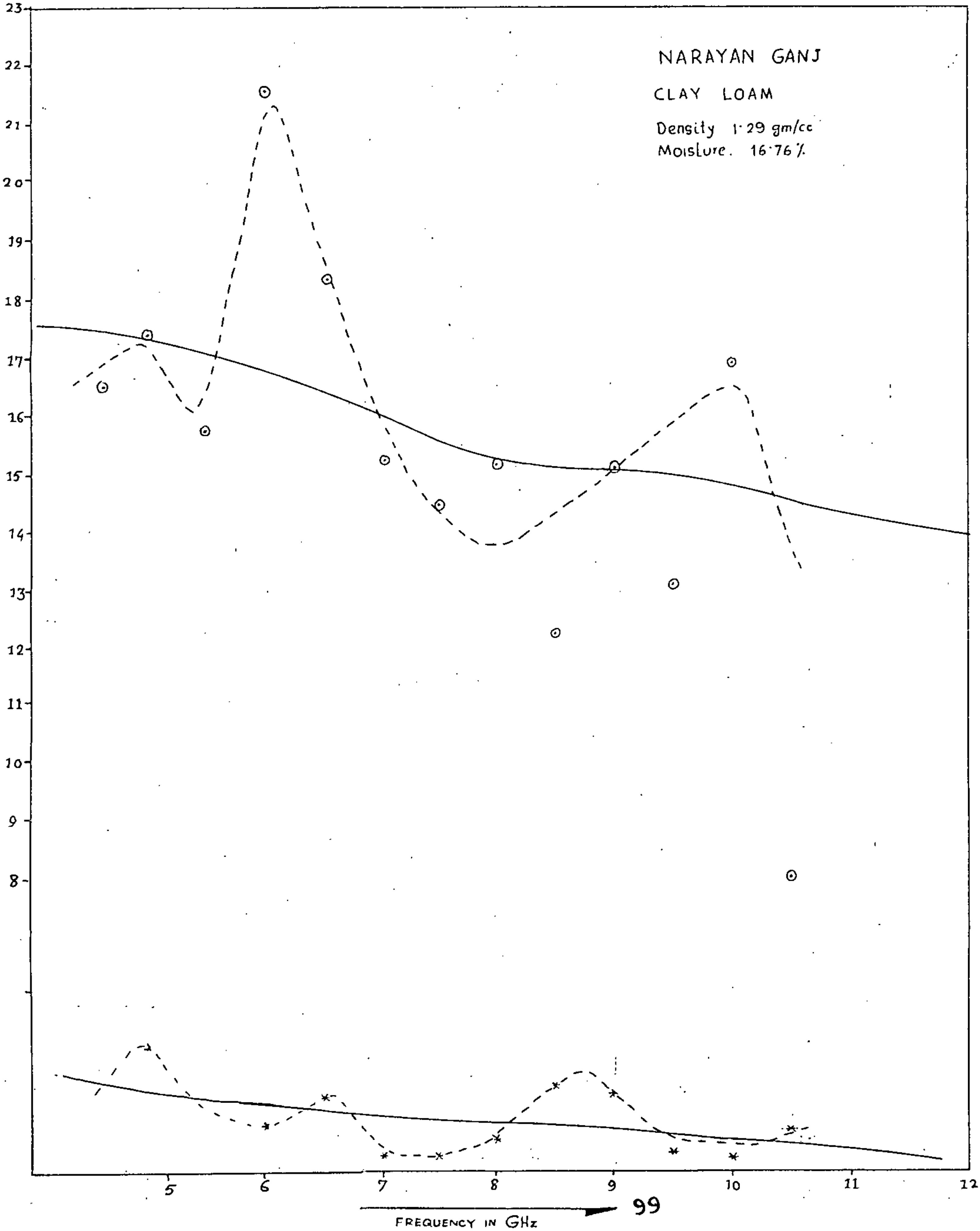

NARAYAN GANJ
CLAY LOAM
Density 1·29 gm/cc
Moisture. 16·76%
23
22
21
20
19
18
17
16
15
14
13
12
11
10
9
8
5
6
7
8
9
10
11
12
FREQUENCY IN GHz

TABLE 9A

f in GHz	4·6	5	5·5	6·0	6·5	7·0	7·5	8·0	8·5	9 0	9·5	10·0	10·5
VSWR	10·0	6·7	6 0	6·0	5·2	4 7	8·0	6·7	5·55	5·65	4 7	5·5	2 65
	10·0	6 9	6·1	6·3	5·2	4·5	7 7	6 8	5·45	5·55	4·7	5·4	3·1
	10·2	8·4	6·2	6·5	5·9	5·0	7·7	6·8	5·25	5·65	4·75	5·2	3·45
	10·4	8·0	6·2	6·5	5·7	4·8	7·7	6 8	5·3	5·6	4·7	5·45	4·1
	10·6	6·3	6·5	7·0	5·9	5·0	7·85	6·7	5·4	5·5	4·8	5·3	4·0
	10·5	8 2	6·4	7·1	5·8	5·1	7·8	6·8	5·35	5·6	4·85	5·4	3·8

AVERAGE

S	10 28	7 75	6·23	6 57	5·62	4·85	7 79	6·77	5·38	5·59	4·75	5 38	3·52
ρ	·82	·77	·723	736	·698	·66	·77	·74	·687	·696	·65	·686	·56
K	16·51	17·4	15·76	21·6	18·34	15·27	14·45	15·19	12·24	15·11	13·12	16·19	8·01

TABLE 9B (DRY)

VSWR	4·6	4 1	2·9	2·9	2·45	2·1	3·2	2·9	3 1	2·8	2·2	2·3	2·3
	4·5	3·9	2·8	2·9	2·4	2 1	3·18	2·9	3 1	2·8	2·25	2·35	2·3
	4 6	4·0	3·1	2·3	2·8	2·2	3·3	3·0	3·12	2·9	2·5	2·3	2·4
	4·7	4·3	3·1	2·4	2·7	2·15	3·3	3·05	3·1	2·9	2·4	2·35	2·3
	4 65	4·2	3·0	2 6	2·6	2·2	3·4	3 0	3·05	2·9	2·3	2·3	2 4
	4·75	4·1	3·05	2 5	2·65	2·1	3·35	2·95	3·1	2·95	2·4	2·3	2·35

AVERAGE (DRY)

S	4·63	4 1	2 99	2·6	2·6	2 14	3·29	2·97	3·31	2·88	2·34	2·32	2·34
ρ	·645	·608	·499	·444	·444	·363	·534	·496	·512	·484	401	·38	·401
k	3·7	5·18	4·13	3·82	4·25	3·24	3·27	3·52	4·45	4·39	3·33	3·25	3·71
k_c	3·66	5·12	4·09	3·78	4·21	3 21	3·24	3·49	4·40	4·34	3·30	3·22	3·67

SAMPLE FROM NARAYN GANJ

TABLE A → Density 1·29 gm/cc

TABLE A → Moisture 16·76%

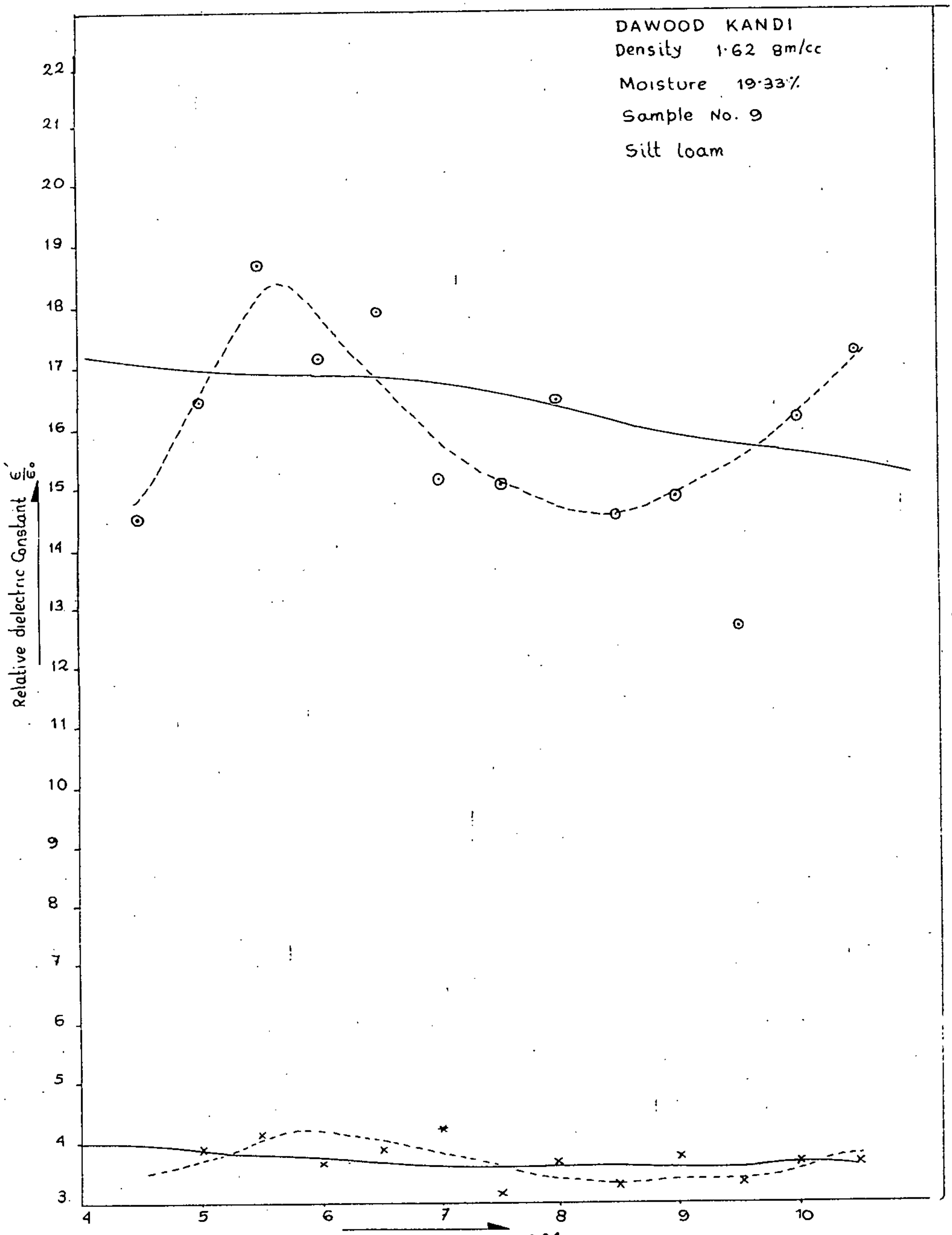
DAWOOD KANDI
Density 1·62 gm/cc
Moisture 19·33%
Sample No. 9
Silt loam
Relative dielectric Constant ε′/ε₀
FREQUENCY IN GHz

TABLE 8A

f in GHz	4.6	5.0	5.5	6.0	6.5	7.0	7.5	8.0	8.5	9.0	9.5	10.0	10.5
VSWR	10.0	7.7	6.7	5.5	5.5	4.8	7.6	7.2	5.8	5.6	5.0	5.4	5.1
	10.2	7.8	6.7	5.8	5.4	4.9	7.4	6.9	6.0	5.5	4.9	5.4	5.2
	10.4	8.0	6.9	6.0	5.7	4.9	8.0	7.0	6.0	5.45	4.8	5.6	5.4
	10.5	7.9	6.9	6.0	5.8	4.8	8.1	6.8	6.1	5.55	4.6	5.0	5.2
	10.3	7.8	6.8	5.8	5.5	4.9	8.0	6.9	5.8	5.6	4.8	4.9	5.4
	10.2	7.8	6.7	5.9	5.4	4.8	7.9	7.0	5.85	5.5	4.8	5.2	5.3

AVERAGE

S	10.27	7.83	6.78	5.83	5.55	4.85	7.88	6.97	5.93	5.53	4.83	5.25	5.27
ρ	.822	.773	.743	.707	.695	.658	.775	.749	.711	.694	.657	.68	.681
K	14.55	16.43	18.69	17.11	17.89	15.06	15.03	16.41	14.57	14.82	12.61	16.15	17.21

TABLE 8B (DRY)

VSWR	4.5	3.55	3.0	2.6	2.5	2.5	3.1	3.0	2.5	2.65	2.4	2.45	2.25
	4.45	2.52	3.0	2.6	2.55	2.5	3.15	3.05	2.7	2.7	2.6	2.45	2.2
	4.5	3.5	2.9	2.55	2.45	2.45	3.3	3.1	2.65	2.6	2.3	2.35	2.25
	4.6	3.6	3.1	2.7	2.5	2.55	3.2	3.1	2.65	2.6	2.3	2.38	2.1
	4.7	3.5	3.2	2.5	2.6	2.6	3.3	3.15	2.7	2.65	2.35	2.4	2.2
	4.5	3.5	3.0	2.55	2.4	2.5	3.35	3.0	2.6	2.7	2.4	2.42	2.15

AVERAGE

S	4.54	3.53	3.03	2.58	2.5	2.52	3.23	3.07	2.63	2.65	2.39	2.41	2.19
ρ	.639	.558	.504	.441	.428	.432	.527	.509	.449	.452	.410	.413	.373
K	3.59	4.03	4.26	3.77	3.96	4.34	3.17	3.74	3.37	3.82	3.46	3.72	3.77
K_c	3.49	3.91	4.13	3.66	3.84	4.21	3.08	3.63	3.28	3.71	3.36	3.61	3.66

SAMPLE FROM DAWOOD KANDI

FOR TABLE A → Density 1.62 gm/cc
→ Moisture 19.33%

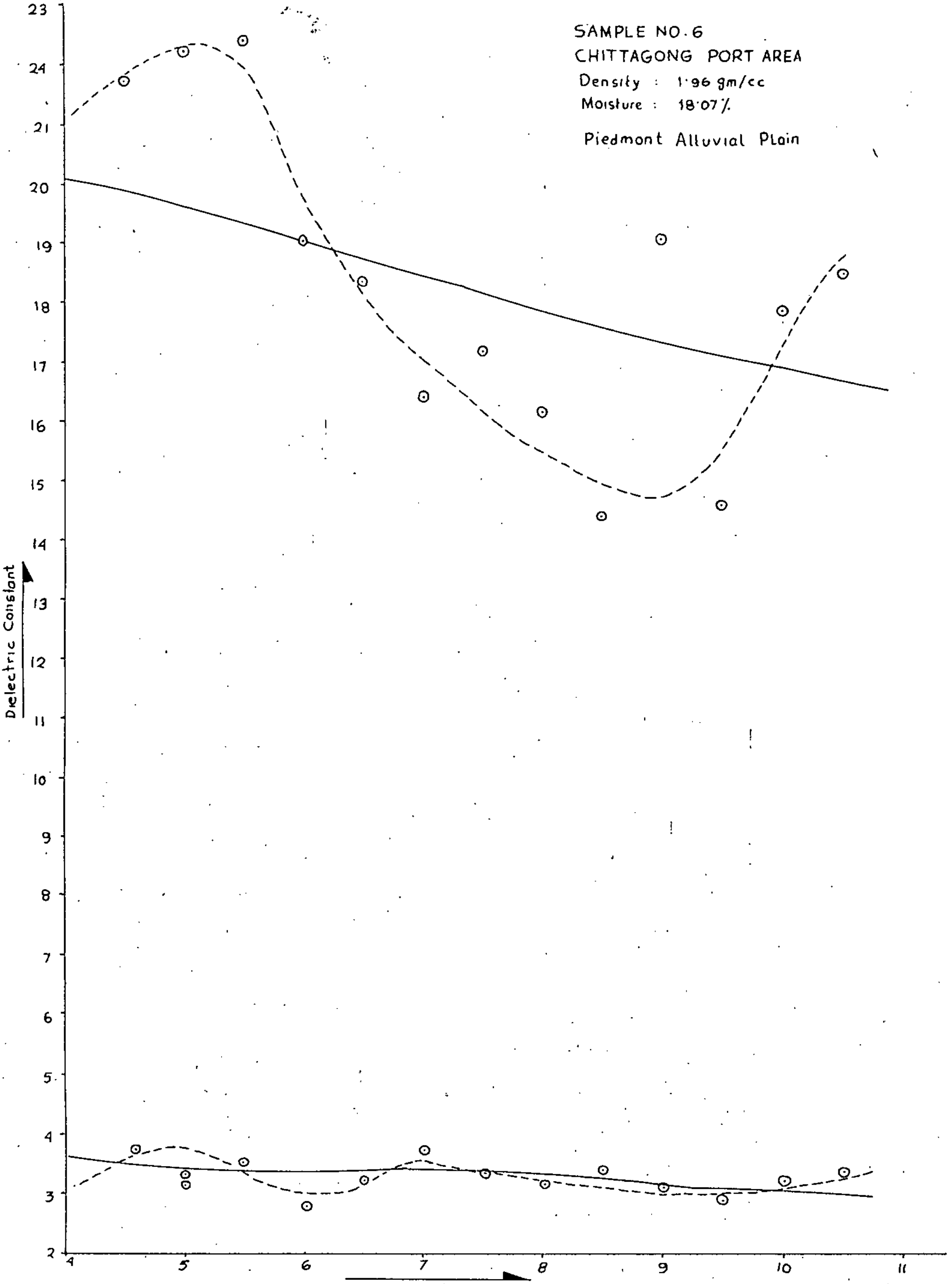
SAMPLE NO. 6
CHITTAGONG PORT AREA
Density : 1·96 gm/cc
Moisture : 18·07%
Piedmont Alluvial Plain
Dielectric Constant
frequency in GHz
23
24
21
20
19
18
17
16
15
14
13
12
11
10
9
8
7
6
5
4
3
2
4
5
6
7
8
9
10
11

TABLE 7 A

f in GHz	4·6	5·0	5·5	6·0	6·5	7·0	7·5	8·0	8·5	9·0	9·5	10·0	10·5
VSWR	12·8	9·0	7·4	6·1	5·55	4·85	8·4	7·0	5·8	6·4	5·3	5·5	5·4
	12·9	9·4	7·4	6·2	5·65	5·0	8·45	6·9	5·9	6·4	5·1	5·6	5·3
	12·0	9·0	7·5	6·2	5·65	5·1	8·3	6·8	5·8	6·3	5·0	5·5	5·1
	12·5	8·8	7·5	6·2	5·8	5·1	8·3	6·8	6·0	6·1	5·3	5·5	5·6
	12·55	8·9	7·5	6·1	5·5	5·2	8·35	6·9	5·9	6·3	5·25	5·6	5·5
	12·6	8·9	7·45	6·1	5·6	5·1	8·4	7·0	5·85	6·35	5·3	5·55	5·4

AVERAGE

S	12·56	9·0	7·46	6·15	5·63	5·06	8·37	6·9	5·88	6·31	5·21	5·54	5·4
ρ	·853	·80	·763	·720	·698	·67	·787	·747	·709	·726	·678	·694	·69
k	21·69	22·2	22·4	19·0	18·34	16·37	17·17	16·13	14·38	19·04	14·58	17·85	18·45

TABLE 7 B (DRY)

VSWR	4·6	3·2	2·75	2·35	2·4	2·3	3·2	2·7	2·6	2·3	2·2	2·05	2·3
	4·7	3·15	2·75	2·4	2·35	2·3	3·25	2·8	2·6	2·25	2·2	2·06	2·25
	4·8	3·2	2·8	2·4	2·4	2·35	3·4	2·85	2·7	2·45	2·18	2·35	2·2
	4·85	3·25	2·85	2·3	2·35	2·4	3·43	2·9	2·7	2·5	2·2	2·4	2·2
	4·9	3·1	2·7	2·35	2·3	2·25	3·46	2·8	2·65	2·4	2·15	2·2	2·3
	4·8	3·15	2·8	2·4	2·4	2·45	3·4	2·75	2·75	2·35	2·13	2·3	2·2

AVERAGE

S	4·775	3·175	2·775	2·37	2·37	2·34	3·37	2·8	2·67	2·38	2·18	2·23	2·24
ρ	·654	·521	·470	·407	·407	·402	·542	·474	·455	·407	·371	·381	·383
K	3·88	3·41	3·63	2·82	3·27	3·81	3·39	3·22	3·46	3·16	2·95	3·26	3·44
K_c'	3·78	3·33	3·54	2·77	3·19	3·72	3·31	3·15	3·38	3·09	2·89	3·19	3·36

SAMPLE FROM CHITTAGONG PORT AREA

TABLE A → Density 1·96 gm/cc
→ Moisture 18·07%

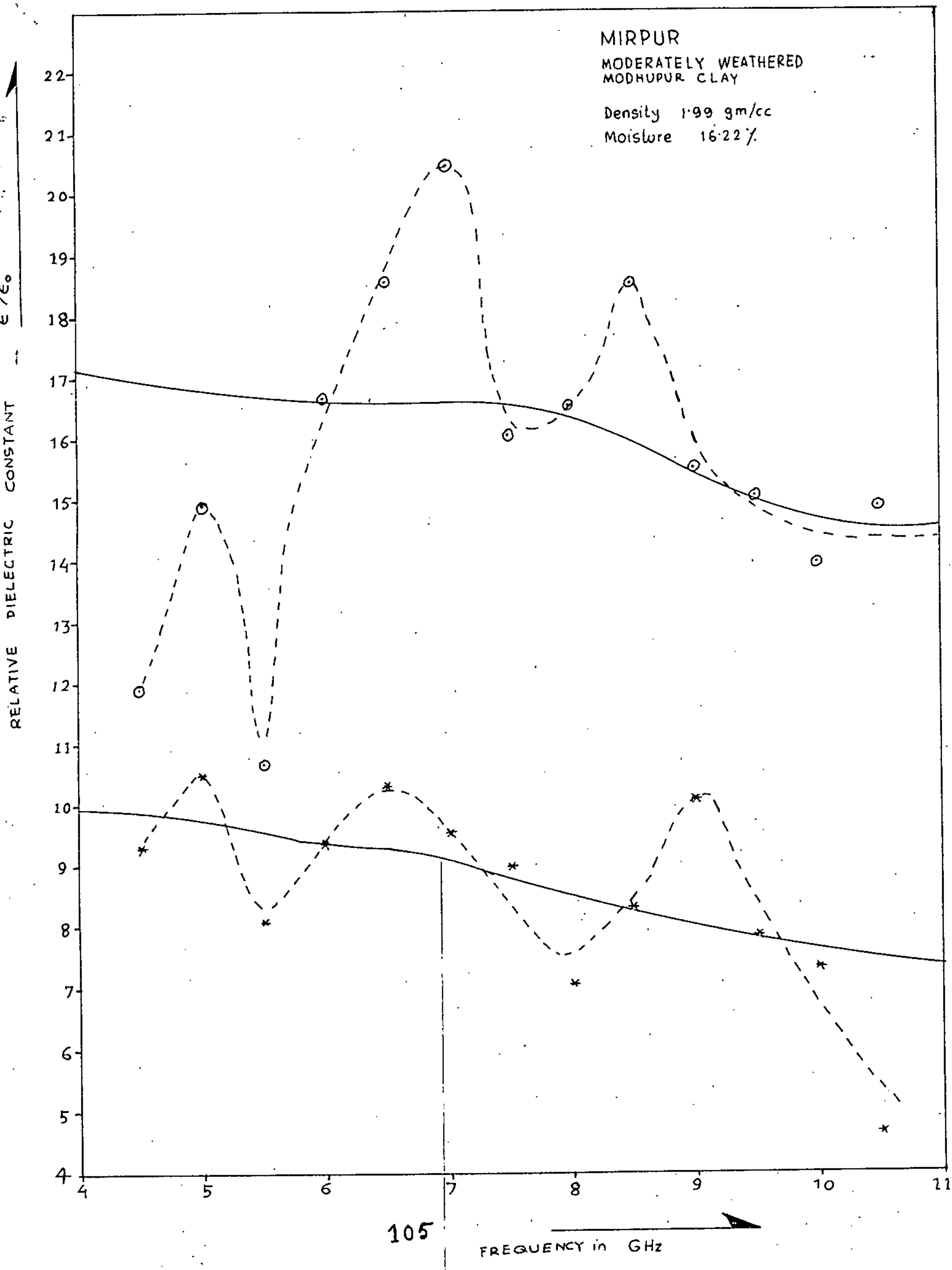
MIRPUR
MODERATELY WEATHERED
MODHUPUR CLAY
Density 1·99 gm/cc
Moisture 16·22%
RELATIVE DIELECTRIC CONSTANT
ε'/ε₀
FREQUENCY in GHz
4
5
6
7
8
9
10
11
12
13
14
15
16
17
18
19
20
21
22

TABLE. 2 A

freq. in GHz	4·6	5·0	5·5	6·0	6·5	7·0	7·5	8·0	8·5	9·0	9·5	10·0	10·5
VSWR	9·11	8·0	4·7	5·85	5·6	5·6	7·4	6·6	5·8	5·2	4·55	4·0	4·4
	9·1	8·0	4·8	5·8	5·6	5·5	7·4	6·5	5·8	5·2	4·6	3·75	4·16
	9·2	8·1	4·75	5·75	5·5	5·5	8·1	6·8	6·2	5·6	4·8	4·8	4·7
	9·1	7·0	5·4	6·0	5·5	5·6	8·1	6·8	6·2	5·58	4·9	4·78	4·8
	9·15	7·8	5·2	5·6	5·8	5·7	8·8	7·1	7·0	5·95	5·3	4·9	4·85
	9·1	7·9	5·35	5·4	5·6	5·6	8·7	7·0	6·9	5·7	5·5	4·8	4·6
	-	-	-	-	-	-	8·7	7·0	6·8	5·7	5·2	4·82	5·4
	-	-	-	-	-	-	8·0	7·35	6·7	5·85	5·35	5·42	5·4
	-	-	-	-	-	-	8·1	7·3	6·6	5·82	5·4	5·5	5·22
	-	-	-	-	-	-	-	7·3	6·7	6·1	5·48	5·3	5·25
	-	-	-	-	-	-	-	7·0	7·1	5·7	5·2	5·5	5·3
	-	-	-	-	-	-	-	6·9	7·0	5·6	5·0	5·3	5·15
	-	-	-	-	-	-	-	6·8	6·8	5·6	5·05	5·25	4·9

AVERAGE

S	9·14	7·92	5·03	5·73	5·6	5·58	8·16	6·96	6·58	5·66	5·1	4·93	4·93
ρ	·803	·76	·67	·703	·70	·70	·78	·75	·74	·70	·67	·66	·66
k	11·87	14·88	10·66	16·66	18·58	20·44	16·02	16·55	18·45	15·5	15·04	13·97	14·86

TABLE. 2 B (DRY)

VSWR	6·9	5·6	3·9	4·0	4·1	3·8	5·4	3·54	3·72	3·65	3·15	3·06	2·25
	7·8	6·0	4·0	4·0	4·3	3·81	5·36	3·75	3·83	3·65	3·15	3·05	2·1
	8·7	6·4	5·0	4·7	4·3	4·0	6·6	5·6	5·6	4·8	4·4	4·3	3·2
	8·0	6·0	4·5	4·6	4·3	3·9	6·5	5·5	5·15	4·37	4·65	4·1	2·9
	8·4	6·2	4·6	4·3	4·2	4·0	6·2	4·2	4·3	4·0	3·55	3·45	2·8
	7·9	6·0	4·35	4·3	4·25	3·9	6·3	4·3	4·1	4·0	3·66	3·48	2·81

AVERAGE

S	7·96	6·04	4·4	4·32	4·24	3·9	6·06	4·48	4·45	4·08	3·66	3·57	2·68
ρ	·78	·72	·63	·624	·628	·59	·717	·635	·633	·606	·57	·56	·456
k	9·59	10·79	8·23	9·67	10·56	9·78	9·27	7·19	8·52	10·33	8·04	7·56	4·74
k_c	9·36	10·53	8·08	9·36	10·3	9·49	8·99	7·02	8·32	10·02	7·85	7·34	4·62

SOIL SAMPLE FROM MIRPUR (WET)

TABLE 2A [Moisture 16·22%
Density 1·99gm/cc

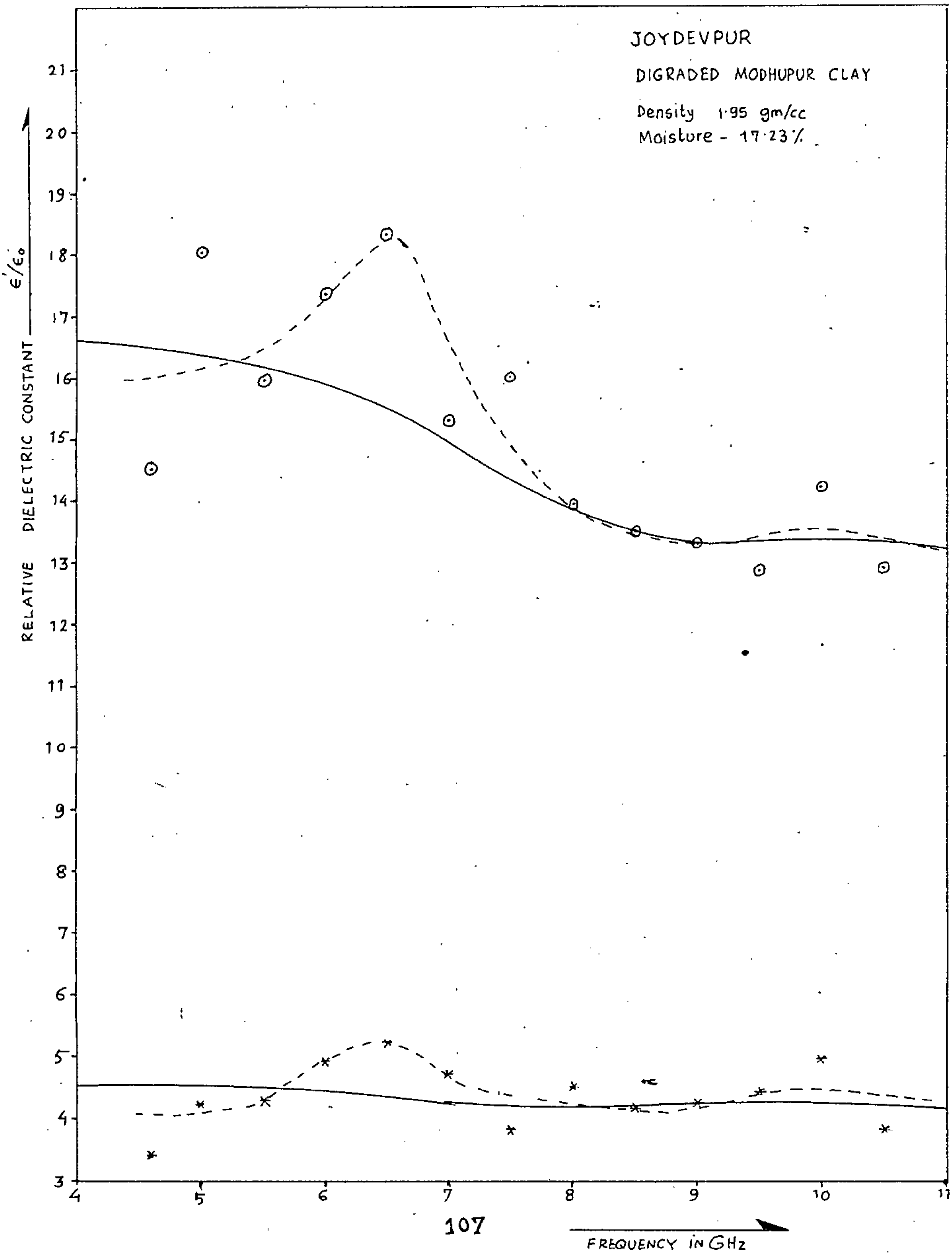
JOYDEVPUR
DIGRADED MODHUPUR CLAY
Density 1·95 gm/cc
Moisture - 17·23%
RELATIVE DIELECTRIC CONSTANT ε′/ε₀
21
20
19
18
17
16
15
14
13
12
11
10
9
8
7
6
5
4
3
4
5
6
7
8
9
10
11
FREQUENCY IN GHz

TABLE 5A

f in GHz	4·6	5·0	5·5	6·0	6·5	7·0	7·5	8·0	8·5	9·0	9·5	10·0	10·5
VSWR	10·25	7·7	6·3	5·6	5·5	4·85	8·0	6·7	5·4	5·3	5·0	5·1	4·6
	10·35	8·0	6·25	5·7	5·55	4·8	7·9	6·4	5·7	5·3	4·9	5·0	4·9
	10·05	7·8	6·3	5·7	5·6	4·8	9·0	6·2	6·0	5·2	4·7	4·8	4·3
	10·03	7·5	6·4	6·0	5·7	5·0	7·5	6·2	6·4	5·3	4·85	4·8	4·6
	10·5	8·2	6·6	5·9	5·65	5·0	7·9	6·4	5·8	5·1	5·0	4·9	4·4
	10·5	8·0	6·5	5·95	5·6	4·9	7·7	6·3	5·7	5·2	4·9	5·0	4·5
	10·4	8·0	6·0	6·0	5·7	5·0	7·97	6·36	5·7	5·25	4·9	4·9	4·56

AVERAGE

S	10·26	7·92	6·27	5·86	5·62	4·92	8·0	6·37	5·67	5·23	4·89	4·93	4·55
ρ	·822	·78	·725	·708	·698	·66	·78	·729	·70	·679	·66	·663	·64
K	14·55	18·08	15·99	17·33	18·37	15·27	16·02	13·87	13·48	13·29	12·89	14·21	12·99

TABLE 5B (DRY)

VSWR	4·3	3·72	3·05	3·0	2·95	2·8	3·75	3·85	3·08	2·95	2·95	2·85	2·55
	4·42	3·65	3·08	2·95	2·85	2·6	3·6	3·75	3·04	2·95	2·95	2·85	2·4
	4·55	3·65	3·05	3·0	2·9	2·6	3·75	3·25	3·0	2·98	2·8	2·85	2·45
	4·56	3·7	3·06	3·0	2·85	2·6	3·8	3·2	3·0	3·0	2·8	2·85	2·1
	4·4	3·6	3·1	3·0	2·8	2·7	3·5	3·4	2·9	2·5	2·6	2·7	2·5
	4·35	3·65	3·05	2·95	2·9	2·6	3·7	3·3	2·95	2·8	2·7	2·8	2·5

AVERAGE

S	4·43	3·66	3·07	2·98	2·88	2·65	3·68	3·46	2·99	2·89	2·80	2·82	2·42
ρ	·63	·57	·51	·50	·49	·45	·57	·55	·50	·48	·47	·48	·41
K	3·43	4·26	4·34	4·92	5·26	4·76	3·85	4·58	4·21	4·33	4·49	5·04	3·86
K_c	3·4	4·22	4·29	4·87	5·20	4·71	3·81	4·53	4·17	4·28	4·44	4·99	3·82

SAMPLE FROM JOYDEVPUR

TABLE A — Moisture : 17·23%
— Density 1·95 gm/cc

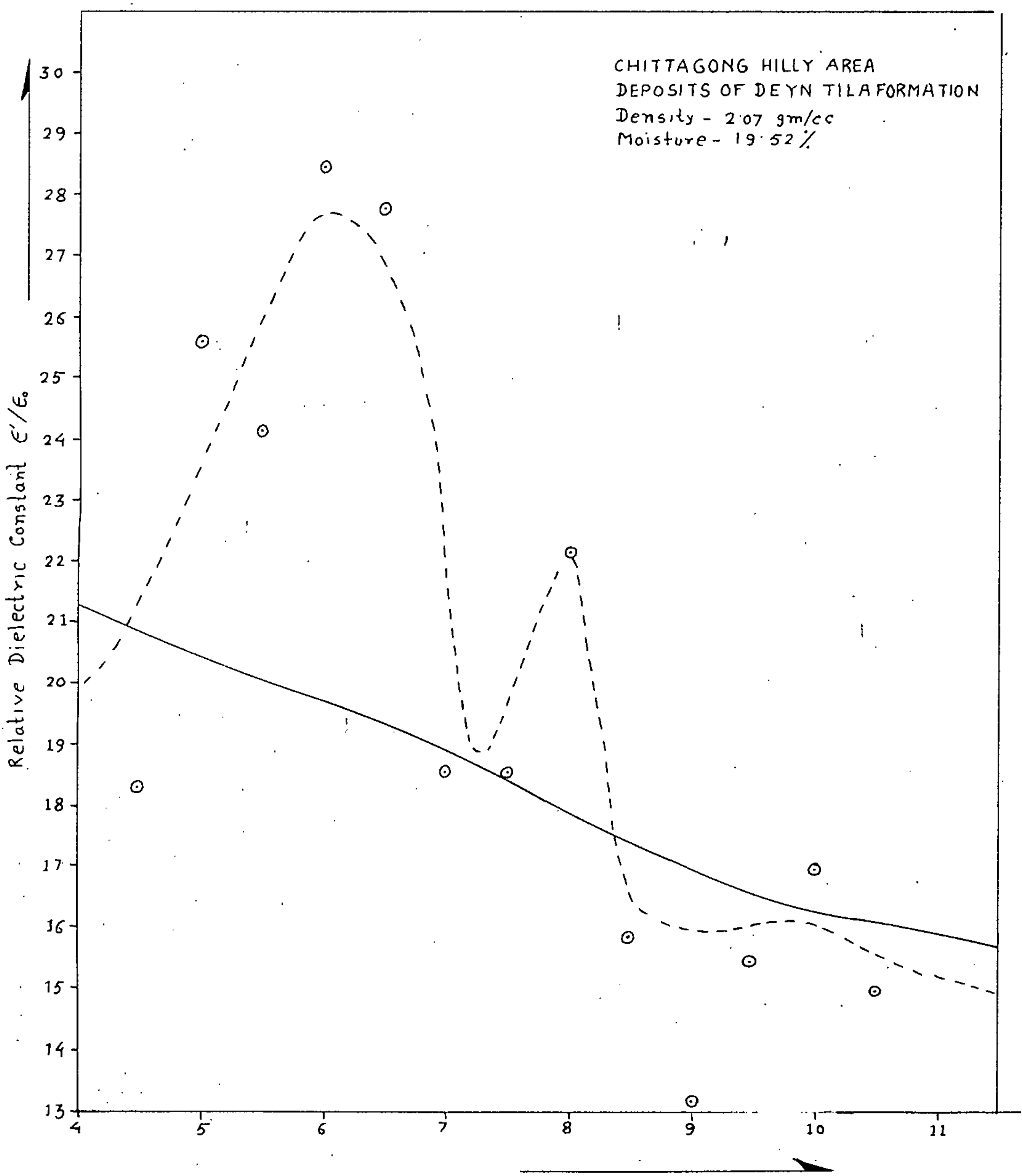
CHITTAGONG HILLY AREA
DEPOSITS OF DEYN TILAFORMATION
Density - 2·07 gm/cc
Moisture - 19·52 %
Relative Dielectric Constant ε'/ε₀
30
29
28
27
26
25
24
23
22
21
20
19
18
17
16
15
14
13
4
5
6
7
8
9
10
11
FREQUENCY IN GHz.

TABLE 10 :

f in GHz	4.6	5.0	5.5	6.0	6.5	7.0	7.5	8.0	8.5	9.0	9.5	10.0	10.5
VSWR	11.5	9.9	7.7	7.2	6.7	6.2	7.0	7.2	6.2	4.9	5.05	5.25	4.95
	11.6	9.8	7.7	7.0	6.7	6.25	7.0	7.2	6.3	4.95	4.9	5.1	4.4
	11.8	9.5	7.8	7.1	6.75	6.10	7.8	7.4	6.0	5.5	5.6	5.6	5.0
	12.0	9.5	7.7	7.3	6.6	5.9	7.7	7.6	6.1	5.5	5.7	5.7	5.0
	11.3	9.6	7.5	6.9	6.4	5.9	7.5	7.4	6.2	5.1	5.5	5.2	4.9
	11.4	9.6	7.6	7.0	6.5	6.0	7.4	7.3	6.1	5.2	5.4	5.4	5.1

AVERAGE

S	11.53	9.65	7.67	7.08	6.61	6.06	7.4	7.35	6.15	5.19	5.36	5.38	4.89
ρ	.84	.812	.769	.752	.737	.717	.762	.76	.72	.67	.685	.686	.66
K	18.33	25.6	24.1	28.4	27.7	8.55	18.45	22.16	15.81	13.19	15.42	16.91	14.86

CHITTAGONG HILLY AREA

DENSITY 2.017 gm/cc

MOISTURE 19.53 %

TABLE NO- 7

FOR DC CONDUCTIVITY OF THE SOIL SAMPLES

Code No.	Resistance in ohm.	Length 1 cm.	Cross sectional area A sq. cm.	Resistivity $P = \frac{AR}{1\ cm}$ ohm.	Conductivity in ohm. /cm.
3	220 K-Ω	5.45	1.25x 2.5	$1.3x10^5$	7.9 μ℧/cm.
1	590 KΩ	5.1	1.5 x 1	$1.7x10^5$	5.8 μ℧/cm
8	470 KΩ	5.3	1.5 x 1	$1.33x10^5$	7.5 μ℧/cm
2	460 K-Ω	6.8	1.25x2.25	$1.9\ x10^5$	5.26 μ℧/cm.
4	320 K-Ω	3.3	1.5x 1	$1.4\ x10^5$	6.9 μ℧/cm.
9	310 KΩ	5.6	1.5x 1	$0.83x10^5$	12.0 μ℧/cm
5	610 K-Ω	5.8	1.5x 1	$1.6X10^5$	6.3 μ℧/cm.

EXPERIMENTAL SETUP FOR MEASURING D-C CONDUCTIVITY

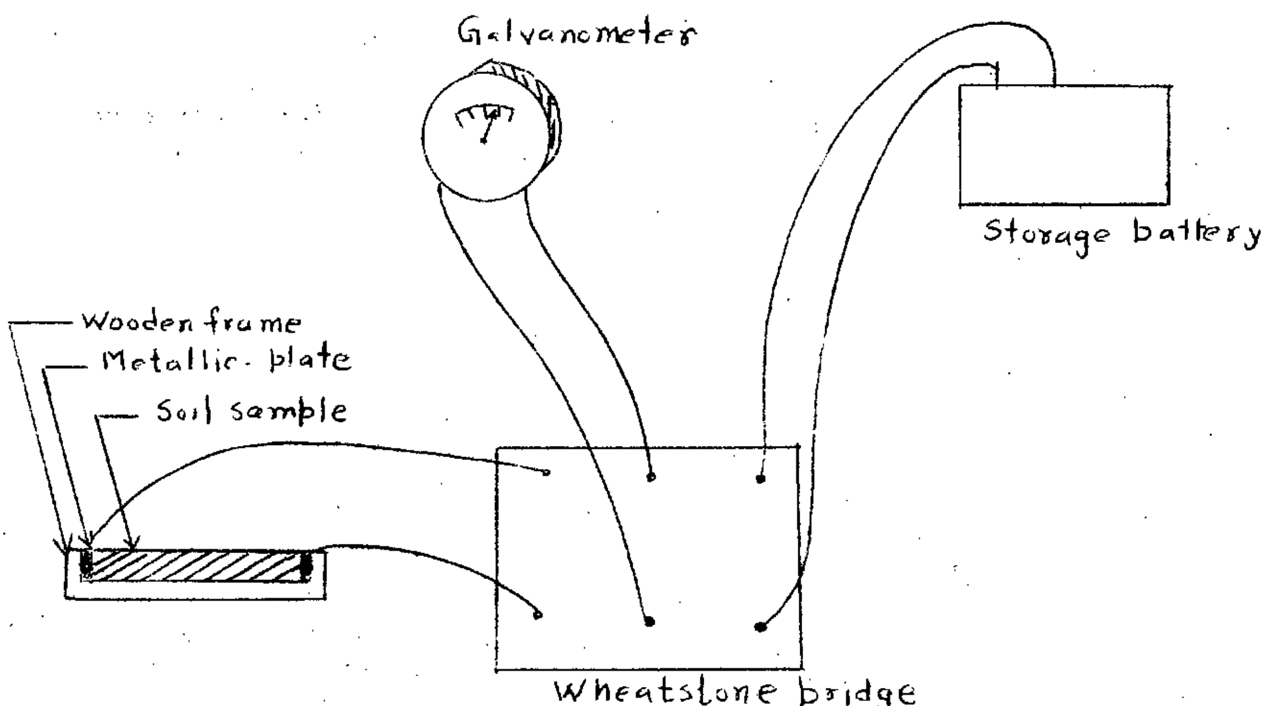

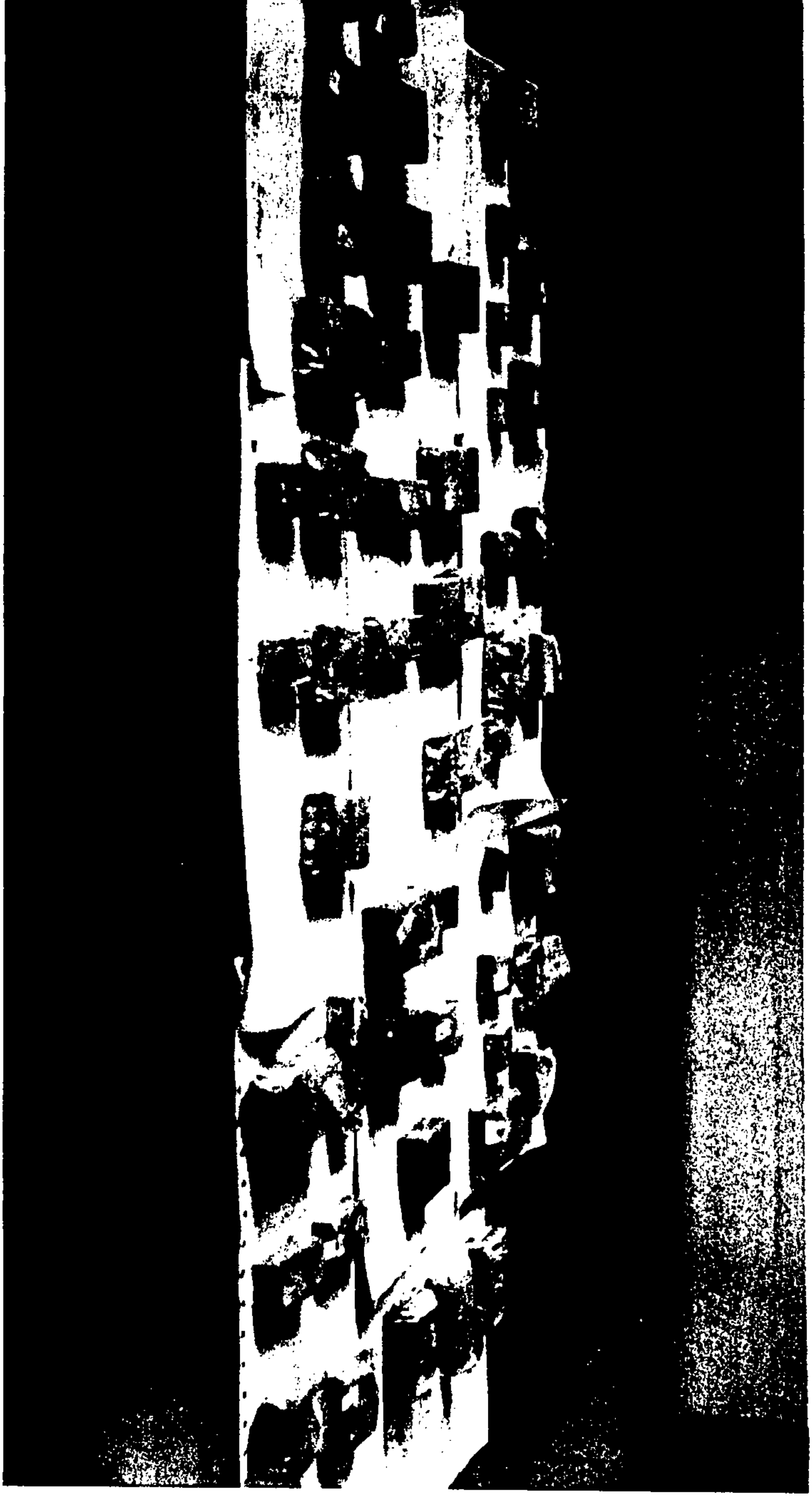

Photographic View of Different Soil Samples.

7.4 **DISCUSSION:**

The curves shown in Fig-18 to Fig-28 reveals some special characteristics of the variation of the dielectric constant of soil with respect to frequencies. The densities of most of the samples were more or less same, but the moisture contents varied appreciably. The characteristices of the curves are listed below:-

(1) It was seen that the presence of moisture in the sample increases the value of the dielectric constant.

(2) An average rise of the values of dielectric constant was observed between 6 to 7 GHz of frequency.

(3) In some samples(Narayn Ganj, Dawood Kandi, Ctg. City) the densities were quite low. It was observed that the dielectric constant of those samples were much less than those of others.

Now, to explain the nature of curve, let us consider the first feature of the curves mentioned in (1) . From the theoretical and experimental investigation it was found that the dielectric constant of water remains more or less constant upto the frequency of about 10 GHz of the applied electromagnetic waves shown in Fig. 30. The typical values within this range of frequency is between 75 and 80. Again, the typical value of dielectric constant of the soil(within 7 to 10 GHz) is about 12. So, it is obvious that the presence of moisture should increase the dielectric constant. It was also observed that there was an average rise in the values of the dielectric constant within 6 to 7 GHz frequency band. From an elaborate study on the dielectric properties of the gases, it is seen that there might be a sharp rise in the value of the dielectric constant of gases, if the vibration of gase molecules forming dipoles are in resonance with the applied frequency of applied electromagnetic waves. Now, in the present case it might happen that some gases have been trapped in the samples and the vibrational frequency of some of the heavy gase molecules forming dipoles falls in the domain of 6 to 7 GHz frequency band. As a result sharp-increase in the value of the dielectric constants are observed. Lastly it was observed that due to lowering of the densities, the dielec-tric constant decreased. It is an accepted fact that, if all other factors remain same, but the densities of the sample decreases, then the value of the dielectric constant gradually decreases towards unity.

It has already been mentioned that the imaginary part of the permittivity of the soil could not be measured. The evalution of this parameter required the shift of the maxima and minima of VSW pattern in the wave-guide section very accurately(of the order of .0001 cm). Since, this shift in the VSW pattern was to calculate manually which was quite impossible, so the imaginary part of the permittivity of the soil at microwave frequencies could not be measured. However to get some idea about the losses in the soil sample, the dc conductivity of the soil samples were calculated. The results agreed fairly with the typical values.

Lastly, in general it may be concluded that there was no appreciable variation of the values of the dielectric constant among the types of the soil samples investigated for different types of thes samples collected from different places.

CHAPTER 8

CONCLUSION

CHAPTER - 8

DISCUSSION

Two different topics have been studied in this thesis. In the first part, study have been made on electromagnetic diffraction phenomena. In chapter-3, the original Fresnel-Kirchoff diffraction theory has been investigated, by incorporating the effect of antenna directivity .This theoretical treatment has been followed by an experiment performed in the laboratory.

From the results shown in the table- 1, it is seen that, on introducing the effect of antenna directivity in the original Fresnel-Kirchoff diffraction theory, the average percentage error between the experimental results and the theoretically calculated values have decreased appreciably. Numerically the figure(percentage deviation) has comedown from 4.51% to 1.36%. The percentage deviation-based on actual field measurement as reported by earlier workers was less than 4.5% . Probably the scale-model technique used and was responsible for this. The antenna diameters of the receiving and the transmitting system was quite comparable to the radius of the first -fresnel-zone and as a result, this zone could not be defined properly. Again, the antennas had high directive patterns and as a result most of the power was concentrated in the first few fresnel-zones resulting inaccuracy in the experiment. Lastly, the experiment was performed in a closed laboratory without absorbing walls. So, the reflection of electromagnetic waves might enhance the inaccuracy of the experiment. The percentage error could be improved by eliminating all thesedifficulties . Again the percentage error (1.36%) could be further decreased by eliminating this following difficulties. It was already mentioned that the antenna patterns were considered along X - Y plane. Due to mathematical complicacy the three dimensional antenna patterns were not considered.

The Knife-edge diffracting sheet was not infinitely long in the transverse direction as assumed theoretically. The finite dimension of the sheet in the transverse direction might cause some diffraction which might be responsible for decrease in the receiving field-strength.

In Chapter-4, a theoretical and experimental investigation was performed on the diffraction of electromagnetic waves by a "building structure". This was also performed in the laboratory using scale-model technique. From the table-2, it is seen that obstacle gain obtained from theoretical and experimental investigations were more or less same. However, a small discrepency was observed. In all three cases, it was found that the theoretical value is slightly less than the experimental results.

One of the major causes of this discrepencies was the negligence of the diffraction due to the edge A(fig). The diffraction due to this edge was neglected for mathematical complicacy. It might happen that the scattered electromagnetic waves from the edge added in phase with the directly received field resulting an increase of over all gain.

The second probable cause might be the finite dimension of the obstacle along the transverse direction. Theoretically the obstacle was assumed to extend infinitely in the transverse direction. The end edges of the obstacle might scatter the electromagnetic wave that added in phase with the direct received field resulting an increase in the over all gain.

Among other causes, the basic optical approach could be one. It has already been mentioned that this method does not consider the characteristics of the diffracting edge i.e. it is immaterial whether the edge is a conducting or an insulating one. But in practice , the case is quite different. When electromagnetic waves are obstructed by a sharp conducting-edge, the upper-side of the sheet is excited by the induced current which radiates eledctromagnetic waves. This radiation from the penumbral region of the conducting sheet is completely neglected in the optical theory. In this problem also, similar radiation from the vertical side of the conducting obstacle facing the receiving antenna might occur.

Lastly, the accuracy of the optical approach depends on the ratio of the dimension of the diffracting obstacle to the wavelength of the transmitted wave. The larger this ratio the more accurate is the approximation. So, the accuracy could be improved by using higher frequency of transmission or making the obstacle dimension larger.

In the part II of the thesis, an investigation was performed on the measurement of dielectric constant of soil at microwave frequencies(X band and J band). Two different procedures were adopted for this purpose. The Ist method known as " Free-space measurement technique", failed to give accurate results. In this procedure, the dielectric constant of water was also measured. However, the conductivity of water could not be measured. It was found that there could be 20 to 30% variation in the result of conductivity for the variation in the magnitude of measured reflection-coefficient. This was one of the main draw-back of the procedure.

From the table-4 it is seen that the relative dielectric constant of the soil is much less than the standard one. The variation might be for loose packing of soil. The loosely packed soil samples acted as a porous medium causing a decrease in the reflected field-strength. Again, due to surface roughness the reflected wave was scattered in different directions resulting a decrease in the field-strength in the receiver. Due to all these factors, the measured dielectric constant was much less than the typical values. These difficulties lead us to adopt a second method.

The 2nd method is known as "measurement of dielectric constant by wave-guide technique" ". In this procedure, soil samples from few places were tested, curves have been plotted showing the variation of value of relative dielectric constant of soil samples with the applied frequency variation, under different moisture contents. One of the important feature of the curves, was that, the presence of moisture increased the value of the relative dielectric constant. This phenomena may be explained as follows. It was found that the dielectric constant of water remains more or less constant(sith 75 & 80) upto the frequency of about 10 GHz . Again, the typical value of dielectric constant of soil (at about 7 to 10 GHz) is about 10. So, it can be concluded that, for the high value of the dielectric constant of water the dielectric constant of soil samples with moisture contents increases. It was also observed that there was an average rise of the values of dielectric constant of soil within 6 to 7 GHz, frequency band. From the dynamic properties of the gases it is seen that there might be a sharp, increase in the value of the dielectric constant of gases, if the vibration of the gas moleclules or electrons in the gases is in resonance with the applied frequency of the electromagnetic waves. Now, in the present case, it might happen that some gases have been trapped in the tested soil samples and the vibrational frequency of some heavy molecules might fall in the domain of 6 to 7 GHz. frequency band resulting peaks in the value of the dielectric constant withint that band of frequency. Throughout the experiment the density of the tested samples were maintained constant except for few cases. In these case it was observed that the dielectric constant of the sample decreased with the decrease of density. It is an accepted fact that, the dielectric constant of any sample gradually approaches towards unity with the decrease in the density, provided all other factors remain same.

The experimental setup was good enough to measure accurately the real part of the permittivity of the soil. Due to lack of instrumental facilities the imaginary part of the permittivity could not be measured. The evaluation of this parameter required the measurement of the shift of maximum or minimum of VSW pattern in the wave-guide section very precisely(of the order of.001 cm), which was very difficult to calculate manually. However, to get some idea about this parameter, the d-c conductivity of the samples were calculated. The results agreed fairly with the typical values.

SCOPE OF THE WORK:

A theoretical and an experimental investigation was done on the electromagnetic diffraction by knife-edge obstacle. The results obtained by incorporating the effect of antenna directivity in the original Fresnel-Kirchoff diffraction theory was quite encouraging. In this case the directivity was considered along the longitudinal vertical plane only. A better result could be expected by considering the three -dimensional variation of the antenna directivity.

Another investigation on the electromagnetic diffraction problem was the study of diffraction by a "flat-top double-edge obstacle". The obstacle was considered as a model of a building structure. The main object of this experiment was to find the effect of electromagnetic diffraction by tall buildings during microwave-communication in modern cities. However, some approximation was considered during the theoretical treatment of the problem. An alternative approach was also considered, which was comparitively more accurate. However the solution could not be found due to mathematical complicacy. [redacted] Again, in our problem only a single obstacle was considered. But in practice, the microwave-signals in the modern cities are diffracted by the presence of a number of building, masts and towers. For considering this effect, a theoretical treatment can be made by considering a statistical distribution of the diffracting obstacle placed in between the transmitter and the receiver. The treatment can also be extended upto consider the formation of radio-pocket in the modern cities during wireless communication. The salution of these problems will surely solve some critical situation that are encountered in the modern cities, especially by the police department.

The main object of the measurement of the dielectric constant of the soil was to prepare a complete Radio-data for Bangladesh soil. Due to limited facilites the study could not be completed. If resources are available for collecting representative soil samples from all over Bangladesh, also facilities are available in the laboratory to measure accurately the phase shift in the NSW pattern, then it would be possible to obtain a complete information about soil characteristics of our country by extending the method adopted in this thesis. Further study could be made to evalute the effective absorption and reflection coefficients of the paddy fields at different stages of their growth. The datas may be quite helpful for establishing the microwave communication link in Bangladesh.

APPENDIX

In Chapter-2, the electromagnetic diffraction by knife-edge obstacle was studied. In this case, an experiment was performed in the laboratory. The received power was detected by an I. F. coplifies. To find the absolute power, the I.F. coplifier was calibrated by means of a power-meter and the curves were then extrapolated for measuring low powers. The calibration curve is shown in Fig. 33.

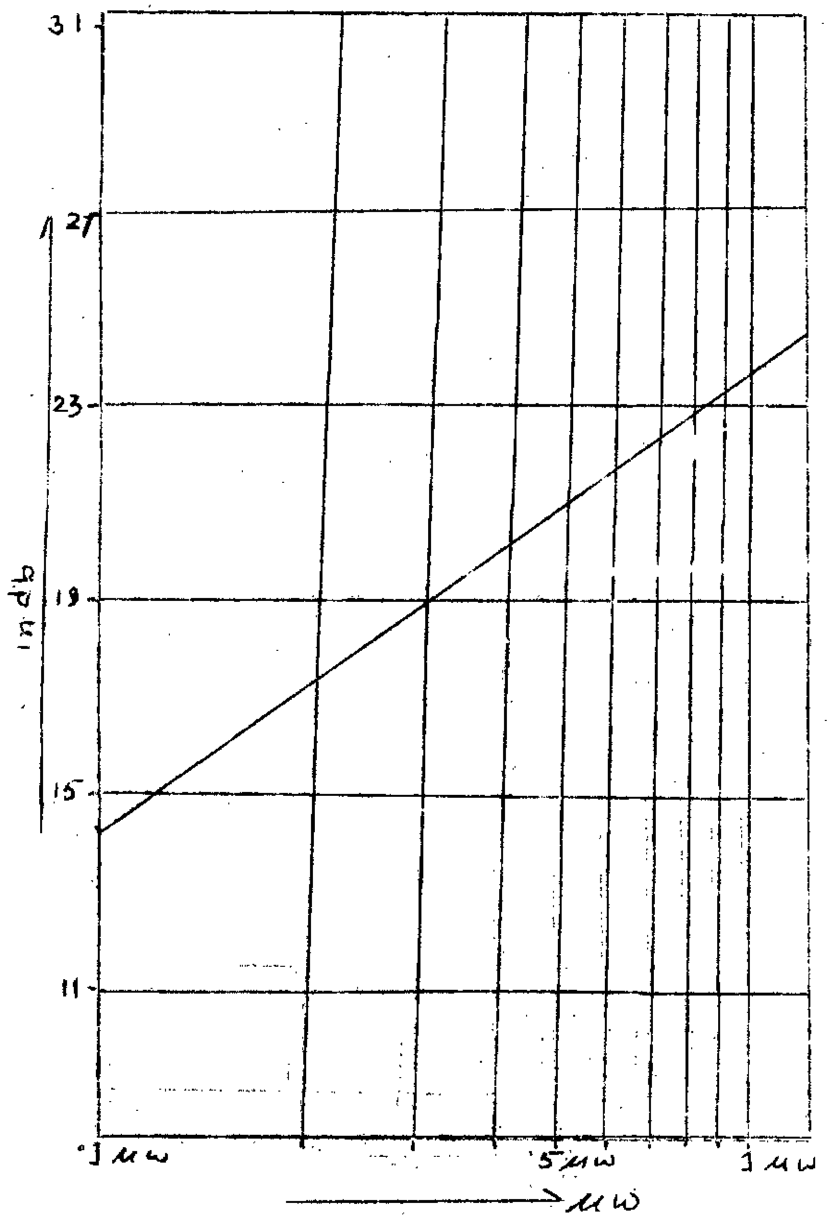

Extrapolated Calibration Curve.
FIG-33

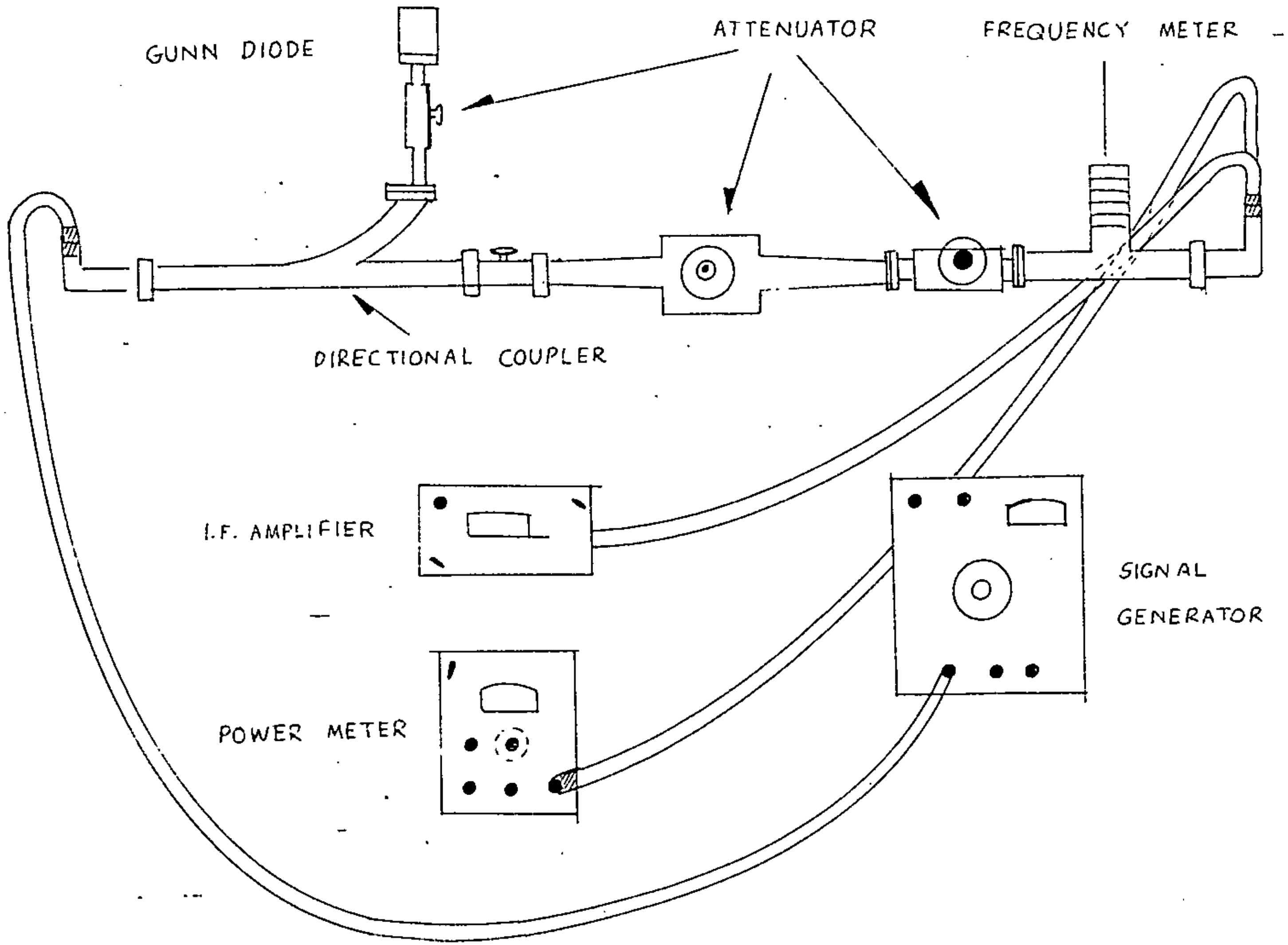

EXPERIMENTAL SET UP FOR CALIBRATION OF I.F. AMPLIFIER

FIG. NO.

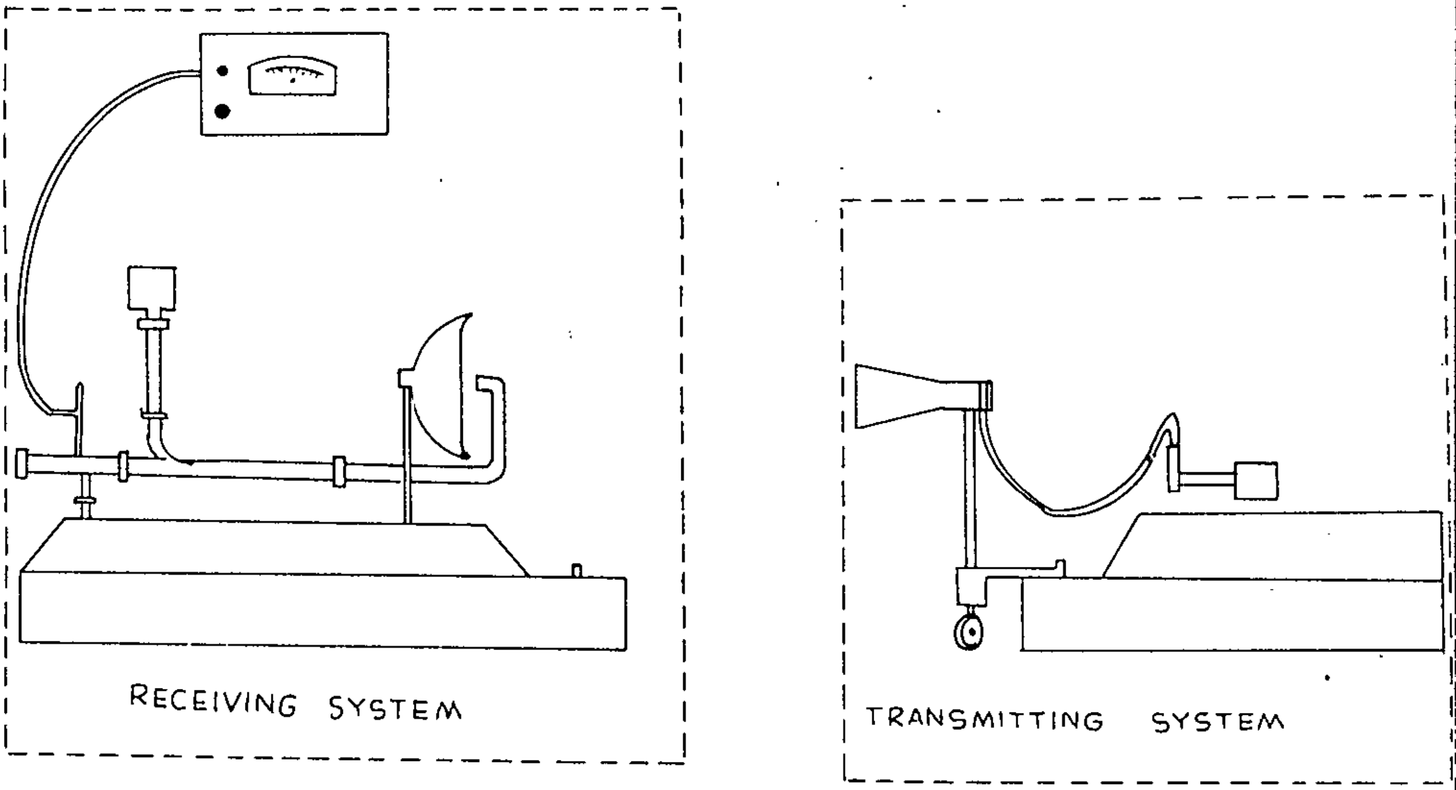

Fig- (a)

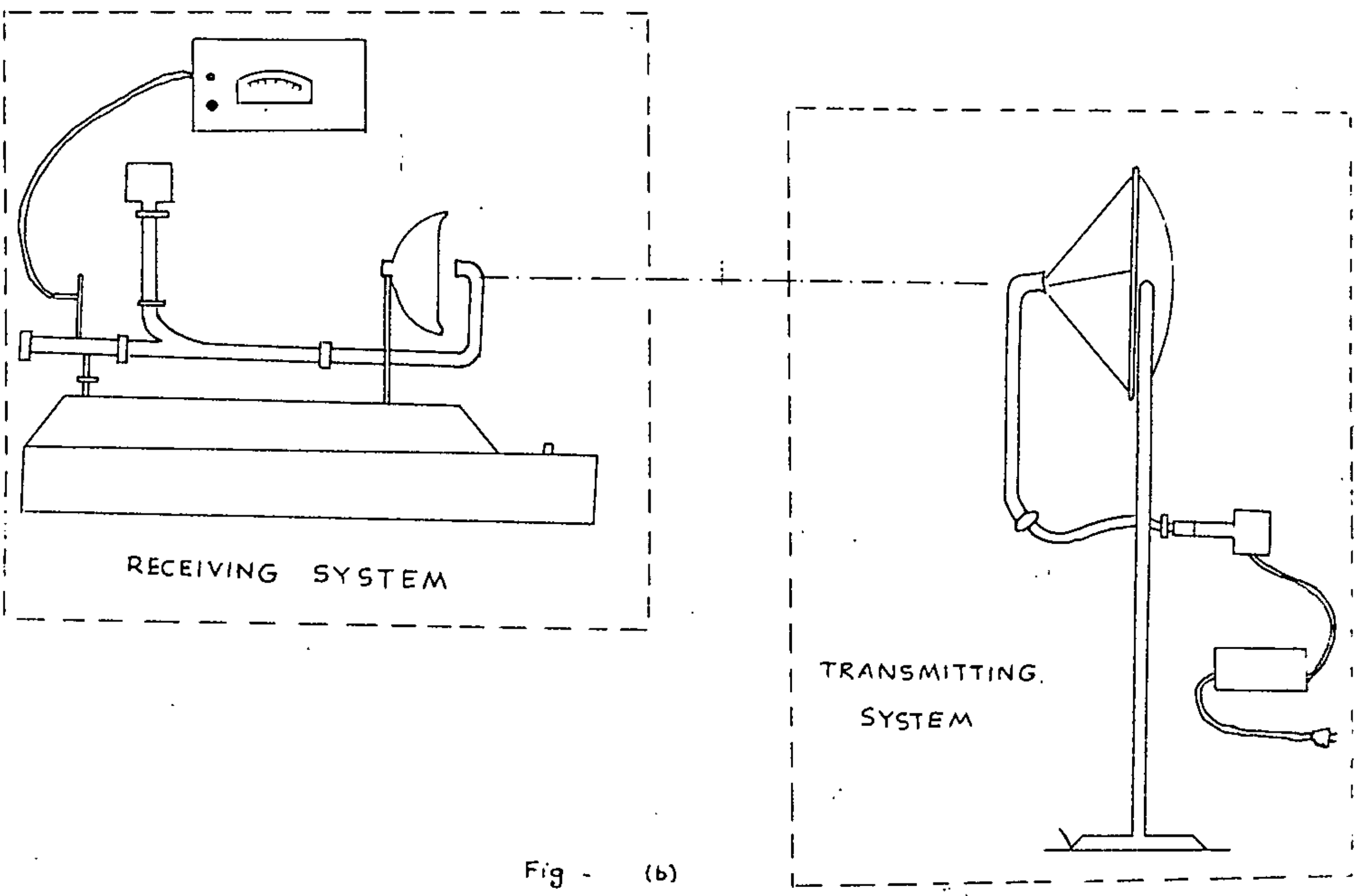

Fig - (b)

EXPERIMENTAL SET UP FOR GAIN MEASUREMENT

APPENDIX-

In Chapter-4, the problem of electromagnetic diffraction by a flat-top double-edged conducting obstacle has been studied. A theoretical formulation of the above problem has been developed. Numerical solutions have been performed with the help of digital computer(IBM-360). For completeness, a sample programming of the above problem have shown below.

```
      DIMENSION   RY(61)
      COMPLEX  DEL,E1,E2,E
      READ (1,25) D1,D2,Y1,Y2,DY,AK,N
   25 FORMAT (6F10.5,I10)
      DEL=(0.0001,0.0001)
      Y=Y1-DY
      E1=(0.0,0.0)
      M=N+1
   26 DO 20  I=1,M
      Y=Y+DY
      R1=D1+Y*Y/(2.*D1)
      R2=D2+Y*Y/(2.*D2)
   20 RY(I)=-AK*(R1+R2)
      CALL EXAR (N,DY,RY,E)
      E2=E1
      E1=E1+E
      WRITE (3,21) E1,Y
*
*
      FORMAT (2E20.8,F10.2)
      IF(Y.GT.Y2) CALL EXIT
      Y=Y-DY
      GO TO 26
      END
```

APPENDIX

To understand the complete phenomena of the response of dielectrics in the presence of alternating electric field onw sould study the frequency-response characteristics of the gases, lequids and solids separately. Considering the dielectric properties of the gases first. In this case, may start with the simple model of electrons grain- elastically bound to equillibrium positions and re-acting to field changes like linear harmonic oscillators. When there is an applied electric-field then the electronic oscillator is considered to be subjected to a driving force eE' ; The law of motion may be written in the following form,[31].

$$\frac{d^2z}{dt^2} + 2\frac{dz}{dt} + w_0^2 z = \frac{e}{m}E' \quad \ldots\ldots\ldots\ldots\ldots\ldots(3.1)$$

where E' is the locally acting electrid field.

The experession can be rewritten in the form of a differential equation for the polarization P. By assuming that the dielectric is composed of N oscillators per unit volume, each of them contributing an induced electric moment.

$$u = eZ$$

$$P = NeZ$$

Again from Mosotti approximation, we can write,

$$E' = E + \frac{P}{3\epsilon},$$

Where E is the applied electric-field. So, the differential equation becomes,

$$\frac{d^2P}{dt^2} + 2\alpha\frac{dP}{dt} + \left(w_0^2 - \frac{Ne^2}{3mt\epsilon_0} \right) P = \frac{Ne^2}{m}E \quad \ldots(3.2)$$

The effect of the polarization of the surrounding is to tower the frequency of the individual oscillator from w_0 to,

$$w'_0 = \sqrt{w_0^2 - \frac{Ne^2}{3m\epsilon_0}} \quad \ldots\ldots(2.3)$$

The steady state solution of the equation 2 is given by,

$$P = P_0 e^{j(wt+\Psi)} = \frac{Ne^2/m}{w_0^2 - w^2 + jw2\alpha} E \quad \ldots\ldots\ldots (2;4)$$

Because of the friction factor 2 a phase-shift occurs between the driving field and the resultant polarization, P became complex. The ratio $P/\epsilon_0 E$ determines the complex relative permittivity of the medium in molecular terms as

$$K^* = 1 + \frac{P}{\epsilon_0 E} = 1 + \frac{Ne^2/\epsilon_0 m}{w_0^2 - w^2 + jw2\alpha} \quad \ldots\ldots\ldots\ldots\ldots (2;5)$$

So; far we have assumed that the dielectric contains only one oscillator type. In the more general case of S oscillertor types which contribute to k* without mutual coupling; the equation may be generalized as,

$$K^* = 1 + \sum_s \frac{N_s e^2/\epsilon_0 M_s}{w_s^2 - w^2 + jw2\alpha_s} \quad \ldots\ldots\ldots\ldots\ldots (2;6)$$

Now, considering the case for, far below the resonance frequency (w ws) , each oscillator type adds a constant contribution

$$\frac{N_s e^2/\epsilon_0 m_s}{w_s^2}$$

to the static dielectric constant of the medium, whereas far above the resonance frequency it's contribution vanishes. To follow the behavior of the lowest oscillator type r through it's resonance region, we lump the effect of vacuum and of the remaining resonator type in a constant contribution.

$$A = 1 + \sum_s \frac{N_s e^2/m_s}{w_s^2} \quad \text{for } s \neq r \quad \ldots\ldots\ (2;7)$$

Furthermore, let us introduce in place of w the deviation from resonance, $\Delta w = w_r - w$

as the variable approximate

$$w_r + w \simeq 2w_r$$

$$\frac{w}{w_r} \simeq 1$$

and then writing the equation 3.6 as ; $K^* = A + \dfrac{B}{\Delta w + j\alpha}$

where, B stands for $B = \frac{N_e e^2/\epsilon_c n_r}{2w_r}$

The frequency dependence of the real part of the relative permittittivity, $K' = A + \frac{B\Delta w}{(\Delta w)^2 + \alpha^2}$ ....(2.8)

described the dispersion characteristics of the dielectric medium near resonance (Fig. 2) . It rises hyperbolically from the low frequency value $A + \frac{2B}{w_r}$ to a maximum

$$K'_{max} = A - \frac{B}{2\alpha}$$

at $\Delta w = \alpha$ and then rises again asymptotically to the constant value A for very high frequencies ($w >> w^2$).

The absorbtion characteristic of the dielectric, identified near resonance by the relative loss factor,

$$K'' = \frac{B\alpha}{(\nabla w)^2 + \alpha^2} \quad ......(2.9)$$

Strats from zero at low frequencies, travers in's maximum B/α at resonance, and falls again symmetrically to zero at high frequencie s ......(2)

Upto this, the frequency dependence character of the dielectric (in gases stato) has been discussed. In case condensed phases, solids and liquids, the case is not so simple. In this case the internal collision should also be considered. The explicit formulation of the problenwas derived by Debye . A brief outline of this formulation is described below:

The basic idea of the dynamic proparties of the solids and lequids is that, in the presence of applied alternating electric fields, the movement of the dipoles are restricted by the intermolecuar collision. According to the casumption of dominating fiction, one may picture the polarmolecular as rolating under torque T of the electric fields with- an angular velocity $\frac{d\theta}{dt}$ proportional to this torque, or

$$T = \xi \frac{d\theta}{dt} \quad ....(2.10)$$

The friction factor will depend on the shape of the molecule and on type of interaction it encounters. If one visualizes the molecule as a sphere of the radius a, rotating in liquid of viscosity according to stokes law, classical hydrodynamics leads to the value

$$\xi = 8\pi\eta a^3 \qquad ....(2.11)$$

Finally, Dyhye calculated the relaxatine time which measures the time required to reduce the dipole moment(when the external field is suddenly removed) of the order to 1/e of it's original value. He found the following relation,

$$\tau = \frac{\xi}{2KT} \qquad ......(2.12)$$

Combining equation 3.11 and 3.12 . Debye obtained for the spherical molecule, it behaves like a ball rotating in oil, the relaxation time ,

$$\tau = \frac{4\pi a^3\eta}{kT} = V\frac{3\eta}{KT}$$

Water at room temperature has viscosity = .01 poises with radius of 2A for the water molecule; a time constant of $.25X10^{-10}$ section results.

However, the variation of real and imaginary past of the promittivity of water can be found to be as shown in Fig. 30.

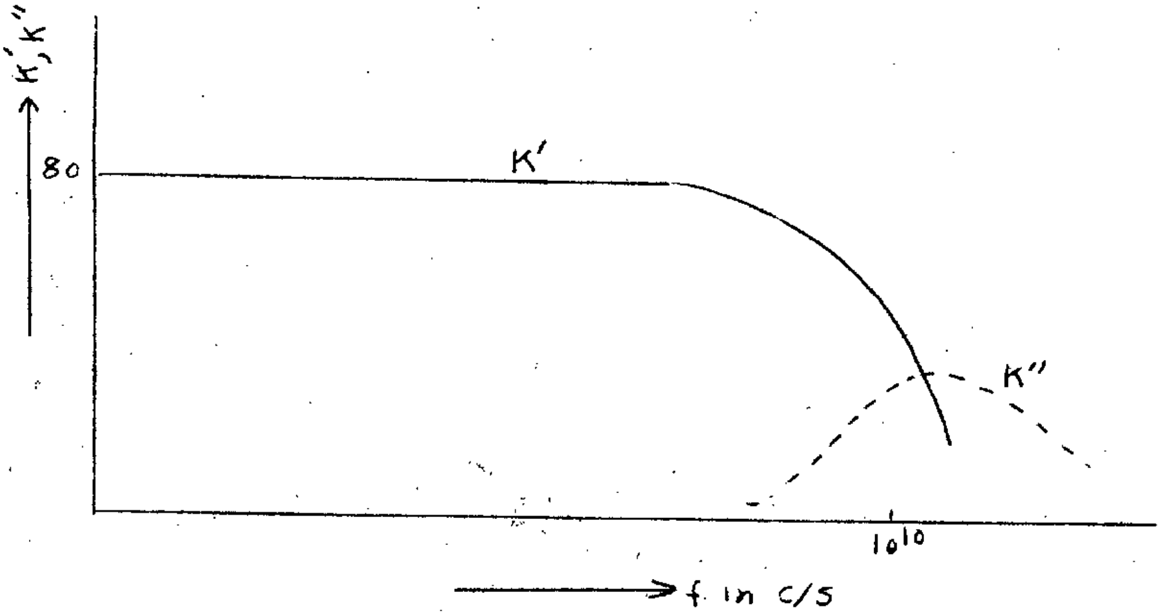

FIG.30

BIBLIOGRAPHY

1. M. Born and E. Wolf, "Principles of Optics," third edition, Pergamon, New York(1965); p-370 et. seq.

2. L. J. Anderson, L. G. Troles and S. Weishbord, "Simplified Method for Computing Knife-Edge Diffraction in Shadow Region" in Electromagnetic Wave Propagation, editted by M. Desirecent and J.L. Michicls, Academic Press, New York(1960); pp 209-214.

3. J. Deygot, " Multiple Knife-Edge Diffraction of Microwaves" Trans. IEEE AP-14, 480-489(1966).

4. C. T. Tai--"A Concise formulation of Huygen's principle for electromagnetic field" I. E. E. Trans. AP Vol. AP-8 P-634 Nov. 1960

5. H. Levine & J. Schwinger- "On the theory of electromagnetic diffraction by an aperture in an infinite half-conducting plane" Comm. Pu Appl. Math Vol. 3, PP-355-391 Dec. 1955.

6. G. W. Swenson, Jr. " VHG diffraction by mountains of the Alaska Range" Proc. IRE(correspondence) Vol. 44 PP-1049-1050 Aug. 1956.

7. B. N. Harden--"Diffraction of Electromagnetic waves by Two parallel Half-Plane" Proc. I. E. E. Part-III, Vol. 100, P-348(1953).

8. K. Bullington--"Reflection Coefficients of Irregular Terrain" Proc. IRE, 42, 1258--1262(1954).

and

K. Bullington ". Radio Propagation at Freq. above 30 Mc" PROC. IRE - 1954, Vol-35

9. Epstin and Peterson "An experimental study of wave propagation at 850 Mc" Proc IRE, Vol. 41, PP. 595-611, May. 1953, especially Fig. 30, Page-609.

10. G. Millington, R. Hewitt, F. S. Immirzi," Double Knife-edge diffraction in field-strength predictions, "IEE Monograph 507E PP-419-429 March, 1962.

11. F. A. Jenkis, Fundamentals of Physical Optics, Mc-Graw-Hill New York(1937); P-175 et seq.

12. J. Deygot, " Transmissions Multivoies par Faisceaus Hertziens" E. A. T. (Montagaries) titre 111, Fasc 1, 1961 and titre-1, PP-139-141 1964.

13. "Etude d'une Liaison Hertziene" STA/EMAT, P-5, December, 1963.

14. J.H. Crysdale "Comparison of some Experimental Terrain Diffraction Losses with Prediction Based on Rice's Theory for Diffraction by Parabolic Cylinder. Trans IRE AP-6, 293-295 (1958).

15. S.O. Rice " Diffraction of Plane Radio Waves by Parabolic Cylinder-- Calculation of Shadows behind Hills" BSTJ, 33,417-504(1954).

16. V.A. Fock, "Electromagnetic diffraction and Propagation".

17. H.E.J. Neugebauer and M.P. Bachyniski, " Diffraction by smooth Cylindrical Mountains", Proc. IRE, 46,1619-1627(1958).

18. C.G. Montogomery " Technique of Microwave Measurement" M.I.T. Radiation Laboratory Series. New-York and Lond, Mcgrow-Hill Book Company, Inc. 1947. P-561-676.

19. C.G. Montogomery, R-H. Dicke and E.M. Purcell" Principles of Microwave Circuits" M.I.T. Radiation Laboratory Series. New-York Toronto, London, Mcgraw-Hill Book Company, Inc. 1948, P-365-374

20. Westtphaul and A.D.G. Jelatis " Measurement of Di-electric Constant and Loss in the Range of Centimeter-waves". Dept. of Electrical Engineer M.I.T. March, 1941, PP-1-19.

21. R.H. Barefield, "Some Measurements of Electrical Constants of the ground at short wave-length by the wave-tilt method" Jour-J.E.E. Vol.75, P-214, 1934.

22. R.L. Smith-Rose, "Electrical Measurements of Soil with Alternating Currents" Jour, I.E.E. Vol. 75 P-222, 1934.

23. A. Oliner & H.M.Altschuler " Methods of measuring Dielectric Constant based upon a Microwave Netw rk view Point".

24. G.A. Deschamps J.Appl. Physics. 24,1046(1953).

25. O.J. Lodge," On Opacity" Philosophical Magazine, 1899, Vol.47 P- 385.

26. W. Burstyn, " Wireless Telegraphy, Influence of the counterpoise on Damping". Elcktrotcnch nische Zeitschrift, 1906, Vol. 27, P-1117.

27. J.S. Sache " The influence of the Earth in Wireless Telegraphy", Anndan da Physik, 1905, Vol. 18, P-348; Elcktrotechnische Zeitschrift, 1905, Vol. 26, P-951.

28. A sommerfield " On the Distribution of Waves in Wireless Telegraphy" Annalen der Physik, 1909 Vol. 28 , P-665 and 1926, Vol. 81, P-1135.

29. K. Uller, " The Electrical Conductivity of Sea and Land," Jahrbuch der Drahtlosen Telegraphie and Telephonie, 1911, Vol. 4, P-639.

30. J. A. Ractcliffe and F. W. G. White." The Electrical Properties of the Soil at Radio Frequencies," Philosophical Magazine, 1930, Vol. 10, P-667.

31. A. Hund," Short-wave Radiation Phenomena", Mc. Graw-Hill, New-York (1952); P-1018 et seq.

32. M. Born and E. Wolf, "Principles of Optics, Third edition, Pergamon, New-York(1965) P-

33. Donald C. Livingston, "The Physics of Microwave propagation". Bayside Research Centre General Telephone and Electronics Laboratories, Inc. New Jersey, U. S. A. (1970).

Some more papers and Books for Reference:

JOURNALS :

34. A. B. Carlson and A. T. Waterman, "Microwave Propagation over Mountain Diffraction Paths," Trans IEEE, AP-14, 489-496(1966)

35. K. Furutsn, " Statistical Theory of Ridge Diffraction," Radio Sci, 1, 79-98 (1966) (Highly Mathematical).

36. A. J. Legg., "Propagation Measurements at 11 Gc/S over 35-Km Near-Optical Path Involving Diffraction at Two obstacles," Electronics Letters, 1, 285-286(1965).

37. M. P. Bachynski and M. G. Kingsmill "Effect of Obstacle Profile on Knife-Edge Diffraction," Trans. IRE, AP-10, 201-205(1962).

38. L. J. Anderson and L. G. Trolese, "Simplified Method for Computing Knife-Edge Diffraction in Shadow Region," Trans IRE, AP-6, 281-186(1958

39. M. P. Bachynski, " Propagation of Oblique Incidence over Cylindrical Obstacles", Jour, Res. NBs, 64D, 311-315 (1960).

40. J. C. Schelleng, C-R Burrows and E. B. Ferrell, " Ultra-Short-Wave Propogation," BSTJ, 12, 125-161(1933); Proc. IRE, 21, 427-463(1933).

41. K.Bullington, " Reflection Coefficient of Irregular Terrain," Proc. IRE, 41, 1258-1262 (1954).

42. R. E. Mc. Gavin & L.J. Maloney, " Study at 1046 Mc. of Reflection Coefficient of Irregular Terrain at Grazing Angles", Jour Res. NBS. 63 D, 235-249(1959).

43. A.W. Straiton and C.W. Tolbert, " Measurement of Dielectric Properties of Soils and Water at 3.2-cm. Wavelength," Jour. Frankin Inst. 246, 13-20(1948).

44. G.W.O. Howe, " Wireless Waves at the Earth's Surface,", Wireless Engg., Vol. 17, P- 385, Sept. 1940.

45. C.H. Collie, J.B. Hostel & D.M. Ritson", The cavity resonator method of measuring Dielectric constant of Polar liquids in centimeter band", Proc. Phy. Soc. Vol. 60P-71(1948).

46. F. Horner, T.A. Taylor, R.Dusnuer, J.Lamb and W. Jackson " Resonance methods of dielectric measurements at centimeteric wavelength," Proc. IEE(London) Vol. 93, Pt. III-AP.1447, July 4, 1946.

47. D.E. Kerr, "Propagation of short Radio-Waves" Mc.Graw-Hill, New-York (1951).

48. F.E. Terman," Radio Engineer's Hand Book", McGraw-Hill, New-York (1943).

49. J.K. Robertson, " Introduction to Physical Optics" Third Edition, Van Nostrand, Princeton (1941).

50. B.B. Baker & E.T. Copson, " Mathematical Theory of Huygen's Principle," Second edition, Oxford, London(1950).

51. K. Hennay, " Radio Engineering Hand-Book, Mc-Graw-Hill, New-York (1950) P- 525 & 526.

52. S.A. Schelkunoff," Electro-Magnetic Waves" Van Nostrand, Princeton(1943) P- 354.

53. A Von Hippel, " Dielectrics and Waves".